UC Berkeley
UC Berkeley Electronic Theses and Dissertations

Title

The roles of microbial selenate reduction and selenium sorption on selenium immobilization in littoral sediment from the hypersaline Salton Sea, California

Permalink

https://escholarship.org/uc/item/61j7r946

Author

Villa-Romero, Juan Fernando

Publication Date

2015

Peer reviewed|Thesis/dissertation

The roles of microbial selenate reduction and selenium sorption on selenium immobilization in littoral sediment from the hypersaline Salton Sea, California

By

Juan Fernando Villa-Romero

A dissertation submitted partial satisfaction of the

requirements for the degree of

Doctor of Philosophy

in

Microbiology

in the

Graduate Division

of the

University of California, Berkeley

Committee in charge:

Professor Céline E. Pallud, Chair
Professor Mary K. Firestone
Professor Norman Terry

Fall 2015

Abstract

The roles of microbial selenate reduction and selenium sorption on selenium immobilization
in littoral sediment from the hypersaline Salton Sea, California

by

Juan Fernando Villa-Romero

Doctor of Philosophy in Microbiology

University of California, Berkeley

Professor Céline Pallud, Chair

The Salton Sea in California was formed between 1905-1907 by an accident that diverted Colorado River water to the Salton Sea Basin of the Colorado desert. Since 1924 the Salton Sea serves as an agricultural drainage reservoir maintained by agricultural and municipal wastewater inputs from the Coachella and Imperial Valleys in California and the Mexicali Valley in Mexico. Today, the Salton Sea is California's largest lake by area (975 km^2) and constitutes a vital habitat for more than a million birds belonging to more than 400 species, including migratory and endangered populations. The Salton Sea, however, has been called an "ecological time bomb" given the threat that the convergence of selenium accumulation, chemical pollution, water diversion and climate change poses to this unique environment.

Selenium (Se) is considered an "essential toxin" due to its role as both an essential nutrient and an environmental contaminant. Selenium contamination is a concern in important areas of the United States, Canada, Mexico, Egypt and Israel where mining, agriculture and the extraction and refinement of fossil fuels and metals lead to selenium release from seleniferous parent rock material and selenium bioaccumulation in wildlife.

In aquatic ecosystems, selenium bioaccumulation is preceded by the accumulation of selenium in sediment which is driven by sorption and microbial activity, more specifically, the assimilatory and dissimilatory reduction of water-soluble selenium oxyanions. For the Salton Sea it remains unclear whether the sorptive and reductive capacity of sediments will suffice to prevent dissolved selenium concentrations in water from increasing in the future.

In order to characterize the transfer of selenium from water to underlying sediments in the Salton Sea, in this dissertation I describe the spatial variability in sediment parameters controlling selenate reduction rates across seven geographical locations and four depth intervals. I identify organic carbon content in sediment as an important driver of selenium accumulation in Salton Sea littoral sediment due to its dual nature as a sorbant for selenium oxyanions and as a source of reducing power

1

for sediment microbial communities capable of selenate reduction. In the the first chapter, I quantify organic carbon content, selenate reducer abundance, selenium content and potential selenate reduction rates using sediment slurries in sediment collected from seven Salton Sea littoral locations. I show a broad diversity of sediment characteristics and the effect of sediment organic carbon content on selenate reduction potential.

In the second chapter, I show a range of K_m and R_{max} values for selenate and selenate reduction, respectively, comparable to that obtained in sediment collected from eleven geographical locations in the states of California and Nevada. K_m values for selenate in evaluated sediment are well above ambient selenate concentrations and therefore microbial communities capable of selenate reduction operate well below their selenate reduction potential. I also show unexpectedly high selenate sorption which, under present conditions, contributes more than microbial activity to selenium retention in sediment.

In the third chapter, I use sediment slurries and a microbial consortium recovered from Salton Sea littoral sediment to suggest that nitrate reducers play an important role in selenium accumulation in the Salton Sea. I discuss this data in the context of our current knowledge regarding the microbial pathways of selenate reduction and the thermodynamic constraints associated with selenate respiration and microbial biomass synthesis.

Dedication

A Vicente, Teresa, Alfonso, Marieta, Jorge, Silvia, William, Jo Ann, Karina, Verónica, Mike, Katherine, Mariana, Manuel, Louis, Iván, Damián, Nina y el resto de mi familia y amigos. Porque la muerte es olvido y ahora somos inmortales.

"La gente que dice que algo es imposible no debe interrumpir el trabajo de aquellos que hacen lo imposible realidad"

George Bernard Shaw

Table of contents

Chapter 1 — Selenate reduction and adsorption in littoral sediments from a hypersaline California lake, the Salton Sea..1

Introduction

The Salton Sea is located in the Colorado desert area of Southeast California, approximately 80 km Southeast of Palm Springs, and is the state's largest lake by area (975 km^2) (Reese et al., 2008). The lake is a shallow (8 m mean depth), eutrophic and moderately hypersaline body of water (current salinity 48 g L^{-1} total dissolved solids) (VillaRomero et al., 2013) with no outlets and a surface elevation of 69.5 m below sea level (Schroeder et al., 2002; Reese & Anderson, 2009; VillaRomero et al., 2013). The Salton Sea was formed between 1905-1907 by an accident that diverted Colorado River water to the Salton Sea Basin, and was legally designated as an agricultural drainage reservoir by the US government in 1924 (Reese et al., 2008). Today, the Salton Sea is maintained by agricultural drainage and municipal wastewater inputs from the Alamo, New and Whitewater Rivers (Reese et al., 2008), the former two accounting for approximately 80% of the lake's total annual inflow (Schroeder et al., 2002). As wetlands in California have decreased by 90% in the last 150 years, the Salton Sea is currently a major habitat for migratory waterfowl using the Pacific Flyway (Kausch & Pallud, 2013; VillaRomero et al., 2013). More than a million individual birds from 400 species use the Salton Sea area annually, including migratory and endangered populations (Hurlbert et al., 2007; Moreau et al., 2007). The Salton Sea is the most important body of water in California's 303(d) list of impaired water bodies (US Environmental Protection Agency, 2012). The lake is eutrophic to hypereutrophic characterized by high nutrient concentrations, high biological productivity (Robertson et al., 2008), and ongoing contamination of organochlorine compounds in sediments and fish species (Sapozhnikova et al., 2004). The lake is expected to shrink due to water diversion and climate change. Selenium is particularly toxic and poses a substantial long-term risk to waterfowl (Lemly, 2002). In Salton Sea littoral sediment, selenium accumulation represents a threat to important waterfowl populations that rely on vital resources the Salton Sea habitat provides. The black-necked stilt (*Himantopus mexicanus*) population is of special concern, with 4.5-7.6% of its eggs potentially impaired by selenium in 1993 and 2004.

Selenium (Se) is a chalcogen described as an "essential toxin" due to its role as both an essential nutrient and an environmental contaminant (Lenz & Lens, 2009; Nancharaiah & Lens, 2015). Selenium has the narrowest concentration range between deficiency and toxicity of all essential elements in animals (Chapman et al., 2010). In humans, for example, selenium is required at a 0.8 µg kg^{-1} concentration, but becomes toxic when ingested beyond 5 µg kg^{-1} (Navarro et al., 2015). Selenium is one of the most common toxic trace elements in environments impacted by mining, agriculture and the extraction and refinement of fossil fuels and metals (Gladyshev et al., 2012; Winkel et al., 2012; Nancharaiah & Lens, 2015; Navarro et al., 2015). Selenium can be uptaken by plankton and algae and can substitute for sulfur in stagnant marine sedimentary deposits when biological detritus derived from these organisms reaches the sediment surface (Presser, 1994). Therefore, selenium is a common trace element in shales rich in organic matter, minerals, including pyrite, and alkaline soils in the Western US (Presser et al., 1994; Stolz & Oremland, 1999; Nancharaiah & Lens, 2015).

Selenium naturally occurs in four oxidation states: -II, 0, IV, and VI, each displaying unique mobility and environmental behavior (Nancharaiah & Lens, 2015). In oxic environments, water-soluble selenium oxyanions predominate with more than 90% of selenium present as selenate (Se(VI), SeO$_4^{2-}$) and less than 10% as selenite (Se(IV), HSeO$_3^-$, SeO$_3^{2-}$) (Martin et al., 2011), the latter one being considered immobile since it is sorbing strongly to clay minerals and organic matter (Saha & Huang, 2010; Amrhein & Doner, 2014). The most reduced form of selenium (-II) occurs in soluble organo-selenides (selenomethionine, e.g.), solid metal-selenides (FeSe, e.g.), or gaseous methylated forms (dimethylselenide, e.g.) (Hamilton, 2004; Nancharaiah & Lens, 2015). Selenate, selenite and organic

selenides are toxic and known to bioaccumulate (Lemly, 2014) while elemental selenium is solid, insoluble, virtually immobile and biologically inert (Gladyshev et al., 2012; Nancharaiah & Lens, 2015).

The geochemical cycle of selenium in sediment is driven by microbes via reduction, oxidation, methylation and demethylation reactions (Stolz et al., 2006; Nancharaiah & Lens, 2015). In anoxic sediment, microbes couple the oxidation of organic carbon to the reduction of selenium oxyanions through a variety of pathways, including assimilatory reduction that incorporates selenium into aminoacids (Gladyshev et al., 2012) and dissimilatory reduction that couples growth to the reduction of selenate to selenite and of selenite to elemental selenium (Stolz et al., 2002, 2006). Selenite, elemental selenium and selenides can be incorporated into particulate matter through adsorption and copreciptation, with elemental selenium often being the dominant species in estuarine and freshwater sediment (Turner, 2013). The resulting selenium species become available to microorganisms, animals and plants that can bioaccumulate selenium to concentrations 1-3 orders of magnitude higher than those present in water (Turner, 2013; US Environmental Protection Agency, 2015). Selenium is particularly toxic and poses a substantial long-term risk to waterfowl (Lemly, 2002). In Salton Sea littoral sediment, selenium accumulation represents a threat to important waterfowl populations that rely on vital resources the Salton Sea habitat provides. The black-necked stilt (*Himantopus mexicanus*) population is of special concern, with 4.5-7.6% of its eggs potentially impaired by selenium in 1993 and 2004. The US national water quality criterion for the protection of aquatic wildlife 3.1 µg L^{-1} for selenium (US Environmental Protection Agency, 2015) but is currently being reviewed to account for the risk associated with dietary exposure (US Environmental Protection Agency, 2015).

Only minor loss of selenium through volatilization occurs in the Salton Sea (Schroeder et al., 2002) and virtually all of the selenium mobilized to the Salton Sea since its formation in 1905-1907 remain sequestered in sediments. Salton Sea sediments are considered major selenium sinks for selenium mobilized from marine pyritic shales that outcrop in the Green, San Juan and Gunnison River watersheds of the Colorado River Basin (Schroeder & Rivera, 1993; Schroeder et al., 2002; Seiler, 2003). Irrigation of this area dissolves and mobilizes selenium salts, leading to high selenium concentrations that often exceed regulatory selenium limits in subsurface drainage water (up to 300 µg L^{-1}) and in the Alamo, New and Whitewater Rivers (2.4-8 µg Se L^{-1}) (Schroeder & Rivera, 1993; Holdren & Montaño, 2002; Schroeder et al., 2002). Salton Sea sediments showed a high selenium content that ranged between 0.6 and 15 µg g^{-1}, about 30 times larger than that in surrounding soil (Schroeder & Rivera, 1993; Schroeder & Orem, 2000; Schroeder et al. 2002; Vogl & Henry, 2002; Byron & Ohlendorf, 2007).

The monetary benefits of preserving the Salton Sea are under debate (Schwabe et al., 2008) but selenium toxicity in this key stopover for migrating birds could jeopardize the survival of entire species, including the endangered desert pupfish (*Cyprinodon macularius*) (Saiki et al., 2011). The Salton Sea is also one of the most important bird habitats in the American Southwest and supports hundreds of thousands of waterfowl including resident and migratory waterfowl using the Pacific Flyway and endangered species including the brown pelican (*Pelecanus occidentalis* L.). Similar to the events that led to selenium accumulation and widespread deformities in waterfowl at the Kesterson Reservoir (California) in 1983, the Salton Sea today receives seleniferous agricultural wastewater from more than 2263 km of drains serving nearly 2023 km^2 of agricultural land in the Imperial Valley of California (Saiki et al., 2011; Kausch & Pallud, 2013). Selenium in organic matter, invertebrates and

fish pose exposure risks to fish, wildlife and humans in the Grand Canyon of the Colorado River and wetlands of the Great Salt Lake, in Colorado and Utah, respectively (Ackerman et al., 2015; Walters et al., 2015).

It remains unclear whether the sorptive and reductive capacity of Salton Sea sediments will suffice to prevent dissolved selenium concentrations from increasing in the future. Furthermore, selenium contamination in water, sediment and biota around the world is expected to increase due to increasing demand for energy covered by fossil fuel mining (Lenz & Lens, 2009; Chapman et al., 2010) and the irrigation of agricultural seleniferous land (Presser et al., 1994; Chapman et al., 2010; Lemly, 2014). In addition, the threat that selenium poses globally to agriculture and human health is only expected to increase due to the effect of climate change (El-Ramady et al., 2014).

Predicting the likely distribution of selenium across sediment depth requires data regarding the rates of selenate reduction in sediment and the half-saturation constants that describe the affinity of sediment towards selenate. While reaction rate constants for biogeochemical reactions obtained from laboratory experiments may be directly applied to natural environments, half-saturation constants are best-determined using samples retrieved from the environment of interest (Jin et al., 2013). In order to better understand and quantify selenium cycling and selenium transfer between water and underlying sediments in the Salton Sea, I focused on littoral sediments since these will be the locations most affected by a decrease in the size of the lake. I characterized the spatial variability in reaction rates and their relationships with sediment characteristics. Kinetic parameters R_{max} and K_m describe the relationship between substrate concentration and the rate of an enzyme-catalyzed reaction with R_{max} being the maximal rate of reaction when the enzyme is saturated with substrate, and K_m representing the affinity of the enzyme towards the substrate, calculated as the substrate concentration at which the rate of reaction is equal to half R_{max}. The overall objective of this dissertation is to identify the sediment parameters that lead to selenium accumulation in the Salton Sea littoral and to quantify kinetic parameters K_m and R_{max} for selenate reduction using sediment samples that preserve the sediment tridimensional architecture and distribution of resident microbes. To accomplish this, I used slurries containing sediment collected from seven littoral sites to quantify maximum potential selenate reduction rates and flow-through reactor (FTR) experiments containing intact sediment slices from North and South locations to identify the sediment characteristics that control selenium retention, and the centimeter-scale vertical distribution of R_{max} values for selenate and selenate half-saturation constants, K_m, in sediment collected across a vertical depth gradient.

In the the first chapter, I will describe the physical, chemical and microbiological characteristics relevant to the selenium cycle in sediment collected from seven littoral locations in the Salton Sea. I showed a broad diversity of sediment environments with different selenate reduction potentials that are affected by the sediment organic carbon content.

In the second chapter, I will describe sediments collected from a 0-8 cm depth gradient at 2 cm interval in two of the littoral locations characterized in Chapter 1. I showed a broad range of sediment characteristics and a diversity of K_m and R_{max} values for selenate and selenate reduction, respectively, comparable to that obtained in a 1990 study focused on sediment collected from eleven geographical locations in California and Nevada. Also, I showed that selenate sorption in sediment can contribute importantly to the well-established accumulation of selenium driven by microbial activity.

The third chapter presents experiments performed with sediment slurries and a microbial

consortium recovered from one of the evaluated littoral sites that suggest nitrate reducers play an important role in selenate reduction. Given the relative scarcity of data pertaining selenate reduction in microbes I review available data regarding the assimilatory and dissimilatory pathways that lead to selenium accumulation in sediment.

References

Ackerman, J., M. Herzog, C. Hartman, J. Isanhart, G. Herring, S. Vaughn, J. Cavitt, C. Eagles-Smith, H. Browers, C. Cline, & J. Vest, 2015. Mercury and selenium contamination in waterbird eggs and risk to avian reproduction at Great Salt Lake, Utah. U.S. Geological Survey, Reston, VA: 178.

Amrhein, C., & H. Doner, 2014. Biogeochemistry of Trace Elements: Reactions in Soils. In Chang, A. C., & D. B. Silva (eds), Salinity and Drainage in San Joaquin Valley, California. Springer Netherlands: 123–146.

Byron, E., & H. Ohlendorf, 2007. Diffusive flux of selenium between lake sediment and overlying water: Assessing restoration alternatives for the Salton Sea. Lake and Reservoir Management 23: 630–636.

Chapman, P., W. Adams, M. Brooks, C. Delos, S. Luoma, W. Maher, H. Ohlendorf, T. Presser, & P. Shaw, 2010. Ecological assessment of selenium in the aquatic environment. 368 pp.

El-Ramady, H., N. Abdalla, T. Alshaal, É. Domokos-Szabolcsy, N. Elhawat, J. Prokisch, A. Sztrik, M. Fári, S. El-Marsafawy, & M. S. Shams, 2014. Selenium in soils under climate change, implication for human health. Environmental Chemistry Letters 13: 1–19.

Gladyshev et al. (ed), 2012. Selenium - Its Molecular Biology and Role in Human Health. Springer Biochemistry and Biophysics.

Hamilton, S., 2004. Review of selenium toxicity in the aquatic food chain. Science of the total environment 326: 1–31.

Holdren, G., & A. Montaño, 2002. Chemical and physical characteristics of the Salton Sea, California. Hydrobiologia 473: 1–21.

Hurlbert, A., T. Anderson, K. Sturm, & S. Hurlbert, 2007. Fish and fish-eating birds at the Salton Sea: a century of boom and bust. Lake and Reservoir Management 23: 469–499.

Jin, Q., E. Roden, & J. Giska, 2013. Geomicrobial Kinetics: Extrapolating Laboratory Studies to Natural Environments. Geomicrobiology Journal 30: 173–185.

Kausch, M., & C. Pallud, 2013. Science, Policy, and Management of Irrigation-Induced Selenium Contamination in California. Journal of Environment Quality 42: 1605.

Lemly, A., 2002. Selenium Assessment in Aquatic Ecosystems: A Guide for Hazard Evaluation and Water Quality Criteria. Springer Science & Business Media.

Lemly, A., 2014. Teratogenic effects and monetary cost of selenium poisoning of fish in Lake Sutton, North Carolina. Ecotoxicology and Environmental Safety 104: 160–167.

Lenz, M., & P. Lens, 2009. The essential toxin: The changing perception of selenium in environmental sciences. Science of the total environment 407: 3620–3633.

Martin, A., S. Simpson, S. Fawcett, C. Wiramanaden, I. Pickering, N. Belzile, Y. Chen, J. London, & D. Wallschläger, 2011. Biogeochemical Mechanisms of Selenium Exchange between Water and Sediments in Two Contrasting Lentic Environments. Environmental Science & Technology 45: 2605–2612.

Moreau, M., J. Surico-Bennett, M. Vicario-Fisher, D. Crane, R. Gerads, R. Gersberg, & S. Hurlbert, 2007. Contaminants in tilapia (*Oreochromis mossambicus*) from the Salton Sea, California, in relation to human health, piscivorous birds and fish meal production. Hydrobiologia 576: 127–165.

Nancharaiah, Y., & P. Lens, 2015. Ecology and Biotechnology of Selenium-Respiring Bacteria. Microbiology and Molecular Biology Reviews 79: 61–80.

Navarro, R., T. Aoyagi, M. Kimura, H. Itoh, Y. Sato, Y. Kikuchi, A. Ogata, & T. Hori, 2015. High-Resolution Dynamics of Microbial Communities during Dissimilatory Selenate Reduction in Anoxic Soil. Environmental Science & Technology 49: 7684–7691.

Presser, T., 1994. "The Kesterson effect." Environmental Management 18: 437–454.

Presser, T., M. Sylvester, & W. Low, 1994. Bioaccumulation of selenium from natural geologic sources in western states and its potential consequences. Environmental Management 18: 423–436.

Reese, B., & M. Anderson, 2009. Dimethyl sulfide production in a saline eutrophic lake, Salton Sea, California. Limnology and Oceanography 54: 250–261.

Reese, B., M. Anderson, & C. Amrhein, 2008. Hydrogen sulfide production and volatilization in a polymictic eutrophic saline lake, Salton Sea, California. Science of the total environment 406: 205–218.

Robertson, D., S. Schladow, & G. Holdren, 2008. Long-term changes in the phosphorus loading to and trophic state of the Salton Sea, California. Hydrobiologia 604: 21–36.

Saha, U., & P. Huang, 2010. Surface coverage effects on the desorption kinetics of selenite from a hydroxyaluminum–montmorillonite complex. Journal of colloid and interface science 350: 320–329.

Saiki, M., B. Martin, & T. May, 2011. Selenium in aquatic biota inhabiting agricultural drains in the Salton Sea Basin, California. Environmental Monitoring and Assessment 184: 5623–5640.

Sapozhnikova, Y., O. Bawardi, & D. Schlenk, 2004. Pesticides and PCBs in sediments and fish from the Salton Sea, California, USA. Chemosphere 55: 797–809.

Schroeder, R., W. Orem, & Y. Kharaka, 2002. Chemical evolution of the Salton Sea, California: nutrient and selenium dynamics. In Barnum, D. A., J. F. Elder, D. Stephens, & M. Friend (eds), The Salton Sea. Springer Netherlands: 23–45.

Schroeder, R. & W. Orem, 2000. Nutrient Dynamics in the Salton Basin--implications from Calcium, Uranium, Molybdenum, and Selenium. U.S. Geological Survey.

Schroeder, R., & M. Rivera, 1993. Physical, chemical, and biological data for detailed study of irrigation drainage in the Salton Sea area, California, 1988-90. U.S. Department of the Interior, U.S. Geological Survey.

Schwabe, K., P. Schuhmann, K. Baerenklau & N. Nergis, 2008. Fundamentals of estimating the net benefits of ecosystem preservation: The case of the Salton Sea. Hydrobiologia 604: 181–195

Seiler, R., 2003. Irrigation-induced contamination of water, sediment, and biota in the western United States-synthesis of data from the National Irrigation Water Quality Program. U.S. Department of the Interior, U.S. Geological Survey.

Stolz, J., P. Basu, & R. Oremland, 2002. Microbial transformation of elements: the case of arsenic and selenium. International Microbiology 5: 201–207.

Stolz, J., P. Basu, J. Santini, & R. Oremland, 2006. Arsenic and Selenium in Microbial Metabolism. Annual Review of Microbiology 60: 107–130.

Stolz, J., & R. Oremland, 1999. Bacterial respiration of arsenic and selenium. FEMS Microbiology Reviews 23: 615–627.

Turner, A., 2013. Selenium in sediments and biota from estuaries of southwest England. Marine Pollution Bulletin 73: 192–198.

VillaRomero, J., M. Kausch, & C. Pallud, 2013. Selenate reduction and adsorption in littoral sediments from a hypersaline California lake, the Salton Sea. Hydrobiologia 709: 129–142.

Vogl, R., & R. Henry, 2002. Characteristics and contaminants of the Salton Sea sediments. Hydrobiologia 473: 47–54.

Walters, D., E. Rosi-Marshall, T. Kennedy, W. Cross, & C. Baxter, 2015. Mercury and selenium accumulation in the Colorado River food web, Grand Canyon, USA. Environmental toxicology and chemistry 34: 2385–2394.

Acknowledgements

JUAN F. VILLAROMERO, PhD

SUMMARY OF QUALIFICATIONS

Academic: PhD, Microbiology, Plant and Microbial Biology Department, University of California, Berkeley, CA
BSc, Environmental Sciences, University of Idaho, Moscow, ID

Areas of expertise: Microbial ecology, metabolism, and evolution; biogeochemistry; fermentation; bioremediation; microbial fuel synthesis and oil recovery; synthetic biology; synthetic ecology; biodiversity conservation; US CFR (21, 820: Quality System Regulation), ISO 17025-2005, Access & Benefit Sharing (ABS) regulations

---

PROFESSIONAL EXPERIENCE

University of California, Berkeley   **Berkeley, CA**

EPA-STAR Fellow 2011, Laboratory of Soil Biogeophysics and Biogeochemistry, **Principal**   *8/2009 – 12/2015*
Investigator: *Dr. Céline Pallud*
- Identified the environmental parameters that control selenium retention in littoral sediments from California's largest lake, the hypersaline Salton Sea
- Refined multidisciplinary protocols to quantify selenate reduction rate kinetics and selenate reducer abundance in flow-through reactors
- Recovered, domesticated and characterised halophilic microbes capable of removing high selenium concentrations from hypersaline agricultural wastewater
- Graduate-level courses: environmental chemistry; microbial genetics, microbial metabolism, microbial ecology and microbial evolution

Graduate Student Instructor   *4/2010 – 5/2015*
- Microbial genetics and genomics; Introductory biology; Environmental issues

Graduate Student Projects   *8/2008 – 8/2009*
- Characterization of solvent tolerance, carbon utilization kinetics and growth requirements for *Geobacillus thermoglucosidasius* in bench-scale fermenters. **Principal Investigator:** Dr. Douglas Clark, Department of Chemical Engineering
- Heterologous expression of thermostable galactosidases from *Sulfolobus* in *E. coli*. **Principal Investigator:** Dr. Jay Keasling, Department of Chemical and Biomolecular Engineering
- DNA microarrays in compost microbiology and microbial diversity applied to *Agrobacterium tumefaciens* suppression in walnut crops. **Principal Investigator:** Dr. Norman Terry, Department of Plant and Microbial Biology
- Method development for recalcitrant fungal DNA extraction and qPCR detection of microbial laccases in rainforest soil. **Principal Investigator:** Dr. Mary Firestone, Department of Plant and Microbial Biology

General Automation Lab Technologies (GALT) Inc.   **San Francisco, CA**
Scientist   *5/2015 – 8/2015*
- Optimised diffusion chambers and culturomic approaches to maximise the recovery of environmental microbes using high-density cultivation
- Optimised protocols for high-throughput domestication and screening of low-abundance water, soil and human gut microbes
- Developed protocols and statistical analyses to evaluate novel antimicrobial production
- Implemented sample-to-data pipelines to quantify and interpret microbial diversity
- Researched architecture and operation protocols for commercially available platforms for high-throughput microbial analysis

Spanish Speaking Citizen Foundation   **Oakland, CA**

Consultant for Science Education   *5/2007 – 8/2008*

- Developed a bilingual science curriculum for Lazear School After School Program
- Implemented online education resources for parents and students still lauded as one the most innovative in the district

Cel Analytical Inc.   **San Francisco, CA**

Laboratory Manager   *8/2006 – 1/2007*

- Performed chemical, microbiological and molecular biology analysis of air, water, soil and sludge samples following EPA and CDPH methods
- Implemented Sample-based Laboratory Information Management Systems (SLIMS)
- Documented sampling, client interactions, laboratory supply chains, equipment maintenance, and protocol updates

University of Idaho, Moscow   **Moscow, ID**

Research Assistant   *8/2004 – 8/2006*

- Investigated the role of earthworms in soil aggregate formation and carbon-nitrogen cycling in rural and urban soils
- Assisted the validation of *Brassica*-derived soil amendments for carrot and strawberry
- Part of the team that rediscovered the Palousse earthworm *Driloleirus americanus*

CRITICAL LEADERSHIP INITIATIVES

Government of Ecuador

- *Instituto Ecuatoriano de Energías Renovables (INER), Ecuador – All Power Labs (APL), Berkeley, CA.* A collaboration to optimize gasification protocols for power generation using agricultural waste   *2015*
- *Universidad Amazónica IKIAM, Ecuador – Harvard University, Cambridge, MA.* Investigator of the "Arca de las Bacterias" project, a joint exploration of microbial diversity to develop applications for environmental quality and bioenergy   *2015*
- *Embassy of Ecuador, Washington DC – University of California, Berkeley, CA.* A collaboration to implement sustainable models of scientific and commercial production based on biotechnology development in Ecuador and US institutions   *2014*
- *Instituto de Altos Estudios Nacionales (IAEN), Ecuador.* Led an international team reviewing the legal frameworks that regulate access and development of traditional knowledge and biological resources   *2013*

alGAS Biotechnologies Inc.

- Led company to a $17,000 prize for DNA synthesis   *2015*
- Led research and development activities aimed at optimizing the electrical properties of treated algae biomass for the manufacture of biodegradable batteries   *2014*

Latin American Science

- Covered Latin American teams participating in the international Genetically Engineered Machines (iGEM) 2013 competition

EDUCATION

University of California, Berkeley, Plant and Microbial Biology Department   **Berkeley, CA**
PhD, Microbiology   *2008 – 2015*
University of Idaho, Moscow   **Moscow, ID**
BSc, Environmental Sciences   *2004 – 2006*
Pontificia Universidad Católica del Ecuador   **Quito, Ecuador**
Biology   *1999 – 2004*

PUBLICATIONS & PRESENTATIONS

Golinelli, S., K. Vega-Villa, K. & **J. VillaRomero**. **2015**. "Biodiversidad: Ciencia ciudadana, saberes ancestrales y biodiversidad aplicada en la economía social del conocimiento". Buen Conocer – Free Libre Open Knowledge Society: Modelos sostenibles y políticas públicas para una economía social del conocimiento común y abierto en el Ecuador. Vila-Viñas, D. & Barandiaran, X. (eds.). Quito, Ecuador: IAEN-CIESPAL

VillaRomero J., K. Schilling, C. Pallud, **2014**. "Surficial Littoral Sediments of Hypersaline Lake, the Salton Sea, a Sink for Selenium Mobilized from the Colorado River Delta" 24th V.M. Goldschmidt 2014 Conference, Sacramento, CA, United States

VillaRomero J., M. Kausch & C. Pallud, **2013**. Selenate reduction and adsorption in littoral sediments from an hypersaline California lake, the Salton Sea. Hydrobiologia 709, 129-142

VillaRomero J., C. Pallud, **2012**. "Selenate reduction rates in littoral sediments of a hypersaline lake, the Salton Sea, CA". 22nd V.M. Goldschmidt 2012 Conference, Montréal, Canada

TRAINING

▪ Computational Genomics Resource Laboratory, "Unix, Perl, Mothur and QIIME for Sequence Data Analysis", University of California, Berkeley, CA	*2015*
▪ Biocurious, "Liquid handling, microfluidics and optics of the Illumina HiSeq platform", Mountain View, CA	*2015*
▪ SynBERC Communications Workshop, "Engaging general audiences about the impacts of engineering biology", M.I.T., Boston, MA	*2014*
▪ Institute for Data Science, "Software Carpentry Bootcamp: Program design, version control and task automation", University of California, Berkeley, Berkeley, CA	*2014*
▪ Institute for Data Science, "Programming and statistical work in R, Python", University of California, Berkeley, CA	*2014*
▪ Joint Genome Institute User Meeting, 2012: Integrated Microbial Genome and Metagenome (IMG-M) database, Walnut Creek, CA	*2012*

AWARDS & RECOGNITIONS

▪ University of California, Berkeley, CITRIS Foundry Applied Tech Incubator	*2015*
▪ Synbiobeta, San Francisco, Blue Sky Competition	*2015*
▪ Embassy of Ecuador, United States of America, Startup Ecuador Competition	*2014*
▪ SynBERC Leadership Excellence Accelerator Program	*2014*
▪ Goldschmidt International Conference 2014 Travel Grant; CAN$450	*2014*
▪ M.I.T. Knight Science Journalism Tracker Recognition	*2013*
▪ University of California, Berkeley, Plant and Microbial Biology Department Travel Grant; US$500	*2012*
▪ Goldschmidt International Conference 2012 Travel Grant; CAN$450	*2012*
▪ U.S. Environmental Protection Agency STAR Fellowship Grant #91727201-0; US$125,000	*2011*
▪ Environmental Science Program Scholarship, University of Idaho, Moscow; US$8,000	*2005*
▪ International Program Office Scholarship, University of Idaho, Moscow; US$1,500	*2004*

Chapter 1 — Selenate reduction and adsorption in littoral sediments from a hypersaline California lake, the Salton Sea

Juan Fernando Villa-Romero[1], Céline Pallud[1,2]
[1] Department of Plant and Microbial Biology, University of California, Berkeley
[2] Department of Environmental Science, Policy and Management, University of California, Berkeley

Abstract

The Salton Sea, a hypersaline lake located in Southern California, is a major habitat for migratory waterfowl, including endangered species, whose survival could be jeopardized by selenium toxicity. Selenium is an essential micronutrient and a contaminant whose speciation and cycling are driven by microbial activity. In the absence of oxygen, microorganisms can couple the oxidation of organic matter with the reduction of soluble selenate and selenite to elemental selenium. In order to better understand and quantify selenium cycling in the Salton Sea and selenium transfer between water and underlying sediments, we measured maximum potential selenate reduction rates and selenate adsorption isotherms in sediments collected from seven littoral locations in July 2011, for which we also measured salinity, organic carbon, nitrogen, and elemental selenium content, and abundance of selenate-reducing prokaryotes. Our results showed a high potential for selenate reduction and for selenate adsorption in all studied sites, both affected by sediment C_{org} content, with selenate adsorption potential about an order of magnitude higher than what is reported for soils. We suggest that both selenate adsorption and reduction are driving selenium removal from the lake's water and selenate retention in littoral sediments of the Salton Sea.

1. Introduction

The Salton Sea, located in the Colorado desert area of southeastern California (Fig. 1), is the largest lake in the state (984 km^2). It is a shallow (8 m mean depth), eutrophic and moderately hypersaline (current salinity 48 g L^{-1} total dissolved solids) lake with no outlets (Schroeder et al., 2002; Cohen, 2008; Reese & Anderson, 2009). The Salton Sea was legally designated as an agricultural drainage reservoir by the federal government in 1924 (Reese et al., 2008) and is maintained by runoff from agricultural irrigation through the Alamo, New and Whitewater Rivers (Fig. 1), the former two accounting for approximately 80% of the lake's total annual inflow (Schroeder et al., 2002).

The Salton Sea area has become a major habitat for migratory waterfowl on the Pacific Flyway, as wetlands in California have decreased by 90% in the last 150 years (Setmire & Schroeder, 1998). More than a million individual birds and 400 species use the Salton Sea area annually, including several endangered species (Setmire & Schroeder, 1998; Cohen & Huyn, 2006). Lately, however, increased salinity and selenium (Se) concentrations, together with accelerated eutrophication, have been implicated in the periodic deaths of over 200,000 migratory water birds and millions of tilapia (Kaiser, 1999; Schroeder & Orem, 2000; Jehl, 2002; Marti-Cardona et al., 2008), resulting in the listing of the Salton Sea in the California Clean Water Act section 303(d) list of impaired waters (US-EPA, 2010). In the Salton Sea, selenium concentrations recorded in fish tissues are elevated enough to negatively affect fish health and reproduction as well as the immune systems of piscivorous birds (Moreau et al., 2007). The black-necked stilt (*Himantopus mexicanus*) population is of special concern, with 4.5-7.6% of its eggs having been estimated to be impaired by selenium both in 1993 and 2004. This phenomenon is expected to be exacerbated in the near future since the Salton Sea is predicted to shrink due to water diversion and the arid climate of the region (US-DOI, 2007), and since water salinity, as well as salts and selenium concentrations are expected to increase dramatically (Cohen &

Huyn, 2006).

Selenium has been described as an "essential toxin" (Lenz & Lens, 2009) due to its role as both an essential nutrient and an environmental contaminant. Of all essential elements for animals, selenium has the narrowest concentration range between deficiency and toxicity (Chapman, 1999). In aquatic habitats, selenium is particularly toxic and poses a substantial long-term risk (Lemly, 2004) mainly because it bioaccumulates within the base of food chains and biomagnifies within trophic webs (Cherry & Guthrie, 1977; Furr et al., 1979). Selenium occurs in four oxidation states: -II, 0, IV and VI, each displaying unique mobility and environmental behavior. Predominant forms of selenium in aerobic environments are the oxyanions selenate (SeO_4^{2-}) and selenite (SeO_3^{2-}) (Haudin et al., 2007). Both anions have been shown to adsorb to the surface of synthetic and natural Al-, Fe- and Mn-oxy-hydroxides (Balistrieri & Chao, 1990; Su & Suarez, 2000; Saha et al., 2005; Catalano et al., 2006; Martínez et al., 2006; Rovira et al., 2008; Mandal et al., 2009) and clays (Balistrieri & Chao, 1987; Bar-Yosef & Meek, 1987; Duc et al., 2003); however, compared to selenate, selenite adsorbs more strongly (Neal & Sposito, 1989; Hyun et al., 2006) and is thus less mobile. Elemental selenium (Se^0) is the predominant selenium form under reducing and weakly acid to alkaline conditions (Stolz & Oremland, 1999; Masscheleyn et al., 1991). The speciation and cycling of selenium are driven by microbial activity *via* reduction, oxidation, methylation and demethylation reactions (Sager, 2002). In the absence of oxygen, microorganisms can couple the oxidation of organic matter with the reduction of selenate and selenite to elemental selenium (Stolz & Oremland, 1999), which is insoluble in water and poorly mobile (Masscheleyn et al., 1991). End products of selenium reduction may also include volatile gases such as hydrogen and alkyl selenides (Schroeder et al., 2002) and organic selenides, which occur in the cells or tissues of living organisms (Bowie et al., 1996).

Selenium in the Salton Sea originates from marine pyritic shales that outcrop in the Upper Colorado River Basin. Irrigation of this area resulted in the dissolution and mobilization of selenium, leading to high concentrations in subsurface drainage water (up to 300 µg L^{-1}; 2.1 µM) and in the Alamo, New and Whitewater Rivers (2.4-8 µg Se L^{-1}; 0.02-0.06 µM) (Setmire & Schroeder, 1998; Holdren & Montaño, 2002; Schroeder et al., 2002), often exceeding the national water quality criterion of 5 µg L^{-1} (0.035 µM) for the protection of aquatic life (US-EPA, 1987). Despite the elevated selenium concentrations in water delivered to the Salton Sea, dissolved selenium concentrations in its Salton Sea water column are low (0.5-2 µg L^{-1}, 0.003-0.014 µM) (Holdren & Montaño, 2002; Schroeder et al., 2002). In fact, the Salton Sea sediments act as a major sink for selenium, with reported measurements ranging from 1.5 to 15 mg Se kg^{-1} (Setmire & Schroeder, 1998; Schroeder & Orem, 2000; Schroeder et al., 2002; Vogl et al., 2002), which is about 30 times higher than average selenium concentrations in surrounding soils (Schroeder et al., 1993).

Only minor loss of selenium through volatilization occurs in the Salton Sea (Schroeder et al., 2002). The observation that virtually all of the selenium entering the Salton Sea is sequestered within its sediments indicates that reduction to insoluble Se(0) and sorption are important processes driving selenium cycling in the Salton Sea. Anoxic conditions occurring in sediments could promote the reduction of selenium, resulting in its adsorption and/or reduction to insoluble Se(0), and consequently immobilization. This has been shown to occur often at depths of only a few millimeters from the sediment surface at other sites (Tokunaga et al., 1998; Martin et al., 2011).

The monetary benefits of preserving the Salton Sea are under debate (Schwabe et al., 2008). However, selenium toxicity in this key stopover for migrating birds could jeopardize the survival of

2

entire species (Cohen & Hyun, 2006) and it is unclear whether the sorptive and reductive capacity of the sediments will suffice to prevent increasing dissolved concentrations in the future. In order to better understand and quantify selenium cycling in the Salton Sea, and selenium transfer between water and underlying sediments, we measured maximum potential selenate reduction rates and selenate adsorption isotherms in sediments collected from seven littoral locations in July 2011, for which we also measured salinity, organic carbon, nitrogen, and elemental selenium content, and abundance of selenate-reducing prokaryotes. We focused our study on littoral sediments, since these will be the most affected by future changes in the lake. We specifically aimed at characterizing the spatial variability in reaction rates and their relationships with sediment characteristics along the littorals of the Salton Sea. Our results suggest that both adsorption and microbially-mediated selenate reduction are important processes controlling selenate retention in littoral sediments of the Salton Sea.

2. Materials and Methods
2.1. Study sites

Seven sites were investigated around the littoral region of the Salton Sea (Fig. 1). Four sites were located in close proximity to the drainage area of agricultural lands, namely A, B, E and F. Sites A (coordinates: N33.52098°; W116.01469°) and B (N33.52521°; W115.98254°), were located in the North of the lake, close by the Whitewater River head, whereas E (N33.20550°; W115.59513°) and F (N33.15324°; W115.64909°) were located in the South end of the lake, close by the Alamo and New Rivers heads, respectively. It should be noted that site E was actually located in the Alamo River Delta itself. Two sites were located close to major cities, with C (N33.34735°; W115.72967°) being located at Bombay Beach and G (N33.32885°; W115.94119°) at Salton City. Finally, D (N33.33844°; W115.66612°) was located away from both agricultural and urban influences.

2.2. Field sampling and physico-chemical characterization of sediment and overlying water

All sites were sampled in July 2011. Intact sediment core samples (4.2 cm ID × 5 cm L) were collected from the water/sediment interface down to a depth of 5 cm using a hand pushed corer 1-2 m from the shore line at water depths no greater than 0.5 m. Overlying water at each of the sampling sites was collected before disturbing the sediment. All samples were preserved at 4°C in sealed anaerobic bags until experiments or analyses were performed. Dry bulk density (ρ_d) and porosity (ϕ) were determined on five replicate samples for only sites F and G sampled in 2010. Total carbon (C), total organic carbon (C_{org}), and total nitrogen (N) contents, and abundance of selenate-reducing prokaryotes (SeRP) were determined in triplicate sediment samples collected from all of our study sites, with the exception of site C. Dry bulk density (ρ_d) was calculated after drying a known volume of sediment for 48 hours at 105°C. Porosity (ϕ) was calculated from the bulk density (ρ_d) and particle density (ρ_S) estimated at 2.65 g cm^{-3}, the density of quartz) as $1-(\rho_d/\rho_S)$. Total carbon, organic carbon and nitrogen contents were measured in 60 mg of air-dried sediment samples using a NC 2100 Soil Analyzer (CE Instruments, USA). Water pH was measured in the field, as well as water salinity measured *via* conductivity using an OAKTON CON 6/TDS 6 hand-held conductivity/TDS meter (Eutech Instruments, USA). Data will be presented as mean standard errors of replicates.

2.3. Elemental selenium quantification in sediment samples

Elemental selenium was extracted from sediments following a protocol adapted from Kulp & Pratt (2004) and Chen et al. (2006). Air-dried sediment samples (0.5 g) were mixed with 5 mL of 99.99% carbon disulfide (CS_2) and agitated for 8 hours at 21°C. Samples (3 mL) were then filtered using a 0.22 μm MCE filter and placed in a graduated digestion tube. The filtrate was heated to evaporate the CS_2 until dry using a water bath adjusted to 70°C. After the CS_2 evaporated, one glass

bead, 10 mL of 14N HNO_3 and 5 mL of 70% $HClO_4$ were added and this mix was heated to 130°C for 1 hour and gently vortexed every 15 minutes. The mixture was left to cool at 21°C for 1 hour and diluted to 25 mL with water. From this mix, 1 mL and 5 mL of sample were collected in two different graduated digestion tubes. One glass bead, 1 mL of 14N HNO_3 and 1 mL of 70% $HClO_4$ were combined, and the mix was heated to 210°C for 15 minutes. The resulting mix was diluted to 25 mL using 3M HCl and analyzed immediately using ICP-OES. Selenium extraction was performed in duplicate sediment samples.
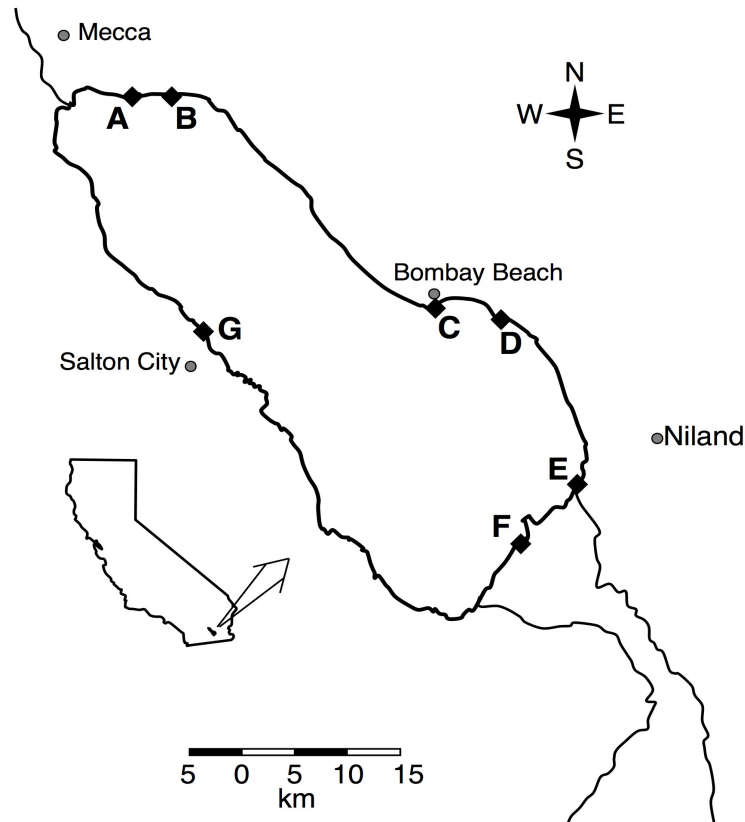
Figure 1. *Map showing the location of the Salton Sea in California and of the seven sites (diamonds) sampled along the littoral of the Salton Sea in July 2011.*

2.4. Enumeration of selenate reducers in sediments

The abundance of selenate-reducing prokaryotes in sediment was estimated using the most probable number (MPN) method (Woomer, 1994) on triplicate sediment samples. Five grams of wet sediment were suspended in 45 mL of sterile saline solution (NaCl, 2%; $MgCl_2$, 0.3%) and shaken thoroughly. Tenfold dilution series (eight replicates) were made directly in sterile culture medium dispensed in 96-well microtiter plates. The composition of the medium (in L^{-1}) was: NaCl, 20 g; $MgCl_2 \cdot 6H_2O$, 3 g; KH_2PO_4, 0.2 g; NH_4Cl, 0.3 g; KCl, 0.3 g; Na_2SO_4, 0.3 g; yeast extract, 0.1 g; Na_2SeO_4, 1.89 g (10 mM); ATCC MD-TMS (trace mineral solution), 10 mL; ATCC MD-VS (vitamin

solution), 10 mL; Na-lactate, 20 mM; and the pH was adjusted to 7.5. The reducing agent in the medium was mercaptoacetic acid, added shortly before dispensing the medium into the wells. Plates were anaerobically incubated at 30°C in the dark for 6 weeks. The presence of selenate-reducing prokaryotes was scored positive upon the formation of elemental selenium that forms a red precipitate.

2.5. Slurry experiments and calculation of selenate reduction rates

Anaerobic slurries (50% w/v) were prepared by mixing 65 g of fresh sediment sample with 65 mL of sterile NaCl simulating the salinity of the Salton Sea (45 g L^{-1}) and containing 0.5 mM selenate (as Na$_2$SeO$_4$). Previous selenate reduction rates measured in brackish to hypersaline sediments showed that selenate reduction activity followed Michaelis-Menten kinetics in relation to selenate concentration, with K$_m$ for selenate ranging from 7.9 to 34 µM (Steinberg & Oremland, 1990). The selenate concentration used here was well above the K$_m$ for selenate, and the reported rates correspond to maximum rates of selenate reduction. Slurries were incubated under gentle orbital shaking to maintain the sediment in suspension for 150 hours at 21°C and were regularly sampled under anaerobic conditions. The samples were immediately centrifuged and the supernatant was filtered through a 0.2 µm pore size MCE syringe filter. Maximum rates of selenate reduction were calculated from the initial linear decreases in selenate concentrations as a function of time. Five replicates per experiment were performed.

2.6. Selenate adsorption isotherms

Selenate adsorption isotherms were obtained in duplicate samples using sieved sediment (<2 mm). Selenate adsorption isotherms were performed by mixing 1 g of air-dried sterile sediment with 10 mL of a sterile solution of NaCl simulating the salinity of the Salton Sea (45 g L^{-1}) amended with concentrations of 0.6, 1.3, 3.2, 6.3, 9.5, 12.7, 31.7, or 63.3 µM of selenate (as Na$_2$SeO$_4$). Sediment suspensions were allowed to equilibrate for 48 hours in the dark on a rotary shaker at 21°C. Supernatants were then collected, filtered through a 0.45 µm MCE syringe filter, acidified with a drop of 6M HCl, and analyzed using inductively coupled plasma optical emission spectrometry (ICP-OES). The amount of selenate sorbed (C$_s$, mg kg^{-1}) was calculated by the difference between aqueous phase initial and equilibrium concentrations (C$_e$, mg L^{-1}). Selenate sorption data were fit with Freundlich sorption model:

$$C_s = K_f \times C_e^{nf} \qquad (1)$$

where K$_f$ is the Freundlich sorption coefficient and nf is a measure of isotherm curvature. The R software (R Development Core Team, 2005) was used to fit the Freundlich adsorption isotherm models on untransformed data and to obtain sorption coefficients (K$_f$ and nf). The non-linear least squares iterative method based on the Gauss-Newton algorithm was used.

2.7. Analytical methods

Concentrations of selenate in slurry filtrates were determined using ion chromatography (IC; Dionex ED40/GP40). Total selenium concentrations in samples collected from adsorption isotherms, elemental selenium extractions, and Salton Sea water samples were measured using a Perkin Elmer 5300 DV Inductively Coupled Plasma-Optical Emission Spectrometer (ICP-OES). Selenium standards were prepared from certified reference stock solutions (VHG Labs) in a matrix with 45 g L^{-1} NaCl, in order to match the composition of samples. Detection limits for IC and ICP-OES in a matrix with 45 g L^{-1} NaCl were 38.0 and 0.6 µM, respectively.

3. Results

3.1. Littoral Salton Sea water and sediment physico-chemical characteristics

Water pH was slightly alkaline (7.5-8.0). Water salinity in six out of the seven study sites averaged 47.5±1.3 g L^{-1}; the exception was site E with a salinity of 3.0 g L^{-1}. Selenium concentrations in water overlying all sampled sites were below the ICP-OES detection limit (0.63 μM). Dry bulk density and porosity were respectively 1.4±0.4 g cm^{-3} and 0.46±0.13 for site F and 1.3±0.1 g cm^{-3} and 0.51±0.04% for site G.

Total sediment N and C_{org} contents were measured in sites A, B, D, E, F and G. Total sediment N content varied by almost one order of magnitude between these sites, with five out of six sites having a N content ranging from 0.04 to 0.10%, whereas site E had a much higher value of 0.32% (Fig. 2 b). Similarly, total sediment C_{org} content varied by more than one order of magnitude between the sites, with four out of six sites ranging between 0.13 and 0.27%, whereas site E had a much higher value of 1.66% and site F had intermediate values of 0.68% (Fig. 2 a). Sites B and D showed the lowest values both for sediment N and C_{org} contents (Fig. 2 a, b). Total C_{org} content was strongly correlated with total N content (Pearson's r=0.98) (Fig. 2 d). Molar C_{org}/N ranged from 3.0 to 8.1 (Fig. 2 c). Sites A, B, D and G all showed values lower than 5.1, whereas site F the highest value and site E showed an intermediate value (Fig. 2 c). Elemental selenium content ranged between 1.7 and 5.9 μg per gram of dry sediment (Fig. 3), with values higher than 3.5 μg g^{-1} for sites A, B and G and lower values for sites C, D, E and F, with especially low concentrations (<2 μg g^{-1}) for site E.

3.2. Abundance of selenate-reducing prokaryotes in sediments

The abundance of selenate-reducing prokaryotes (SeRP) in sediments from a 0-5 cm depth interval was the lowest in site D with (1.4±0.1)×10^3 SeRP cm^{-3} of sediment, and site F with (3.1±0.6)×10^3 SeRP cm^{-3} of sediment (Fig. 4). Sites A, B and C showed similar densities with respectively (4.5±1.7)×10^3, (4.0±0.7)×10^3 and (3.6±1.8)×10^3 SeRP cm^{-3} of sediment. Site G showed a slightly higher density with (6.7±3.0)×10^3 SeRP cm^{-3} of sediment. Site E, however, showed a density of selenate-reducing prokaryotes that was more than an order of magnitude higher with (8.4±0.5)×10^4 cells SeRP cm^{-3} of sediment.

3.3. Sediment selenate reduction rates

Maximum potential selenate reduction rates measured at 45 g L^{-1} NaCl varied by one order of magnitude between all sites and ranged between 29.1±13.3 and 294.9±40.8 nmol SeO$_4^{2-}$ cm^{-3} h^{-1} (Fig. 5). Four sites (A, B, C and G) exhibited selenate reduction rates that were lower than 75.0 nmol SeO$_4^{2-}$ cm^{-3} h^{-1}, whereas the three other sites (D, E and F) showed selenate reduction rates higher than 184 nmol SeO$_4^{2-}$ cm^{-3} h^{-1}, and the highest rate was measured in site E.

3.4. Selenate adsorption isotherms on Salton Sea sediments

Fits of the Freundlich sorption model (Eq. 1) to the sorption experimental data from our seven study sites are shown in Fig. 6 and corresponding sorption parameters are summarized in Table 1. Isotherms were well described by the Freundlich model with all correlation coefficients falling between 0.996 and 0.999. With the exception of site E, which exhibited a larger Freundlich constant (109 mg^{1-nf} kg^{-1} L^{nf}) than the other sites, K_f calculated for Salton Sea littoral sediments were fairly similar among most sites, ranging between 77 (Site A) and 88 (Site B) mg^{1-nf} kg^{-1} L^{nf}. Freundlich nf coefficients usually departed from unity and ranged between 0.87 (Site B) and 1.06 (Site E). The linearity assumption could not be accepted and linear K_d partition coefficients were therefore not calculated. Since nf values varied among sites, K_f units varied consequently, and direct comparisons of K_f values

should be done very carefully.
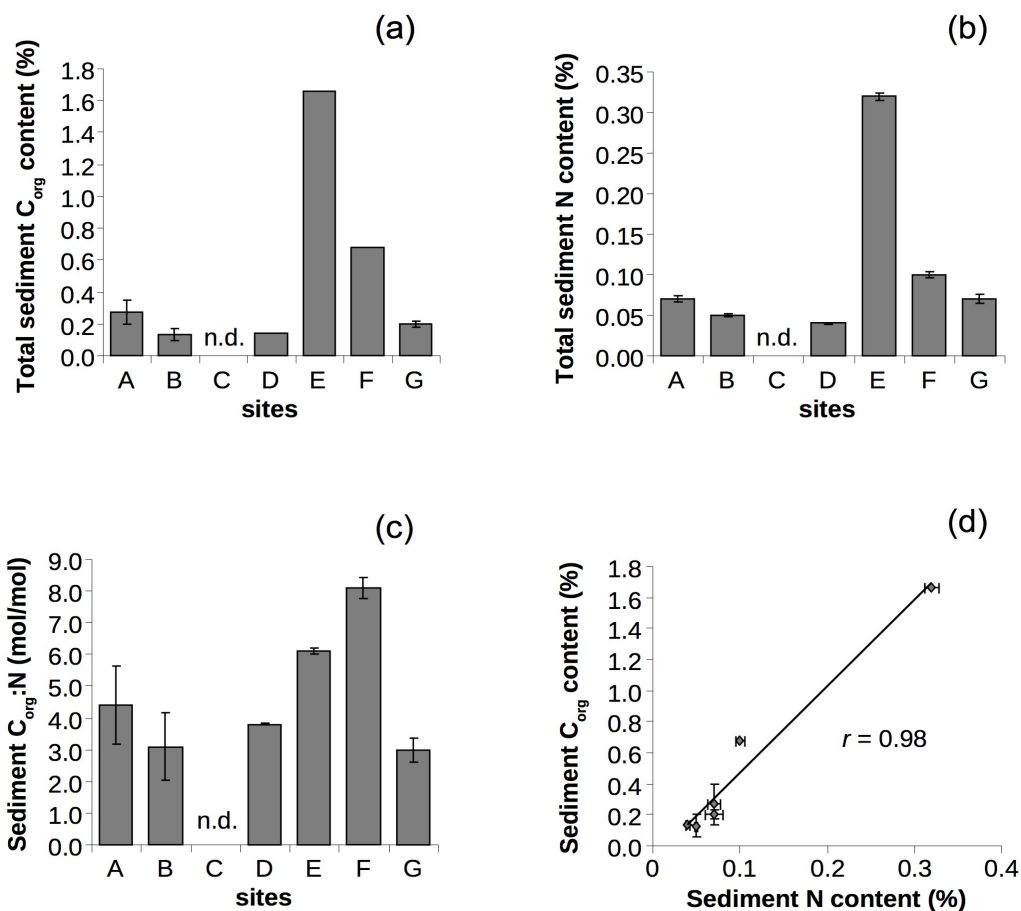
Figure 2. (a) Total organic carbon (C_{org}) content, (b) total nitrogen (N) content, and (c) molar C_{org}/N in sediment samples collected from the 0-5 cm depth interval in six Salton Sea littoral sites in July 2011, and (d) correlation between sediment N and C_{org} content. n.d. means not determined and error bars indicate the standard errors of three replicates.

4. Discussion

We found relatively low N and C_{org} contents in littoral sediments of the Salton Sea, with the highest values being 0.32 and 1.66% for total N and total C_{org}, respectively, both occurring in site E. These values are lower than the averages of 0.43±0.28 and 4.17±3.08% reported by Anderson et al. (2008) for sediment total N and total C_{org} content for 90 sites of the Salton Sea sampled in 2001, including both littoral and deep sediment locations. The same study and previous ones (Arnal, 1961; Schroeder et al., 2002) report lower levels of N, C_{org} and P in sediments near the Salton Sea margins, compared to deeper sediments from the north and south basins of the lake. Our measurements in littoral locations thus fit within the lowest range of total N and C_{org} contents in Salton Sea sediments measured by Anderson et al. (2008), which were 0.06-1.3%, and 0.13-12.5%, respectively. Due to the lack of vegetation around the Salton Sea, the main source of organic matter for the sediments is the phytoplankton (Arnal, 1961; Anderson et al., 2008). The action of currents in the Salton Sea concentrates organic residues in zones of quiet waters with low currents, and consequently little

organic matter accumulates along the coasts of the lake (Arnal, 1961), which explains the low N and C_{org} contents we measured in littoral sediments.
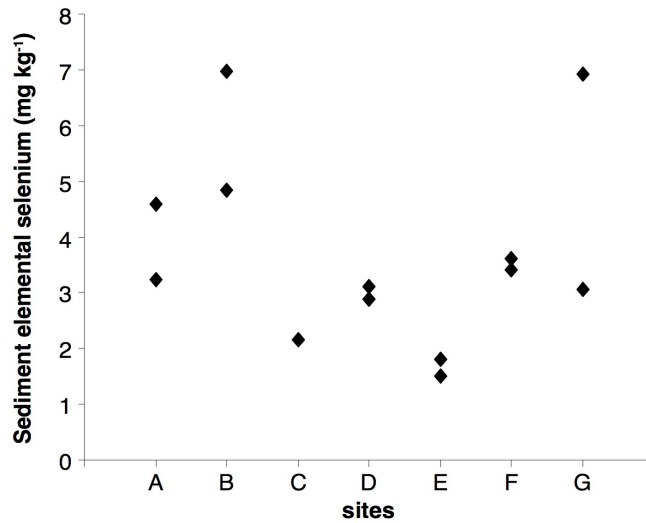
Figure 3. *Concentration of elemental selenium, Se(0), in sediment samples collected from the 0-5 cm depth interval in seven Salton Sea littoral sites in July 2011. Duplicate measurements are indicated.*
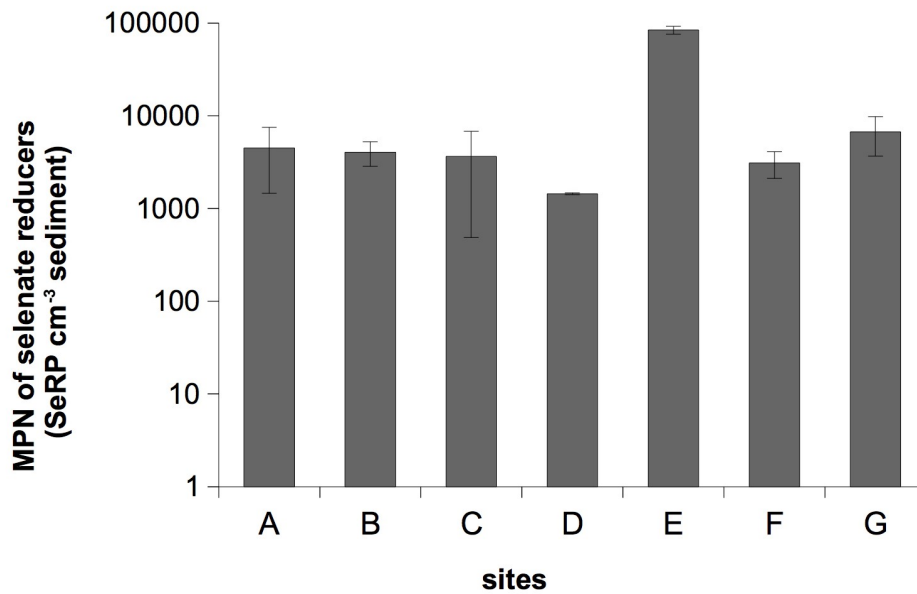
Figure 4. *Most Probably Numbers (MPN) of selenate-reducers (SeRP) in sediment samples collected in July 2011 from the 0–5-cm depth interval in seven Salton Sea littoral sites. Error bars indicate the standard errors of eight replicates.*
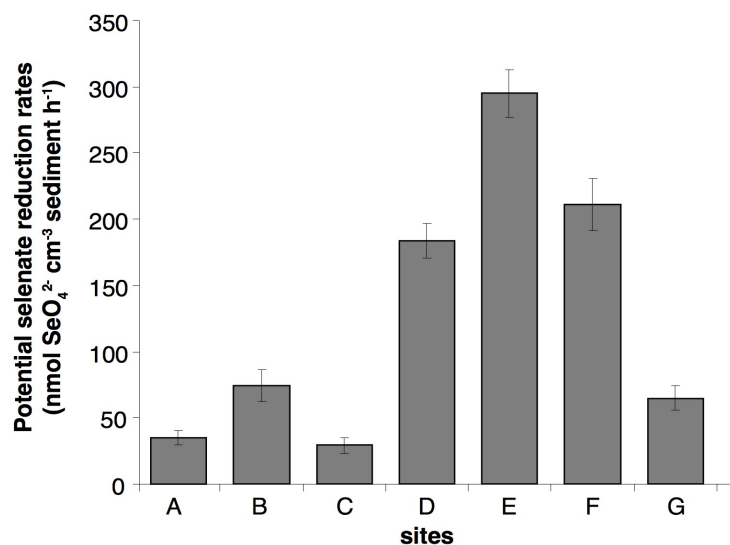
Figure 5. *Maximum potential selenate reduction rates measured in slurry experiments performed at salinity 45 and at 21 C on sediment samples collected in July 2011 from the 0-5 cm depth interval in seven Salton Sea littoral sites. Error bars indicate the standard errors of five replicates.*

The higher N and C_{org} contents observed in site E could be explained by the location of this site in the Alamo River Delta. It has been shown that nutrient concentrations in the Salton Sea tributaries were much higher than those in the lake itself, for example with 30-120 times higher concentrations of total N (Holdren & Montaño, 2002). Whereas the New and Whitewater Rivers also contain wastewater treatment plant effluents, nearly all of the water in the Alamo River originates from agricultural runoff in the Imperial Valley, and consequently, the N in the Alamo River is mostly from chemical fertilizers (Holdren & Montaño, 2002; Schroeder et al, 2002). More specifically, 70% of the total N in the Alamo River exists as oxidized forms (nitrate or nitrite) (Holdren & Montaño, 2002).

With the exception of site F with a C_{org}/N of 8.1, our sites exhibit very low C_{org}/N (Fig. 2 c). In fact, averaged over all our study sites, the molar C_{org}/N for Salton Sea littoral sediments is 4.8±2.0, which is half of the average value reported by Anderson et al. (2008) for the whole Salton Sea basin. It is lower than the range of 5.8-7.9 reported for deep Salton Sea sediments but fits within the range of 1.5-7.2 reported for shallow sediments by Schroeder et al. (2002). This reflects different sources of N for the littoral and deep sediments. As discussed earlier, due to the action of currents in the Salton Sea, organic residues from phytoplankton, with typical C_{org}/N ratio of 6 to 9 (Sampei & Matsumoto, 2001) will mainly accumulate in the deeper parts of the lake. The very low C_{org}/N ratios measured at sites A, B, D and G could reflect a greater relative contribution of ammonium (Schroeder et al., 2002). Littoral sediments receive more N derived from fertilizers than sediments from deeper parts of the lake. In addition, littoral sediments seasonally receive high amounts of organic residues following massive fish die-offs that can reach up to 10,000,000 individuals (Marti-Cardona et al., 2008). Fish die-offs at the Salton Sea typically occur in May to August when the lake is thermally stratified (Marti-Cardona et al., 2008), and poorly decomposed fish carcasses were common in all sampling sites in July 2011. Since most fish species have C_{org}/N that range between 3.8 and 5.7 (Czamanski et al., 2011), this could explain the especially low C_{org}/N observed in all sites.

9
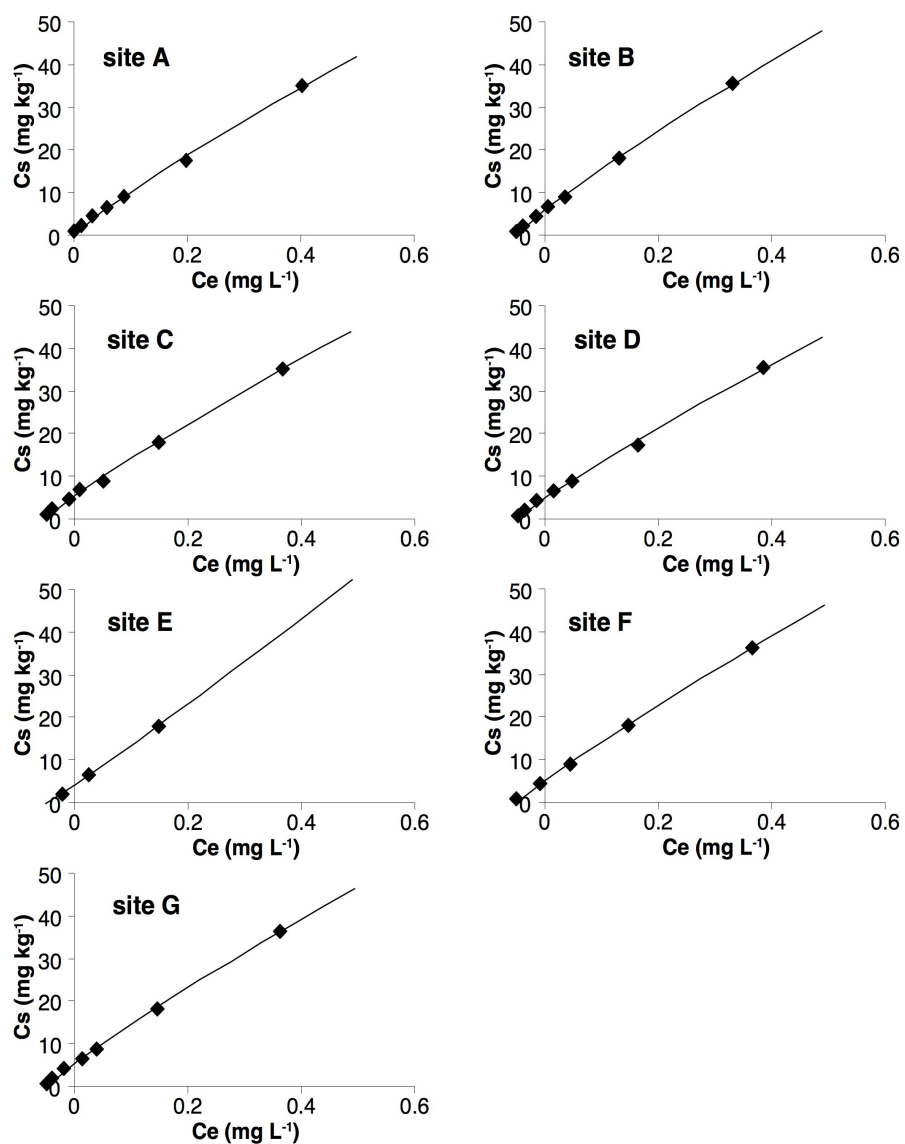
Figure 6. *Measured (symbols) Se(VI) sorption isotherms and corresponding Freundlich sorption model fits (solid lines) for seven Salton Sea littoral sediments.*

Table 1. K_f and nf parameters calculated from isotherm data fitted to the Freundlich model for our seven study sites sampled in July 2011.

sites	R^2	K_f	nf
A	0.9964	77.4	0.88
B	0.9986	87.9	0.87
C	0.9964	82.6	0.90
D	0.9978	80.1	0.90
E	0.9975	109.2	1.06
F	0.9966	87.0	0.92
G	0.9985	84.7	0.89

The concentrations of elemental selenium in littoral sediments of the Salton Sea measured in this study (1.7-5.9 mg kg^{-1}) fit within the lower range of sediment selenium concentrations reported previously (0.58 up to 16 mg kg^{-1}) (Setmire & Schroeder, 1998; Schroeder & Orem, 2000; Schroeder et al., 2002; Vogl et al., 2002). The highest concentrations reported in the literature (>9-15 mg kg^{-1}) correspond to deep sediment locations, which contrast with our focus on littoral sediments. In addition, we found elemental selenium sediment concentrations to be higher in the northern Salton Sea littoral (sites A, B and G) and lower in the southern part of the lake (C, D, E and F), with the lowest value recorded in site E, located in the Alamo River Delta. This heterogeneity in the spatial distribution of selenium in Salton Sea sediments has been observed previously with concentrations that were consistently more elevated over the northern half of the lake (Redlands Institute, 2002; Vogl et al., 2002). The much lower concentrations of 1.5-1.8 mg kg^{-1} recorded in site E are similar to previous measurements of Setmire & Schroeder (1998), who reported selenium concentrations ranging between 0.2 and 2.5 mg kg^{-1} in sediments from the Alamo River Delta. Site E is located in the Alamo River Delta, where selenium concentration in water is about 6.25 µg Se L^{-1} or 0.044 µM (Holdren & Montaño, 2002), present as selenate (60%) and selenite (40%) (Setmire & Schroeder, 1998). The low concentrations of elemental selenium in sediment of site E, located in the Alamo River Delta, could indicate that selenate reduction is incomplete and only proceeds to selenite. It is also possible that selenate reduction proceeds to elemental selenium, but that the concentrations of elemental selenium in surface sediments are diluted due to the sedimentation of suspended particles that have low selenium concentrations. In fact, being located in the River Delta where the flow channel opens into the Salton Sea, site E is in a zone of low flow velocity and consequently high sedimentation rates. Although selenium volatilization is only minor in the Salton Sea (Schroeder et al., 2002), it could contribute to the lower selenium concentration recorded in sediments at site E. In fact selenium volatilization is enhanced at low salinity (Frankenberger et al., 2004), and consequently selenium volatilization could have contribute selenium loss in water at that location. On the other hand, we suggest that at site D, the low concentrations of elemental selenium are due to substrate-limited *in situ* selenate reduction. In fact, this site exhibits extremely low N and C$_{org}$ contents, which results in the lowest abundance of selenate-reducing microorganisms of all studied sites. As a consequence, limited rates of selenate reduction occur *in situ* at this location, which results in limited production of elemental selenium.

Only very limited amount of data reporting selenate reduction rates in natural sediments are available. The rates obtained using slurry experiments are referred to as ''potential'' rates because they correspond to selenate reduction activities when the only terminal electron acceptor being supplied to the bacterial community is selenate. It should be noted that the slurry experiments were designed such that selenate reduction would not be limited by the availability of selenate and consequently the measured rates correspond to "maximum" potential rates of selenate reduction. The experimental data demonstrate a potential for selenate reduction at all study sites. The range of potential selenate reduction rates we obtained is an order of magnitude higher than the range reported by Steinberg & Oremland (1990) for 11 sediments with salinities ranging from freshwater to hypersaline. The difference could partly be due to the inclusion of several sites which did not receive selenium-rich agricultural drainage in the Steinberg & Oremland (1990) study. In addition, the authors used core incubations to obtain their rates, whereas we employed slurry experiments. Sediment slurries involve mixing sediments and water and consequently remove transport limitations on the supply of reactants to the microorganisms, which tends to enhance rates of microbially mediated reactions (Marxsen & Fiebig, 1993; Meile & Tuncay, 2005; Pallud & Van Cappellen, 2006).

The potential for selenate reduction varied widely between sites. The highest potential rate of

selenate reduction was observed at site E, which is exposed *in situ* to the lowest salinity and contains 2.4-13 times more C_{org} and 3-8 times more N than the other sites. At lower salinity and with higher carbon and nitrogen availabilities, microbial communities capable of reducing selenate can reach higher numbers. In fact, we observed a density of selenate-reducing microorganisms that was 10 times higher in site E than in the other sites. Under the anoxic conditions during slurry experiments, the higher numbers of selenate-reducing microorganisms combined with higher availability of C_{org} and N resulted in potential rates of selenate reduction that are much higher than the six other sites.

We also argue that the higher potential selenate reduction rate obtained for site E is not only due to more numerous selenate-reducing microorganisms, but also to more diverse communities of selenate-reducing microorganisms than the other sites, due to its low *in situ* salinity of 3.0 g L^{-1}. This more diverse microbial community would respond better to the high salinity in experimental slurries, thus achieving higher selenate reduction rates. In fact, higher salinities have been associated with lower microbial diversities (Parnell, et al., 2011), particularly in hypersaline anaerobic environments (Oren, 1999). In addition, it was shown that highly uneven communities were less resistant to salinity and achieved lower nitrate reduction rates (Wittebolle et al., 2009).

Except for site D, the spatial heterogeneity in potential selenate reduction rates we measured in littoral sediments reflects the sediment N and C_{org} content. Since N is not limiting in the Salton Sea (Holdren & Montaño, 2002; Schroeder at al., 2002), we actually argue that C_{org} content is the main factor limiting selenate reduction rates in our experiments. In fact, the lowest potential selenate reduction rates were measured in sites A, B and G, all characterized by very low C_{org} content. Low substrate concentrations in those sites consequently limit microbial activity in general, including selenate reduction. Conversely, both sites E and F were characterized by the highest potential selenate reduction rates, which we attributed partly to their high C_{org} content. Since microorganisms couple the oxidation of organic carbon to the reduction of terminal electron acceptors, including selenate, without C_{org} limitation, microorganisms can reduce more selenate.

Although comparing K_f values among several sites should be done extremely cautiously given the slight differences in K_f units (depending on nf values), we observed that the sorption potential of site E is higher than the one of all other sites. Organic matter has been shown to play a very important role in the sorption of selenate to various soils (Pezzarosa et al., 1999). The highest sorption potential of site E is likely to be due to its high organic matter content, as reflected by the much higher N and C_{org} content of all studied sites. In addition, both laboratory experiments involving synthetic and natural Fe-oxy-hydroxides (Balistrieri & Chao, 1987; Su & Suarez, 2000; Martínez et al., 2006; Rovira et al., 2008) and experiments with natural soils concluded to the importance of Fe(III) as sorbents for selenate. Considering that the highest Fe(III)-oxides concentrations in the Salton Sea have been reported in the littoral zone surrounding the Alamo River Delta (De Koff et al., 2008) where site E is located, Fe(III)-oxides content, in addition to organic matter content, could explain why the selenate sorption potential for site E is the highest.

Only a limited number of studies have investigated selenate sorption in natural sediments and soils, since most studies focused on selenite, which adsorbs more strongly than selenate (Neal & Sposito, 1989; Hyun et al., 2006). Interestingly, our K_f data were up to one order of magnitude higher than those reported in the literature for Mediterranean soils (Pezzarosa et al., 1999), tropical soils (de Abreu et al., 2011), and human-affected soils such as coal mine soils (Sharmasarka & Vance, 2002) or ash landfill soils (Hyun et al., 2006). The high partition coefficients calculated in our study may be

explained by the high (up to 23.8%) $CaCO_3$ content measured in littoral sediments of the Salton Sea (Anderson et al., 2008). In fact, calcium has been implicated in increased selenium sorption (Afzal et al., 1999; Pezzarosa et al., 1999; Wang et al., 2007; Wang et al., 2009) especially for selenite (Duc et al., 2003), even though sulfate has been reported to suppress selenium sorption well above enhancements by calcium (Hyun et al., 2006). Our results suggest that selenate sorption may be a more important factor contributing to the sequestration of selenium in the Salton Sea littoral sediments than previously thought. In the context of future changes that will affect the Salton Sea, including increasing salinity, selenate sorption potential might become less significant. In fact, Su & Suarez (2000) showed that increasing salinity results in decreased selenate sorption to iron oxides, although it does not affect selenite sorption.

5. Conclusions

Our study investigating seven littoral sediments of the Salton Sea, CA, showed a high potential for selenate reduction and for selenate adsorption in all studied sites. We observed a high spatial variability in selenate reduction rates and in selenate sorption potential controlled mainly by the sediment C_{org} content. The measured maximum potential selenate reduction rates were overall quite high, which is important in the context of an ecosystem like the Salton Sea, where the water that feeds it has concentrations of selenium above the national water quality criterion for the protection of aquatic life. Selenate adsorption potential was also high, by about an order of magnitude higher than that expected from previous work on soils. Consequently, both selenate reduction and selenate adsorption are responsible for selenium sequestration in the Salton Sea sediments. Since selenium volatilization is only minor at the Salton Sea, we suggest that both selenate reduction and adsorption are major processes removing selenium from its water. Whereas selenium immobilization in the Salton Sea sediments has prevented aqueous selenium concentrations from reaching levels that pose an environmental hazard, sedimentary selenium is potentially available to benthic organisms and could thus enter the food chain. This is of special concern considering that the lake is expected to shrink and littoral sediments will be increasingly affected by sediment resuspension or sediment oxygenation. With the expected increase in the lake's salinity, we suggest that selenate adsorption might become less important. However, the effects of increasing salinity on selenate reduction still remained to be investigated.

6. References

Afzal, S., M. Younas & K. Hussain, 1999. Selenium speciation of surface sediments from saline lakes of the Soan-Sakesar Valley Salt-Range, Pakistan. Water Quality Research Journal of Canada, 34:575-588.

Anderson, M., L. Whiteaker, E. Wakefield & C. Amrhein, 2008. Properties and distribution of sediment in the Salton Sea, California: an assessment of predictive models. Hydrobiologia, 604:94-110.

Arnal R., 1961. Limnology, sedimentation, and microorganisms of the Salton Sea, California. Geological Society of America Bulletin, 72:427-478.

Balistrieri, L. & T. Chao, 1987. Selenium adsorption by goethite. American Journal of the Soil Sciences Society, 51:1145-1151.

Balistrieri, L. & T. Chao, 1990. Adsorption of selenium by amorphous iron oxyhydroxide and manganese dioxide. Geochimica et Cosmochimica Acta, 54:739-751.

Bar-Yosef, B. & D. Meek, 1987. Selenium sorption by kaolinite and montmorillonite. Soil Science, 144:11-19.

Bowie, G., J. Sanders, G. Riedel, C. Gilmour, D. Breitburg, G. Cutter, & D. Porcella, 1996. Assessing selenium cycling and accumulation in aquatic ecosystems. Water, Air and Soil Pollution, 90:93-104.

Catalano, J., Z. Zhang, P. Fenter & M. Bedzyk, 2006. Inner-sphere adsorption geometry of Se (IV) at the hematite (100)-water interface. Journal of Colloid and Interface Science, 297:665-671.

Chapman, P., 1999. Selenium – A potential time bomb or just another contaminant? Human and Ecological Risk Assessment, 5:1123-1138.

Chen, Y., L. Li, A. D'Ulivo & N. Belize, 2006. Extraction and determination of elemental selenium in sediments - A comparative study. 577-126-133.

Cherry, D. & R. Guthrie, 1977. Toxic metals in surface waters from coal ash. Water Resources Bulletin, 13:1227-1236.

Cohen, M. & K. Hyun, 2006. Hazard – The future of the Salton Sea with no restoration project. Pacific Institute, Oakland, California.

Cohen, M., 2008. Past and Future of the Salton Sea. In Gleick P. H. (ed.), The World's Water 2008-2009. Island Press, Covelo, California.

Czamanski, M., A. Nugraha, P. Pondaven, M. Lasbleiz, A. Masson, N. Caroff, R. Bellail & P. Tréguer, 2011. Carbon, nitrogen and phosphorus elemental stoichiometry in aquacultured and wild-caught fish and consequences for pelagic nutrient dynamics. Marine Biology, 158:2847-2862.

de Abreu, L., G. Santos, N. Curi, L. Guimaraes & J. de Sá e Melo Marques, 2011. Selenium sorption in soils of the Cerrado biome. Revista Brasileira de Ciencia do Solo, 35:1995-2003.

De Koff, J., M. Anderson & C. Amrhein, 2008. Geochemistry of iron in the Salton Sea, California. Hydrobiologia, 604:111-121.

Duc, M., G. Lefevre, M. Fedoroff, J. Jeanjean, J. Rouchaud, F. Monteil-Rivera, J. Dumonceau & S. Milonjic, 2003. Sorption of selenium anionic species on apatites and iron oxides from aqueous solutions. Journal of Environmental Radioactivity, 70:61-72.

Frankenberger, W., C. Amrhein, T. Fan, D. Flaschi, J. Glater, E. Kartinen, K. Kovac, E. Lee, H. Ohlendorf, L. Owens, N. Terry & A. Toto, 2004 Advanced treatment technologies in the remediation of seleniferous drainage waters and sediments. Irrigation and Drainage Systems, 18:19-41.

Furr, A., L. MacDaniels, L. St. John, W. Gutenmann, S. Pakkala & D. Lisk, 1979. Elemental composition of tree nuts. Bulletin of Environmental Contamination and Toxicology, 21:392-396.

Haudin, C., P. Renault, V. Hallaire, E. Leclerc-Cessac, & S. Staunton, 2007. Effect of aeration on

mobility of selenium in columns of aggregated soil as influenced by straw amendment and tomato plant growth. Geoderma, 141:98–110.

Holdren C. & A. Montaño, 2002. Chemical and physical characteristics of the Salton Sea, California. Hydrobiologia 473:1–21. In Barnum, D., J. Elder, D. Stephens, & M. Friend (eds), Proceedings of the Salton Sea Symposium held in Desert Hot Springs, CA, 13-14 January 2000. Kluwer Academic Publishers, Dordrecht, The Netherlands.

Hyun, S., P. Burns, I. Murarka & L. Lee, 2006. Selenium (IV) and (VI) sorption by soils surrounding fly ash management facilities. Vadose Zone Journal, 5:1110-1118.

Jehl, J. & R. McKernan, 2002. Biology and migration of eared grebes at the Salton Sea. Hydrobiologia, 473:245-253.

Kaiser, J., 1999. Battle over a dying sea. Science, 284:28-30.

Kulp, T. & L. Pratt, 2004. Speciation and weathering of selenium in upper cretaceous chalk and shale from South Dakota and Wyoming, USA. Geochimica et Cosmochimica Acta, 68:3687-3701.

Lemly, A., 2004. Aquatic selenium pollution is a global environmental safety issue. Ecotoxicology and Environmental Safety, 59:44-56.

Lenz, M. & P. Lens, 2009. The Essential Toxin: The Changing Perception Of Selenium In Environmental Sciences. Science Of The Total Environment, 407:3620-3633.

Mandal, S., S. Mayadevi & B. Kulkarni, 2009. Adsorption of aqueous selenite [Se(IV)] species on synthetic layered double hydroxide materials. Industrial & Engineering Chemistry Research, 48:7893-7898.

Marti-Cardona, B., T. Steissberg, S. Schladow, & S. Hook, 2008. Relating fish kills to upwellings and wind patterns in the Salton Sea. Hydrobiologia, 604:85-95.

Martin, A., S. Simpson, S. Fawcett, C. Wiramanaden, I. Pickering, N. Belzile, Y. Chen, J. London & D. Wallschläger, 2011. Biogeochemical Mechanisms of Selenium Exchange between Water and Sediments in Two Contrasting Lentic Environments. Environmental Science and Technology, 45:2605–2612.

Martínez, M., J. Giménez, J. de Pablo, M. Rovira & L. Duro, 2006. Sorption of selenium (IV) and selenium (VI) onto magnetite. Applied Surface Science, 252:3767-3773.

Marxsen, J. & D. Fiebig, 1993. Use of perfused cores for evaluating extracellular enzyme activity in stream-bed sediments. FEMS Microbiology Ecology, 13: 1-12.

Masscheleyn, P., R. Delaune & W. Patrick, 1991. Biogeochemical behavior of selenium in anoxic soils and sediments: An equilibrium thermodynamics approach. Journal of Environmental Science and Health, 26:555-573.

Meile, C., & K. Tuncay, 2005. Scale dependence of reaction rates in porous media. Advance in Water Resources, 29:62-71.

Moreau, M., J. Surico-Bennett, M. Vicario-Fisher, R. Gerads, R. Gersberg & S. Hurlbert, 2007. Selenium, arsenic, DDT and other contaminants in four fish species in the Salton Sea, California, their temporal trends, and their potential impact on human consumers and wildlife. Lake and Reservoir Management, 23:536-569.

Neal, R. & G. Sposito, 1989. Selenate adsorption on alluvial soils. American Journal of the Soil Sciences Society, 53:70-74.

Oren, A., 1999. Bioenergetic aspects of halophilism. Microbiology and Molecular Biology Reviews, 63:334-348.

Pallud, C., P. Van Cappellen, 2006. Kinetics of microbial sulfate reduction in estuarine sediments. Geochimica et Cosmochimica Acta, 70:1148-1162.

Parnell, J., G. Rompato, T. Crowl, B. Weimer & M. Pfrender, 2011. Phylogenetic distance in Great Salt Lake microbial communities. Aquatic Microbial Ecology, 64:267-273.

Pezzarosa, B., D. Piccotino & G. Petruzzelli, 1999. Sorption and desorption of selenium in different soils of the Mediterranean area. Communications in Soil Science and Plant Analysis, 30:2669-2679.

R Development Core Team. 2005. R: A language and environment for statistical computing. Vienna, Austria.

Redlands Institute, 2002. Salton Sea Atlas. ESRI Press, Redlands, California.

Reese, B. & M. Anderson, 2009. Dimethyl sulfide production in a saline eutrophic lake, Salton Sea, California. Limnology and Oceanography, 54:250-261.

Reese, B., M. Anderson & C. Amrhein, 2008. Hydrogen sulfide production and volatilization in a polymictic eutrophic saline lake, Salton Sea, California. Science of the Total Environment, 406:205-218.

Rovira, M., J. Giménez, M. Martínez, X. Martínez-Lladó, J. de Pablo, V. Martí & L. Duro, 2008. Sorption of selenium (IV) and selenium (VI) onto natural iron oxides: Goethite and hematite. Journal of Hazardous Materials, 150:279-284.

Sager, M., 2002. Vertical mobility of Selenium, Arsenic and Sulfur in Model Soil Columns. Die Bodenkultur, 53:83-103.

Saha, U., C. Liu, L. Kozak & P. Huang, 2005. Kinetics of selenite desorption by phosphate from hydroxyaluminum- and hydroxyaluminosilicate-montmorillonite complexes. Geoderma, 124:105-119.

Sampei, Y., & E. Matsumoto, 2001. C/N ratios in a sediment core from Nakaumi Lagoon, southwest Japan - usefulness as an organic source indicator. Geochemistry Journal, 35:189-205.

Schroeder, R. & W. Orem, 2000. Nutrient dynamics in the Salton Basin-implications from calcium, uranium, molybdenum, and selenium. Presentation, Spring 2000, Annual Meeting of American Geophysical Union, Washington, DC.

Schroeder, R., M. Rivera, B. Redfield, J. Densmore, R. Michel, D. Norton, D. Audet, J. Setmire & S. Goodbred, 1993. Physical, chemical and biological data for detailed study of irrigation drainage in the Salton Sea area, California, 1988-1990. United States Geological Survey – Open file report 93-083, Sacramento, California.

Schroeder, R., W. Orem, & J. Kharaka, 2002. Chemical evolution of the Salton Sea, California: nutrient and selenium dynamics. Hydrobiologia 473:23–45. In Barnum, D., J. Elder, D. Stephens, & M. Friend (eds), Proceedings of the Salton Sea Symposium held in Desert Hot Springs, CA, 13-14 January 2000. Kluwer Academic Publishers, Dordrecht, The Netherlands.

Schwabe, K., P. Schuhmann, K. Baerenklau & N. Nergis, 2008. Fundamentals of estimating the net benefits of ecosystem preservation: The case of the Salton Sea. Hydrobiologia 604: 181–195

Setmire, J. & R. Schroeder, 1998. Selenium and salinity concerns in the Salton Sea area of California. In Frankenberger, W. & R. Engberg, Environmental Chemistry of Selenium, Marcel Dekker Inc. New York, New York.

Sharmasarkar, S. & G. Vance, 2002. Selenite-selenate sorption in surface coal mine environment. Advances in Environmental Research, 7:87-95.

Steinberg, N. & R. Oremland, 1990. Dissimilatory Selenate Reduction Potentials In A Diversity Of Sediment Types. Applied and Environmental Microbiology, 56:3550-3557.

Stolz, J., & R. Oremland, 1999. Bacterial respiration of arsenic and selenium. FEMS Microbiology Review, 23:615-627.

Su, C. & D. Suarez, 2000. Selenate and selenite sorption on iron oxides: an infrared and electrophoretic study. American Journal of the Soil Sciences Society, 64:101-111.

Tokunaga, T., I. Pickering & G. Brown, 1996. Selenium transformations in ponded sediments. Journal of the American Soil Sciences Society, 60:781-790.

US-DOI (United States of America Department of the Interior), 2007. Reclamation – Managing water in the West: Restoration of the Salton Sea Summary Report. Bureau of Reclamation, Lower Colorado Region, Boulder City, Nevada.

US-EPA (United States Environmental Protection Agency), 1987. Ambient water quality criteria for selenium. U.S. Government Print Office, Washington, DC.

US-EPA (United States Environmental Protection Agency), 2010. California's 2008-2010 Section 303(d) list of impaired waters. In California State Water Resources Control Board, Sacramento, California.

Vogl, R., & R. Henry, 2002. Characteristics and contaminants of the Salton Sea sediments. Hydrobiologia 473:47-54.

Wang, T., J. Wang & J. Burken, 2007. The leaching characteristics of selenium from coal fly ashes. Journal of Environmental Quality, 36:1784-1792.

Wang, T., J. Wang, Y. Tang, H. Shi & K. Ladwig, 2009. Leaching characteristics of arsenic and selenium from coal fly ash: Role of calcium. Energy and Fuels, 23:2959-2966.

Wittebolle, L., M. Marzorati, L. Clement, A. Balloi, D. Daffonchio, K. Heylen, P. De Vos, W. Verstraete & N. Boon, 2009. Initial Community evenness favors functionality under selective stress. Nature, 458:doi:10.1038/nature07840.

Woomer, P., 1994. Most Probable Number counts. In Methods of Soil Analysis, Part 2: Microbiological and Biochemical Properties. SSSA Book Series, No. 5. Madison, Wisconsin

Chapter 2 — Sediment parameters controlling selenium distribution and the kinetics of selenate reduction across depth in littoral sediment of California's largest lake, the hypersaline Salton Sea

Juan Fernando Villa-Romero[1], Kathrin Schilling[2], Céline Pallud[1,2]
[1] Department of Plant and Microbial Biology, University of California, Berkeley
[2] Department of Environmental Science, Policy and Management, University of California, Berkeley

Abstract
Selenium (Se) is an essential micronutrient, and one of the trace elements most highly impacted by human activities. Selenate is the main selenium species in water entering the Salton Sea, a shallow, eutrophic, highly productive, and moderately hypersaline lake with no outlets, that is a vital habitat for more than 100,000 waterfowl, including migratory and endangered bird species. We used flow-through reactor (FTR) experiments containing intact sediment slices from North and South locations characterized by different texture to identify the sediment characteristics that control selenium retention, and the centimeter-scale vertical distribution of maximum selenate reduction potential, R_{max} and selenate half-saturation constants, K_m. In replicate sediment samples, we measured sorption percentages for selenate and selenite. Organic matter content varies widely between locations and across depth and is a strong determinant of selenium content in sediment. In North and South sediment, the sediment surface showed the lowest K_m values while sediment at 6-8 cm showed the highest R_{max} values. This implies that, *in situ*, selenate reduction across sediment depth is limited by the low availability of selenate and that resident selenate-reducing microbial communities operate well below their maximum potential rate. Selenate sorption was unexpectedly high and may contribute significantly to selenium retention in the Salton Sea littoral. This study is the first to quantify kinetic parameters for selenate reduction using undisturbed sediment and suggests that the prevalence of reports regarding selenate reduction at the sediment surface may be an artifact of slurry experiments that obscure spatial differences in selenate half-saturation constants and selenate reduction potential across sediment depth.

1. Introduction

Selenium (Se) is a chalcogen, an essential micronutrient, and one of the trace elements most impacted by mining, the refinement of metals, agriculture and other industrial activities (Frankenberger, 1994; Stolz & Oremland, 1999, Nancharaiah & Lens, 2015). Selenium is present in shales, alkaline soils (Presser, 1994), Se-bearing minerals (e.g., pyrite), and rarely in Se minerals (e.g., ferroselite, challomenite, and schmeiderite) (Stolz & Oremland, 1999; Nancharaiah & Lens, 2015). Selenium occurs in four oxidation states: -II, 0, IV, and VI, each displaying unique mobility and environmental behavior (Stolz et al., 2006). Water-soluble selenium oxyanions predominate in oxic environments, with more than 90% of soluble selenium pools present as selenate (Se(VI), as SeO_4^{2-}) and less than 10% as selenite (Se(IV), as $HSeO_3^-$, SeO_3^{2-}) (Martin et al., 2011). Selenate sorbs weakly to soil or sediment solid particles (Neal & Sposito, 1989), is predominant in surface waters (Martin et al., 2011), and is highly mobile (Neal & Sposito, 1989; Amrhein & Doner, 2014). Selenite, on the other hand, forms strong stable complexes with aluminum-, iron- and manganese-(oxy)hydroxides (Su & Suarez, 2000; Mandal et al., 2009; Saha & Huang, 2010), clay minerals (Balistrieri & Chao, 1987; BarYosef, 1987; Duc et al., 2003) and organic matter (Fernández-Martínez & Charlet, 2009) which reduces its mobility. The reduced from of elemental selenium, Se(0), is solid and immobile (Stolz et al., 2006).

Selenium speciation and cycling in the environment are predominantly governed by microbial activity via reduction, oxidation, methylation and demethylation reactions (Stolz et al., 2006). The most reduced form of selenium (-II) occurs in soluble organo-selenides (selenomethionine, e.g.), in solid metal-selenides (FeSe, e.g.), or in gaseous methylated forms (dimethylselenide, e.g) (Stolz & Oremland, 1999; Chasteen & Bentley, 2003; Hamilton, 2004). Selenate, selenite and organic selenide are toxic, bioavailable and known to bioaccumulate (Frankenberger & Engberg, 1998; Lemly, 2014). Upon its oxidation and release from parent rock material, selenate can be transported by water and upon entering trophic webs, selenium can accumulate in primary producers to concentrations 10^2- to 10^6-fold above ambient concentrations (Chapman et al., 2010). Selenium contamination of water, sediment and biota might amplify in the future if the increasing demand for energy is covered by fossil fuel combustion (Lenz & Lens, 2009; Chapman et al., 2010) and due to increased irrigated agriculture in semi-arid regions and mining of phosphate ores (Presser et al., 1994; Lemly, 2014). The anthropogenic release of selenium to water has led to several contamination events.In the US, Se contamination was reported for the first time in the 1980s at the Kesterson National Wildlife Refuge (California), and it continues to this day with the most recent events at Lake Sutton (North Carolina), after a discharge of coal ash wastewater (Lemly, 2014). In the Western United States, selenium accumulation and soil salinization originate from irrigating seleniferous soils (>0.5 µg Se g^{-1}), which results in the release of water-soluble selenate after selenium oxidation, and the concentration of selenium salts in the soil surface by physical weathering and evapotranspiration (Presser et al., 1994). Together with adsorption and assimilation, microbial dissimilatory selenate reduction is an important process transferring selenium from water to sediment in aquatic environments (Oremland et al., 1989; Steinberg & Oremland, 1990. The reduction of selenate to elemental selenium is highly exergonic (Oremland et al., 1989; Butler et al., 2012), can support anaerobic microbial growth, and leads to the formation of elemental selenium, sometimes in the form of nanoparticles (Butler et al., 2012, Nancharaiah & Lens, 2015). Selenite, elemental selenium and selenides can be incorporated into particulate matter through adsorption and coprecipitation, with elemental selenium often being the dominant species in estuarine and freshwater sediment (Turner, 2013). The top centimeters of sediment constitute a key environment during the introduction of selenium into the trophic chain of piscivorous birds (Steinberg & Oremland, 1990; Presser, 1994; Lemly, 2002). Most of the selenate reduction in lacustrine systems is reported to take place in the upper 0-8 cm of the sediment (Oremland et al., 1990) and to coincide with an accumulation of organic matter (Weres et al., 1989, 1990; Presser et al., 1994; Zhang & Moore, 1997; Vogl & Henry, 2002; Miles et al., 2009) or higher clay content (Oades, 1988).

Among the ecosystems currently most impacted by irrigation-induced selenium contamination in the USA is the Salton Sea (Seiler, 2003), the largest (940 km^2) selenium-impaired body of water in California's 303(d) list (US EPA, 2010). The Salton Sea was created in 1906 by an accident that diverted Colorado River water to the Salton Basin in the Colorado Desert and it has been a federally designated agricultural drainage reservoir since 1924 (Reese et al., 2008). It is a shallow (8 m mean depth), eutrophic, highly productive, and moderately hypersaline lake (salinity 47.5) with no outlets (VillaRomero et al., 2013; Schroeder et al., 2002; Reese & Anderson, 2009). It also became a vital habitat for more than 100,000 waterfowl, including migratory and endangered bird species (Krantz, 2007; Moreau et al., 2007). Fish biomass in the Salton Sea can increase or crash dramatically, however, increasing eutrophication has led to an increase in fish biomass since the early 2000 which becomes evident during seasonal fish die offs that in 2001, for example, reached up to 20 million individuals (Hurlbert et al., 2007). Irrigation runoff from the Coachella and Imperial Valleys maintains the Salton Sea through the Whitewater River at the North, and the Alamo and New Rivers at the South (Fig. 1). New and Whitewater River waters contain wastewater treatment effluents, while Alamo River water

contains mainly agricultural runoff from the Imperial Valley. Selenium concentrations in waters that feed the Salton Sea are low (between 2.4 and 8 µg L^{-1} or 0.017 -0.056 µM mostly as selenate) (Schroeder et al., 2002), but frequently exceed the current national recommended chronic selenium water quality criterion for the protection of aquatic life (3.1 µg L^{-1}, 0.022 µM; USEPA, 2015) or the CA Central Valley criterion for the protection of wetland waterfowl (2 µg L^{-1} or 0.014 µM, USEPA, 2000). However, dissolved selenium concentrations in Salton Sea water are much lower, ranging between 0.5 and 2.0 µg L^{-1} (0.003-0.014 µM) despite more than 100 years of selenium accumulation (Holdren & Montaño, 2002; Schroeder et al., 2002). In part due to high potential selenate reduction rates in Salton Sea littoral sediments (VillaRomero et al., 2013), sediment acts as a selenium sink with concentrations between 0.6 and 15 µg selenium g^{-1} (Schroeder et al., 2000, 2002; Byron & Ohlendorf, 2007; VillaRomero et al., 2013), about 30 times larger than selenium concentrations in surrounding soils (Schroeder et al., 1993, 2002).

Predicting the likely distribution of selenium across sediment depth requires data regarding the maximum potential rates of selenate reduction (R_{max}) in sediment and the half-saturation constants that describe the affinity of sediment towards selenate (K_m). Rates of microbial dissimilatory reduction obtained in the presence of saturating concentrations of terminal electron acceptor are referred as potential. Kinetic parameters R_{max} and K_m can be obtained from sediment slurries, however, sediment slurries destroy the tridimensional structure and spatial distribution of microbes in sediment, and therefore deliver data under conditions that impose almost no limitations on microbial activity (Pallud & Van Cappellen, 2006; Pallud et al., 2007). Alternatively, biogeochemical reaction rates and rate kinetic parameters can be derived from flow-through reactors (FTRs) containing intact sediment samples. Data obtained using this approach more closely reflect *in situ* processes because conditions of mass transfer limitation, microbial spatial distribution, and solid-bound substrate composition are preserved (Pallud & Van Cappellen, 2006).

The objective of this paper is to characterize differences in kinetic parameters K_m and R_{max} for selenate reduction across depth and to identify the sediment parameters controlling selenium distribution in Salton Sea littoral sediment. We use FTRs containing intact Salton Sea sediment collected from North and South littoral locations across a vertical 0-8 cm depth gradient at 2 cm intervals to quantify clay content, organic carbon content, nitrogen content, selenate reducer abundance, selenate sorption and selenite sorption, and to determine selenate reduction rates and kinetics (R_{max} and selenate half-saturation concentration, K_m). Ours is the first study aimed at measuring K_m values and R_{max} values for selenate reduction using a method that preserves the tridimensional architecture of sediments and the tridimensional distribution of sediment microbes.

2. Materials & Methods
2.1. Study Sites
Our work focused on littoral sediments from the Salton Sea in Southern California, USA (Fig. 1). Two sites, called North and South sites hereafter, located in close proximity to the drainage area of agricultural lands. Both sites were sampled in November 2012 (Fig. 1). The North location (N33.52338°; W115.98176°) is about 8 miles Southeast of the Whitewater River head (Fig. 1) on a mudflat bordering an extensive playa covered in barnacle shells and fish bones. Water at the North site was intensely mixed by wave action, which led to the formation of a viscous mud that made a clear identification of the water-sediment boundary difficult. Collected sediments gave a strongly sulfidic smell and were uniformly black. The South location (N33.15329°; W115.64909°) is located halfway between the Alamo and New Rivers heads (Fig. 1) on a narrow sandy playa free from barnacle shells,

fish bones and fish carcasses. Water overlying the sampling site in the South site was calm and clear, and the water-sediment interface was easy to identify. Collected sediments gave a slight smell of hydrogen sulfide and consisted of a thin brown layer (~5 mm depth) underlain by a gray layer.
At each sampling site, sediment cores were taken 1-2 m from the shoreline, at a water depth no greater than 0.5 m. Four intact replicate sediment cores (4.2 cm ID × 8 cm length, each) were collected from the water/sediment interface using a hand pushed corer lined with four stacked Plexiglas reactor cells.

One core was separated into four sediment slices corresponding to four different depth intervals (0-2, 2-4, 4-6 and 6-8 cm) and flow-through reactors were assembled on site using a 0.2 µm pore size nitrocellulose filter, a glass fiber filter and a Plexiglas cap at each end (Roychoudhury et al., 1998; Pallud & Van Cappellen, 2006; Pallud et al., 2007). The remaining three cores were used for the analyses of (i) the physical (bulk density, porosity, and clay content), (ii) chemical sediment characteristics (organic carbon, total nitrogen and selenium content, as well as selenate and selenite sorption), and (iii) the abundance of selenate-reducer microorganisms in sediment, as described below. All samples were preserved at 4°C in sealed anaerobic bags until experiments or analyses were performed.
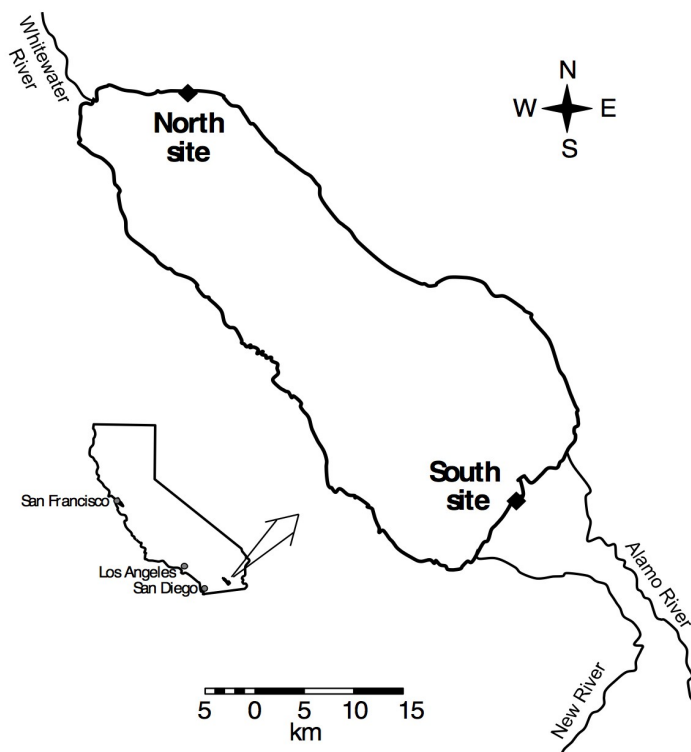
Figure 1: *Map showing the location of the Salton Sea in California and of the two study sites (diamonds) sampled along the littoral of the Salton Sea in November 2012*

2.2. Sediment dry bulk density, porosity, clay content, average particle size and surface area measurements

Dry bulk density and porosity were determined after drying each of the 27.7 cm^3 sediment slices collected for physical characterization at 105°C for 48 hours. Porosity was calculated from the bulk

density (ρ_d) and particle density (ρ_S estimated at 2.65 g cm^{-3}, the density of quartz) as 1-(ρ_d /ρ_S). For every sediment sample, five replicate measurements of clay percentage, mean particle size, and surface area were performed using a LISST-Portable|XR (Sequoia Scientific, WA, USA) laser diffraction-based particle sizer (Agrawal & Pottsmith, 2000). The sediment slurries were obtained by gently disaggregating 5 g of oven-dried sediment using a pestle and mortar, and treating it with 5 mL of 30 % hydrogen peroxide (H_2O_2) overnight to remove organic matter, and with 25 mL of 1 M HCl for 5 hours to remove carbonates. The resulting sample was centrifuged at 6,000 RCF for 15 minutes, and the pellet was resuspended in 20 mL of a 5 g L^{-1} sodium hexametaphosphate solution for 24 hours.

2.3. Sediment organic carbon and total nitrogen content measurements

Sediment organic carbon (C_{org}), and total nitrogen (N) contents were determined in duplicates of air-dried samples. To avoid artifacts derived from the standard procedure applied to remove carbonate (Bianchi, 2012), total N was measured in untreated sediments, and C_{org} content was measured in sediment treated for 20 minutes with 0.7 mL of a 1 M H_2SO_4 5 % $FeSO_4$ solution to remove carbonates (Carter, 1993). Analyses were performed using a NC 2100 Soil Analyzer (CE Instruments, USA). Inorganic carbon content was calculated from the difference between total and organic carbon content.

2.4. Sequential extraction of selenium in sediment

Selenium was extracted and quantified following a modified methodology from Gao et al. (2003). Total selenium content was determined both in original sediment and sediment recovered from flow-through reactors using aqua regia (1:3; HNO_3: HCl). Two mL of water and 2 mL of concentrated HNO_3 were added to 1 gram of sediment placed in a 30 mL Teflon beaker. This mix was placed on a hotplate at 100˚C overnight and evaporated to near dryness. Twelve mL of freshly prepared aqua regia (1:3; HNO_3: Hcl) were added to the remaining sample and evaporated again to near dryness. To the remaining sample, 5 mL of 0.1 M HCl were added and this mix was filtered through a 0.45 μm PTFE filter membrane. Sequential extractions were preformed for sediment recovered after the FTR experiments. The selenium fractions are operationally-defined as soluble, adsorbed, organically-bound, elemental and total fractions, extracted using 0.25 M KCl, 0.1 M K_2HPO_4 (pH 8.0), 0.1 M NaOH, 1.0 M Na_2SO_3 (pH 7), and aqua regia (1:3; HNO_3: HCl), respectively. Briefly, 2 g of oven-dry sediment were mixed with 20 mL of 0.25 M KCl in 50-mL centrifuge bottles and shaken for 2 hours. The suspension was centrifuged at 6,000 g relative centrifugal force (RCF) for 15 minutes and the supernatant was filtered through a 0.45 μm PTFE filter membrane. The remaining sediment was split into two subsamples. To each, 20 mL of 0.1 M K_2HPO_4 solution (pH 8.0) was added and the sediment was resuspended. After shaking overnight for 18 hours, the suspension was centrifuged at 6,000 g relative centrifugal force (RCF) for 15 minutes, and filtered through a 0.45 μm PTFE filter membrane. One subsample from the K_2HPO_4 extraction was ready for analysis. To 2.5 mL of the second subsample, 0.5 mL of concentrated HNO_3 were added. This mix was placed on a hotplate at 100˚C under a fume hood and evaporated to near dryness. To the dry sample, 60 mL of concentrated HNO_3 were added. This mix was evaporated to near dryness under the same conditions and diluted with 3 mL of water after dried.

2.5. Enumeration of selenate and selenite reducers in sediments

The abundance of selenate-reducing bacteria in sediment was estimated by the most probable number (MPN) method (Woomer, 1994). The abundance of selenate-reducing bacteria was estimated in duplicate sediment core samples collected from each location and depth interval and in sediment recovered from the FTR experiments. Five grams of homogenized sediment were suspended in 45 mL of sterile saline solution (45 g L^{-1} NaCl), and shaken thoroughly. Tenfold dilution series (eight

replicates) were made from the slurry directly in sterile culture medium dispensed in 96-well microtiter plates. The composition of the medium for selenate-reducing bacteria was (in L^{-1}; VillaRomero et al., 2013): NaCl, 45 g; $MgCl_2i6H_2O$, 3 g; KH_2PO_4, 0.2 g; NH_4Cl, 0.3 g; KCl, 0.3 g; Na_2SO_4, 0.3 g; yeast extract, 0.1 g; Na_2SeO_4, 1.89 g; ATCC MD-TMS (trace mineral solution), 10 mL; ATCC MD-VS (vitamin solution), 10 mL; Na-lactate, 10 mM; pH was adjusted to 7.5. The reducing agent in the medium was mercaptoacetic acid, added shortly before dispensing the medium into the wells. Plates were anaerobically incubated at 30°C in the dark for 6 weeks. The presence of selenate- reducing bacteria was scored positive upon the formation of elemental selenium as a red precipitate.

2.6. Selenate and selenite sorption

Selenate and selenite adsorption on Salton Sea sediments was investigated using duplicate slurry experiments performed by mixing 1 g of sieved (<2 mm) air-dried sterile (autoclaved at 121°C for 1 h) sediment with 1 mL of a sterile solution of NaCl simulating the salinity of the Salton Sea and amended with 3.3 µM selenite or selenate to mimic dissolved selenium concentrations in river water entering the Salton Sea (Holdren & Montaño, 2002). Sediment suspensions were allowed to equilibrate for 6 and 12 hours for selenite and selenate, respectively, in the dark on a rotary shaker at 18°C. Supernatants were then collected and filtered through a 0.45-µm MCE syringe filter before analysis and total Se concentrations were measured as described earlier. The percentage of selenate and selenite sorption was calculated by the difference between initial aqueous phase and equilibrium selenium concentrations.

2.7. Selenium analysis

For the sequential extraction of selenium in sediment, total selenium was measured using a Perkin Elmer 5300 DV Inductively Coupled Plasma-Optical Emission Spectrometer (ICP-OES) operating in regular mode. Selenium standards were prepared from certified reference stock solutions (VHG Labs) in a matrix with 47.5 g L^{-1} NaCl to match the salinity of the samples. Detection limits in a matrix with 47.5 g L^{-1} NaCl was 0.6 µM.

In samples from the sorption and flow-through reactor experiments, total Se was determined using the ICP-OES operating in regular mode. Selenite concentrations were measured via ICP-OES coupled to a hydride-generation (HG) setup based on the phase separator setup described by Kausch et al. (2012). Elemental and speciation standards were prepared from certified reference stock solutions (VHG Labs) in a matrix matching the composition of measured samples. Flow rate was 1 mL min^{-1}. A sample injection time of 60 s before optical emission reading and a rinse time of 30 s between samples were used due to a memory effect. Selenate concentrations were calculated as the difference between total Se and selenite concentrations. Selenium standards were prepared from certified reference stock solutions (VHG Labs) in a matrix with 47.5 g L^{-1} NaCl to match the salinity of the samples. Detection limits in a matrix with 47.5 g L^{-1} NaCl was 0.6 µM.

2.8. Flow-through reactor experiments setup and calculation of selenate reduction rates

FTR experiments (Roychoudhury et al., 1998; Pallud et al., 2007) were performed to measure potential rates of selenate reduction in response to imposed selenate concentrations,on sediment from depth intervals 0-2, 2-4, 4-6, and 6-8 cm from the North and South sites. The main advantages of using FTRs are that rates are measured under (near) steady-state conditions, dissolved metabolic byproducts do not accumulate, and the solution to solid ratio of the natural sediment is preserved, which is important given that subsurface microorganisms are in most cases particle-bound (Pallud & Van Cappellen, 2006; McMahon & Parnell, 2014). The experiments were run inside a glove box under a 95% nitrogen, 5% hydrogen atmosphere at room temperature. The input solutions consisted of sterile

anoxic 45 g L^{-1} NaCl solutions supplemented with various concentrations of selenate. Five successive selenate concentrations (53, 73, 159, 290 and 423 µM) were supplied to the FTR for about 150 hours each at a constant flow rate (2 ± 0.5 cm^3 h^{-1}) using a peristaltic pump. Selenate concentrations were chosen to include values well above reported K_m values for selenate reduction (7.9 to 34 µM; Steinberg & Oremland, 1990) in order to reach selenate saturation and measure maximum reduction rate (Pallud et al., 2007). Outflow samples were collected every 6 hours using a fraction collector and analyzed for total selenium and selenite, as described earlier. Before analysis, the samples were centrifuged for 25 minutes at 10,000 RCF and 4°C. Total Se and selenite concentrations were determined as described earlier. Selenate concentrations were calculated as the difference between total Se and selenite concentrations. Steady-state potential selenate reduction rates (SeRR) were calculated as:

$$SeRR = \frac{(Cout - C0)Q}{V}$$

(eq. 1)

where C_{out} is the steady-state selenate concentration in the outflow, C_0 is the selenate input concentration, Q is the volumetric flow rate and V is the volume of the sediment in the reactor (Pallud & Van Cappellen, 2006; Pallud et al., 2007). Kinetic parameters R_{max} and K_m for selenate reduction were derived from the steady-state reaction rates calculated with eq. 1, and the average, steady-state selenate concentrations estimated as $(C_0 + C_{out})/2$ using a non linear regression fitting of the Michaelis-Menten expression using KaleidaGraph (Synergy Software, Inc., Reading, Pennsylvania) (Pallud et al., 2007).

2.9. Statistical analysis

The statistical significance of differences between sediment characteristics across sites and depths was determined by one-way ANOVA and post hoc comparison of means with Tukey's Honest Significant Differences with a significance threshold of $P < 0.05$. Correlations between sediment characteristics and percentage of adsorption, reaction rates, and kinetic parameters were evaluated using Pearson's correlation coefficient, r. All statistical analyses were used using R (R Core Team, 2014. URL http://www.R-project.org/).

3. Results
3.1. Potential selenate reduction rates (SeRR) and selenate reduction kinetics

For all depths and sites, selenate concentrations in FTR outflow reached steady-state after less than 50 hours (Fig. 2), with average outflow concentrations varying by less than 4.8% during that steady-state.

The calculated potential SeRR increased with increasing porewater selenate concentration (Fig. 3). The dependence of potential SeRR on selenate concentration followed the Michaelis-Menten rate equation (Fig. 3). Apparent R_{max} were 1.7 to 1.8 times higher at the North site than for the South site except for the depth interval 4-6 cm (Table 1). R_{max} values varied by a factor of up to 3.4 and 2.6 in North and South sediments, respectively, ranging between 8.5 to 29.2 nmol SeO$_4^{2-}$ cm^{-3} h^{-1} in North sediment and between 6.4 to 16.5 nmol SeO$_4^{2-}$ cm^{-3} h^{-1} in South sediment. The lowest R_{max} values were observed at 4-6 cm and 2-4 cm in North and South sediment, respectively (Table 1). For all sediments, R_{max} values were positively correlated with K_m values for selenate ($r= 0.78$; p-value= 0.02), the abundance of selenate-reducing bacteria ($r= 0.71$; p-value= 0.05), and total selenium content ($r= 0.48$; p-value= 0.23). Depending on the site, R_{max} was positively correlated with sediment clay content ($r=$

0.72; p-value= 0.29 for North sediment), and C_{org}:N (r= 0.92; p-value= 0.08 for South sediment). Apparent K_m showed a similar range of values in both sites and varied by more than one order of magnitude with depth, ranging from 10 to 661 μM (Table 1). The highest K_m values were observed for the depth interval of 6-8 cm at both sites, and the lowest values were for the depth interval 0-2 cm for the South site and for the depth interval 2-4 cm for the North site. K_m was negatively correlated with sediment nitrogen content in North sediment (r= -0.74; p-value = 0.263) but positively correlated with nitrogen content in South sediment (r= +0.95; p-value = 0.051). K_m was also correlated with surface area in North sediment (r= -0.81; p-value = 0.18), and with organic carbon content (r= -0.7; p-value= 0.304), C_{org}:N (r= 0.97; p-value = 0.028), and elemental selenium content (r= -0.83; p-value= 0.171) in South sediment.

3.2. Selenate and selenite sorption

Selenite and selenate sorption percentages are shown in Figure 4. Selenite sorption was detected in all evaluated sediments, with percentages of selenite sorbed ranging from 15 to 41% (Fig. 4 A), whereas selenate sorption was detected only in the topmost sediments (0-4 cm) and was highly variable ranging from 10% to 33%. (Fig. 4 B). Selenite sorption increased with depth, however, differences were not statistically significant (p< 0.05). Selenite sorption percentages were positively correlated with C_{org}:N (r= +0.85; p-value= 0.007). Where detected, selenate sorption was positively correlated with C_{org} (r= +0.46; p-value= 0.54) and negatively with clay content (r= -0.94; p-value= 0.063).
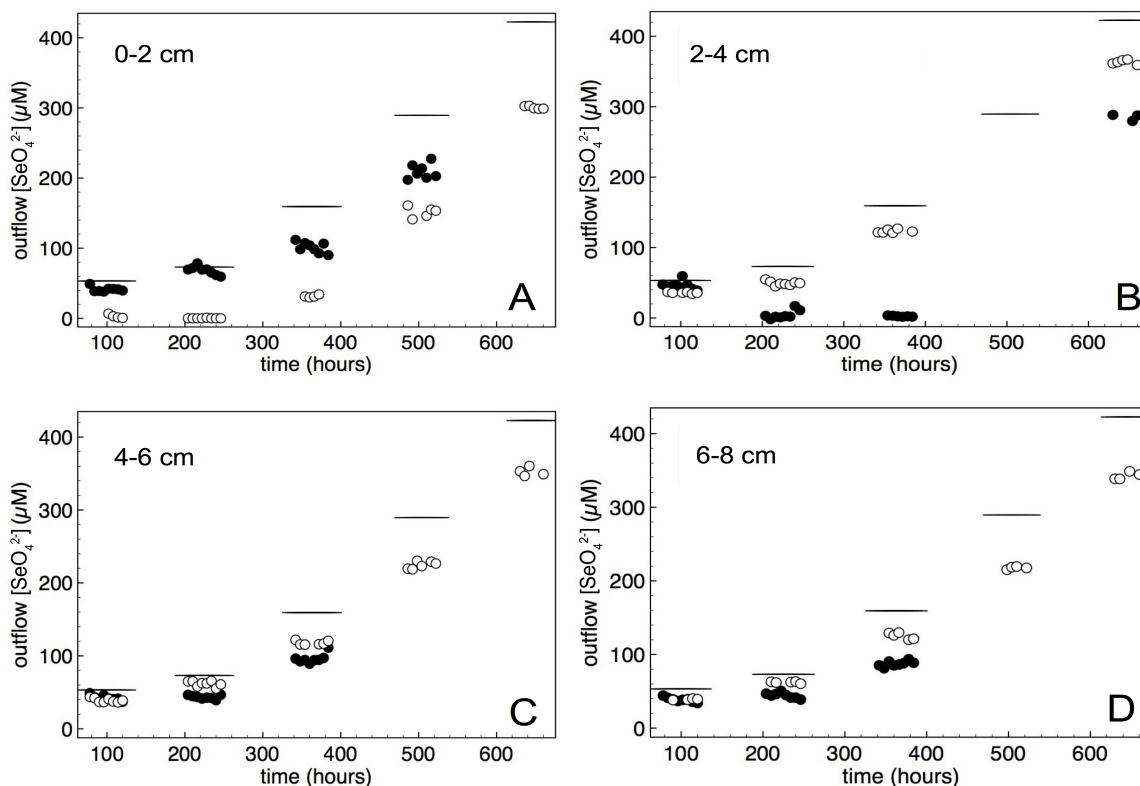
Figure 2: *Selenate concentrations measured in the flow-through reactor outflow as a function of time for the 0-2 cm (A), 2-4 cm (B), 4-6 cm (C), and 6-8 cm (D) depth intervals for the South (white circles) and North site (black circles). Input selenate concentrations are indicated by the black solid lines.*

3.3. Sediment physical characteristics

Figure 5 shows the vertical variation in physical properties of sediment collected in North and South sites. The South site sediment had no gravel, compared to up to 27% in the North site (Fig. 5 A), and had a finer texture than that of North sediment. For the 0-8 cm depth interval, average clay percentages in South sediment were 4 times higher (13.2% ± 4.4 in South sediment vs. 2%±0.3 in North sediment) (Fig. 5 B), average mean particle size 3.2 times lower (76.3 ± 8.3 μm in South sediment vs. 23.7±19.4 μm in North sediment) (Fig. 5 C), and average surface area 5.3 times greater (0.16 ± 0.05 m^2 cm^{-3} in South sediment vs. 0.03±0.01 m^2 cm^{-3} in North sediment) than those in North sediment (Fig. 5 D).

Clay content did not significantly vary with depth in North sediment ($p < 0.05$; Fig. 5 B), but was significantly higher ($p < 0.05$) in the 2-4 and 4-6 cm depth intervals compared to other depths in South sediment. Mean particle size in North sediment ranged between 65.2 μm and 84.4 μm and showed no significant ($p < 0.05$) differences between depths (Fig. 5 C). In South sediment, mean particle size ranged from 8.3 μm to 50.2 μm and was significantly higher ($p < 0.05$) in the 0-2 cm and 6-8 cm depth intervals. Clay content was positively correlated with surface area ($r = +0.98$; p-value= 9.4×10^{-6}), and negatively correlated with particle size ($r = -0.97$; p-value= 7.7×10^{-5}), while mean particle size and surface area were negatively correlated ($r = -0.95$; p-value= 0.0003).

Bulk density and porosity differed only slightly between sites and averaged 1.07±0.1 g cm^{-3} and 59.6%±3.3 in North sediment, and 0.97±0.1 g cm^{-3} and 63.5%±4.7 in South sediment, respectively, for the 0-8 cm depth interval (Fig. 5 E, F). For both sites, porosity was the highest in the top 2 cm of sediments (Fig. 5 F).

3.4. Sediment chemical characteristics

Sediment inorganic carbon content ranged between 1.4% and 2.2%, showing no significant differences ($p < 0.05$) between sites and depths (Fig. 6 A). Sediment C_{org} content and nitrogen content showed no significant differences between the North and South sites for the 0-4 cm depth interval (Fig. 6 B, C). However, for the 4-8 cm depth, sediment C_{org} content was significantly higher ($p < 0.05$) in the North site than in the South site by a factor of 1.32 (Fig. 6 B). Sediment C_{org} content showed opposite trends below 4 cm depth in the two study sites. It increased significantly with depth from 0.4% to 0.51% in the North site ($p < 0.05$; Fig. 6 B), but decreased significantly with depth from 0.4% to 0.34% in the South site ($p < 0.05$; Fig. 6 B). Sediment nitrogen content was not significantly different ($p < 0.05$) between depths at neither North nor South sites, except for depth intervals 4-6 and 6-8 cm in South sediment in which nitrogen content was significantly lower ($p < 0.05$) (Fig. 6 C). C_{org} content was positively correlated with nitrogen content ($r = +0.65$; p-value= 0.078) and negatively correlated with clay content ($r = -0.74$; p-value= 0.034), while both C_{org} and nitrogen content were negatively correlated with surface area ($r = -0.64$; p-value= 0.089 and $r = -0.81$; p-value= 0.015, respectively for C_{org} and N, respectively) at both sites. No significant differences were detected for sediment molar C_{org}:N between the two sites (Fig. 6 D). Molar C_{org}:N showed no significant differences ($p < 0.05$) between depths, ranging between 5.2 and 7.8 at the North site and from 5.8 to 7.5 at the South site (Fig. 6 D). Total selenium content averaged for the 0-8 cm depth interval was 5 times higher in the sediment from the North site than for the South site, with values of 2.21 ± 0.6 and 0.44 ± 0.19 μg g^{-1}, respectively. For both sites, total selenium content increased with depth, with values significantly lower for the top 4 cm of the sediment than for the deeper depth intervals ($p < 0.05$) (Fig. 6 F). Total selenium content in North and South sediments was positively correlated with C_{org} ($r = 0.83$; p-value= 0.0106).

26
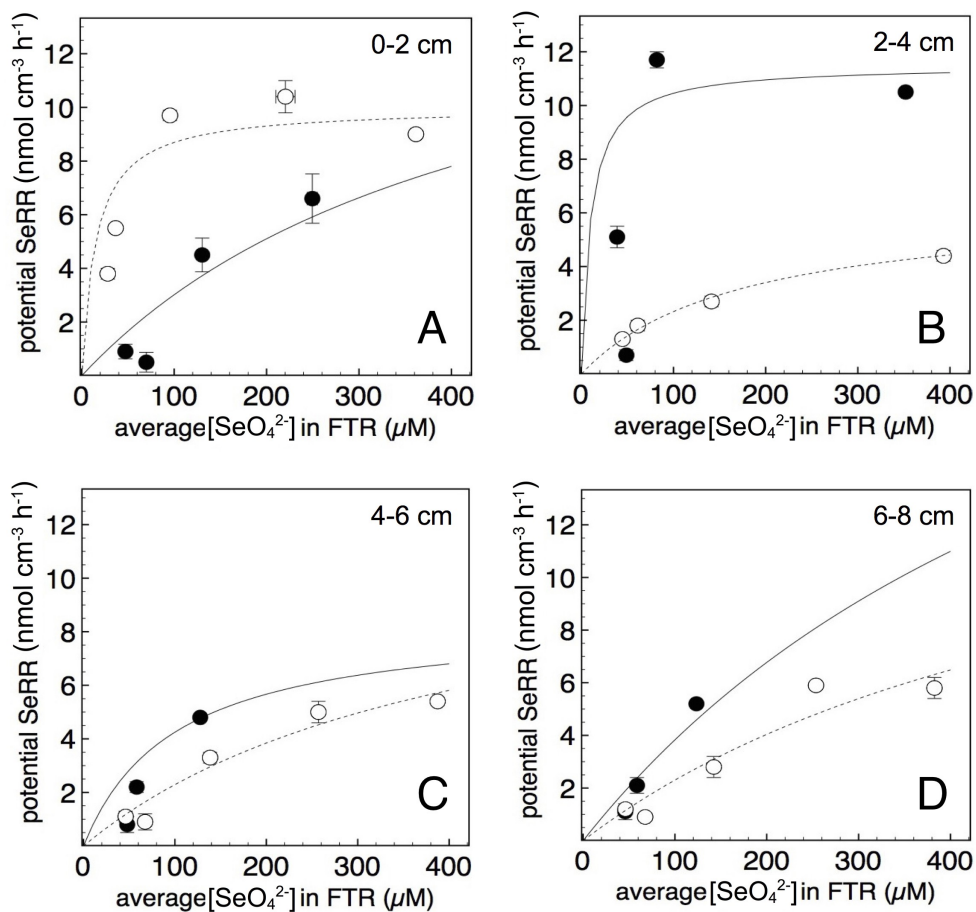
Figure 3: *Steady-state potential selenate reduction rates (SeRR) as a function of average selenate concentration in FTRs measured in sediment from the North (black circles) and South (white circles) sites collected from the 0-2 (A), 2-4 (B), 4-6 (C) and 6-8 (D) cm depth intervals. The lines correspond to the Michaelis-Menten rate expression, using R_{max} and K_m summarized in the adjoining table (E). Values represent the average of five replicates ± standard deviation. When not visible, the X- and Y- error bars fall within the size of the symbols.*

Table 1. Kinetic parameters K_m and R_{max} for selenate reduction

	cm	K_m μM	V_{max} nmol h⁻¹ cm⁻³
NORTH	0-2	448.6	16.6
NORTH	2-4	10.0	11.5
NORTH	4-6	100.0	8.5
NORTH	6-8	661.0	29.2
SOUTH	0-2	15.0	10.0
SOUTH	2-4	173.8	6.4
SOUTH	4-6	420.8	11.9
SOUTH	6-8	616.1	16.5
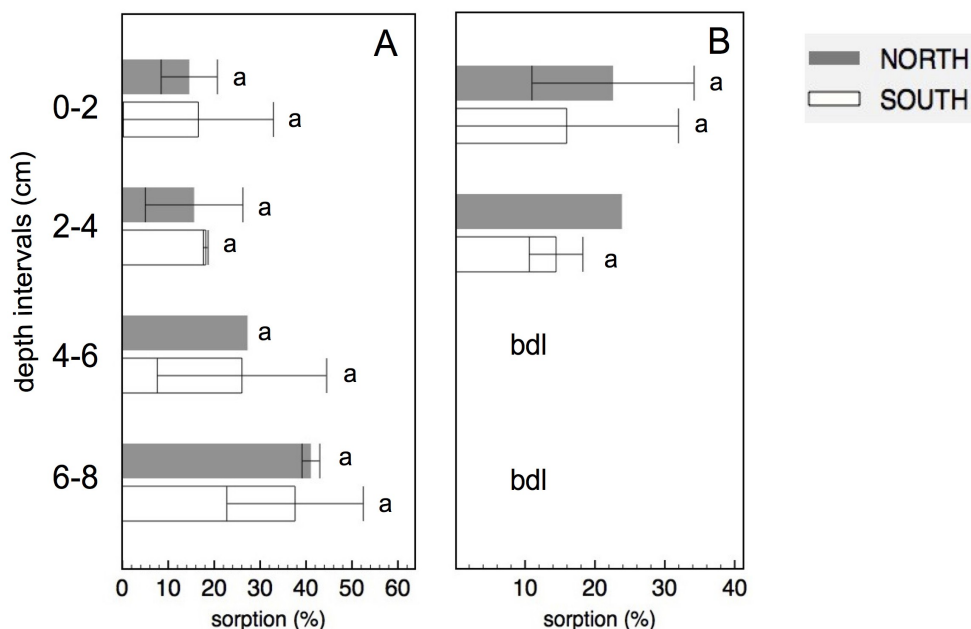
Figure 4: Percentage of selenite (A) and selenate (B) sorbed in North (gray) and South (white) sediment. Values represent the average of two replicates ± standard deviation. Means with different letters are significantly different (Tukey's HSD, p<0.05). bdl= below detection limit. Selenate and selenite sorption values were obtained from duplicate slurry experiments performed by mixing 1 g of air-dried sterile sediment with 1 mL of a sterile NaCl solution amended with 3.25 ± 0.18 μM selenite or 3.28 ± 0.0 μM selenate

3.5. Abundance of selenate-reducing bacteria in sediment

The abundance of selenate-reducing bacteria in sediment varied only slightly with depth and between sites (Fig. 6 E) averaging $3.1\pm0.5\times10^3$ and $2.8\pm0.2\times10^3$ cells cm^{-3}, in the North and South sites respectively. The abundance of selenate-reducing bacteria in North and South sediment correlated positively with C_{org} ($r=+0.52$; p-value= 0.187) and total selenium content ($r=+0.47$; p-value= 0.241). In South sediment, the abundance of selenate-reducing bacteria was positively correlated with N content ($r = 0.78$; p-value = 0.221) and negatively correlated with C_{org}:N ($r = -0.86$; p-value= 0.136).

3.6. Sediment characteristics at the end of the FTR experiments

Sediment C_{org} content increased during the course of the FTR experiments by 21 to 61% across all sediment depths investigated in the North site, and by 10 to 18% for the depth intervals 0-2 and 4-6 cm only, in the South site. In contrast, sediment from the depth intervals 2-4 and 6-8 cm in the South site were characterized by a 15 to 20% decrease in sediment C_{org} over the course of the FTR experiments (Figs. 6 B and 7 D). Except for the depth interval 0-2 cm, sediment C_{org} content at the end of FTR experiments was significantly higher (p< 0.05) in the North site than in the South site (Fig. 7 D).

Total sediment selenium content increased on average by a factor of 2×10^2 and 8×10^2 in the

North and South sites, respectively, over the course of the FTR experiments (Fig. 6 F and 7 A). Total selenium content at termination of the FTR experiments was significantly higher (p< 0.05) in North sediment than South sediment at all depths, with the highest values recorded for the depth interval 0-2 cm at both sites (Fig. 7 A). Both soluble (Se-KCl) and ligand-exchangeable (Se-K_2HPO_4) selenium fractions in all sediments recovered from FTR experiments were extremely small (data not shown).

Organic matter-associated (Se-NaOH) and elemental selenium (Se-Na_2SO_3) accounted for most of the selenium in the depth interval 0-2 cm of the sediment recovered from FTR experiments, representing 43% and 31% of total selenium in North site, respectively, and 25% and 26% of total selenium in South site, respectively (Fig. 7 B and C). The percentage of selenium associated with the organic matter fraction, which includes both selenium adsorbed to the organic matter and selenium incorporated in biomass, represented less than 13% of the total selenium for all the other depths investigated (Fig. 7 B). On the other hand, the percentage of selenium associated with the elemental fraction for the depth intervals 2-4, 4-6 and 6-8 cm varied widely, ranging between 12 and 82% in North site, and between 2 and 51% in South site (Fig. 7 C). The residual selenium fraction, that is, selenium detected in the total extraction but not accounted by the sum of organic matter-associated and elemental selenium ranged between 10 and 76% in North sediment and between 40 and 95% in South sediment.

In North and South sediments recovered from FTRs, organic matter-bound and total selenium content were positively correlated (r= 0.92; p-value= 0.001). In North sediment recovered from FTRs, both elemental and total selenium content were negatively correlated with C_{org}:N (r= -0.99; p-value= 0.003 and r= -0.63; p-value= 0.374 for elemental and total selenium content, respectively) and with C_{org} content (r= -0.97; p-value= 0.023 and r= -0.83; p-value= 0.169 for elemental and total selenium content, respectively). In South sediment recovered from FTR experiments, elemental selenium content was positively correlated with total selenium (r= 0.98; p-value= 0.019) and C_{org} content (r= 0.76; p-value= 0.242).

The abundance of selenate-reducers in sediment recovered from FTR experiments decreased with depth. The abundance of selenate-reducing bacteria at the end of FTR experiments was up to 23 times higher than that in original sediment, with the largest increase observed at the 0-4 cm depth interval at the North site (Fig. 6 E and 7 E). In both sites, selenate-reducer abundance at the end of FTR experiments correlated positively with R_{max} (r= 0.71; p-value= 0.047), selenite-reducer abundance (r= +0.61; p-value= 0.11), and elemental selenium content (r= +0.92; p-value= 0.001), and negatively with C_{org}:N (r= -0.73; p-value= 0.04), and selenite sorption (r= -0.68; p-value= 0.062). The sediment parameters that correlated best with selenate-reducer abundance in North sediment recovered from FTRs were selenite sorption, C_{org} and C_{org}:N (r= -0.9; p-value= 0.098; r= -0.98; p-value= 0.019; r= -0.97; p-value= 0.028, respectively). In South sediment recovered from FTRs, selenate reducer abundance correlated best with clay, C_{org} and total nitrogen content (r= -0.9; p-value= 0.098; r= -0.98; p-value= 0.019; r= -0.97; p-value= 0.028, respectively).

4. Discussion
4.1. Biomass sources and physical controls of the distribution of organic carbon and nitrogen content in littoral sediment

Higher current velocities (>20 cm s^{-1}) and resulting higher intensities in water mixing and sediment resuspension in the Southern Salton Sea Basin, compared to the Northern Basin (Anderson et al., 2008), and the high velocity inflows from the New and Alamo Rivers at the Southern end of the

Salton Sea (Vogl & Henry, 2002) (Fig. 1) may explain the higher clay content measured in South littoral sediment in this study. Higher clay contents in evaluated sediment from the South site may result from higher current velocities resulting when a large volume of water moving at some velocity in the North Salton Sea Basin accelerates when forced into the shallower conditions of the South Basin (Anderson et al., 2008). More intense water currents in the Southern Salton Sea Basin can keep finer particles in suspension and transport them to the littoral zone where they accumulate to a percentage higher than that found in littoral sediment from the North site. Sediment clay contents in North and South sediment were 2-15 times lower, respectively, than the average clay content reported for the whole Salton Sea Basin for sediment collected down to a depth of 182 cm (Vogl & Henry, 2002; Schladow et al., 2007; Anderson et al., 2008). Clay content controls the sediment surface area available for the retention of organic matter and microbial cells (Liao et al., 2015). Anderson et al., 2008 reported a strong positive correlation between clay content and organic carbon content in sediment collected from the whole Salton Sea Basin, however, we found the opposite, a strong negative correlation between clay content and organic carbon content in evaluated sediments from the Salton Sea littoral. This suggests that the processes that lead to organic matter retention by clay in littoral sediment are different to those operating at deeper sediments which constitute the vast majority of the lake. These differences may be due to differences in organic matter degradation between littoral sites and deep sediments, perhaps due to the availability of oxygen versus sulfate as terminal electron acceptors and the different extent to which these terminal electron acceptors can support organic matter oxidation.

The consistently low (<8) C_{org}:N we observed in North and South littoral sediment (Fig. 6 D) suggest that fish and microalgae contribute importantly to biomass accumulation in those sites. Indeed, fish and microalgae have C_{org}:N ranges of 4-6 and 5-7, respectively (Meyers & Ishiwatari, 1993; Czamanski et al., 2011; Bianchi, 2012). The range of C_{org}:N values we observed in North and South littoral sediments is similar to the range of 3.0-8.1 reported for an array of Salton Sea littoral sediments (VillaRomero et al., 2013), but lower than the average C_{org}:N value of 10 reported for the whole Salton Sea Basin (Anderson et al., 2008). This shows that organic matter with higher nitrogen content reaches the Salton Sea littoral, compared to deeper parts of the lake, and could result from the yearly accumulation of million of fish carcasses on the Salton Sea shore. Salton Sea littoral sediments have received biomass derived from fish die-offs yearly since the late 1980s and this die off events can reach up to 20,000,000 individuals (Riedel et al., 2002; Hurlbert et al., 2007; Moreau et al., 2007; Marti-Cardona et al., 2008). Similar to Anderson et al., 2008, we found a strong correlation between C_{org} and N content in sediment.

Differences in sediment C_{org} content observed with depth (Fig. 6 B) reflect differences in biomass accumulation patterns in the Salton Sea littoral or differences in percolation patterns of dissolved organic carbon due to differences in sediment texture between North and South sediment. In North site, a higher C_{org} content below 4 cm compared to the surface sediment would suggests higher productivity in the past, while the opposite can be inferred from C_{org} content data across depth in South sediment. We cannot explain differences in productivity between the North and South Basins with the available data, but they may be due to differences in water mixing intensity as presented above. Autochthonous algae production and increased productivity due to eutrophication have been proposed to explain increasing C_{org} content in Salton Sea sediment sampled between 1961 and 2008 (Anderson et al., 2008). Massive algae deposition, which occurs seasonally in the Salton Sea (California Department of Water Resources, 2013), can tilt the balance between biomass degradation and accumulation towards accumulation, as observed in other shallow and hypereutrophic lakes (Xu et al., 2015). Another possibility is that higher clay content in sediment from the South site results in negligible

30

downward transport of dissolved organic carbon derived from organic matter oxidation at the sediment surface. On the contrary, lower clay content and the presence of gravel in North sediment would lead to increased oxygen diffusion, higher organic matter oxidation and the downward transport of dissolved forms of organic carbon to depths below 4 cm.
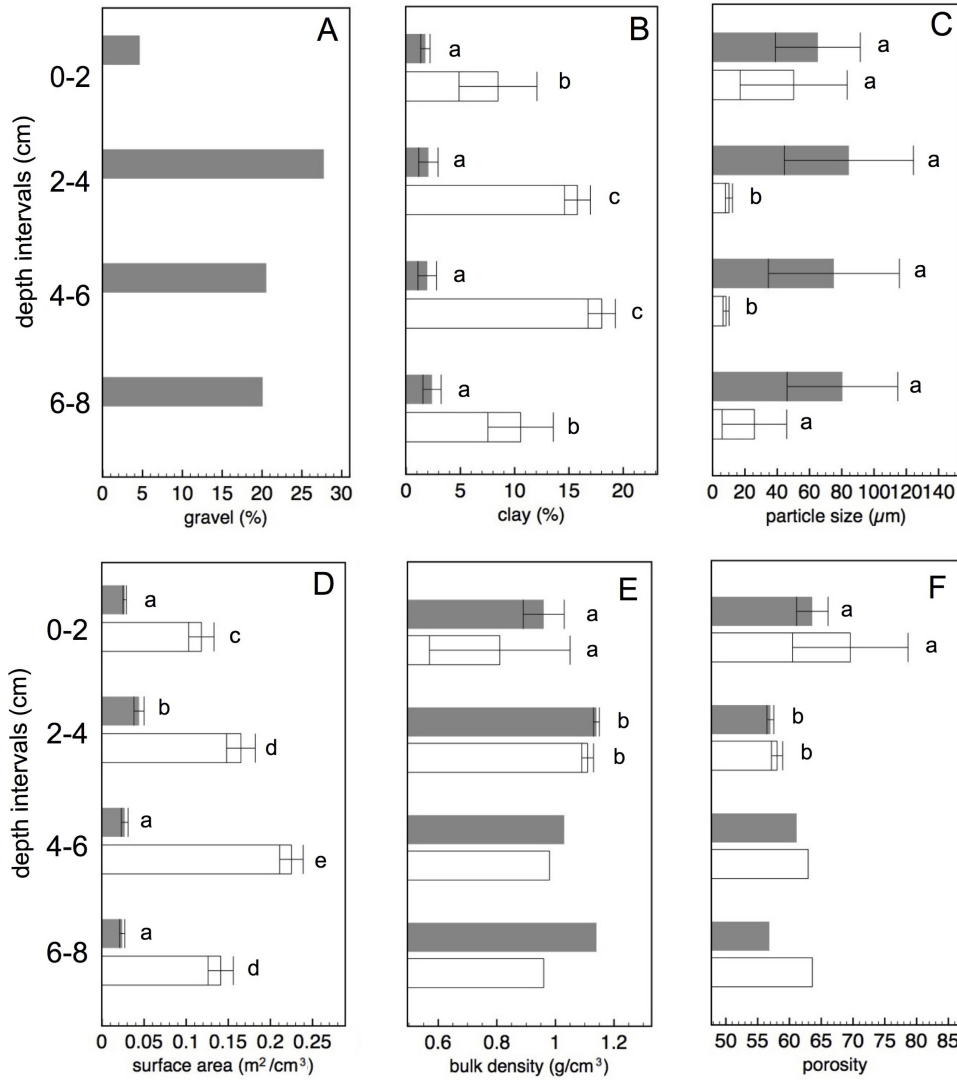
Figure 5: *Sediment gravel percentage (A), clay percentage (B), mean particle size (C), surface area (D), dry bulk density (E), and porosity (F) as a function of depth in North (gray) and South (white) sites. Values represent the average of three replicates ± standard deviation, except for bulk density and porosity at depths 4-6 and 6-8 cm in panels D and E (these data are the result of a single measurement and therefore no standard deviation can be calculated). Means with different letters are significantly different (Tukey's HSD, p<0.05).*

31
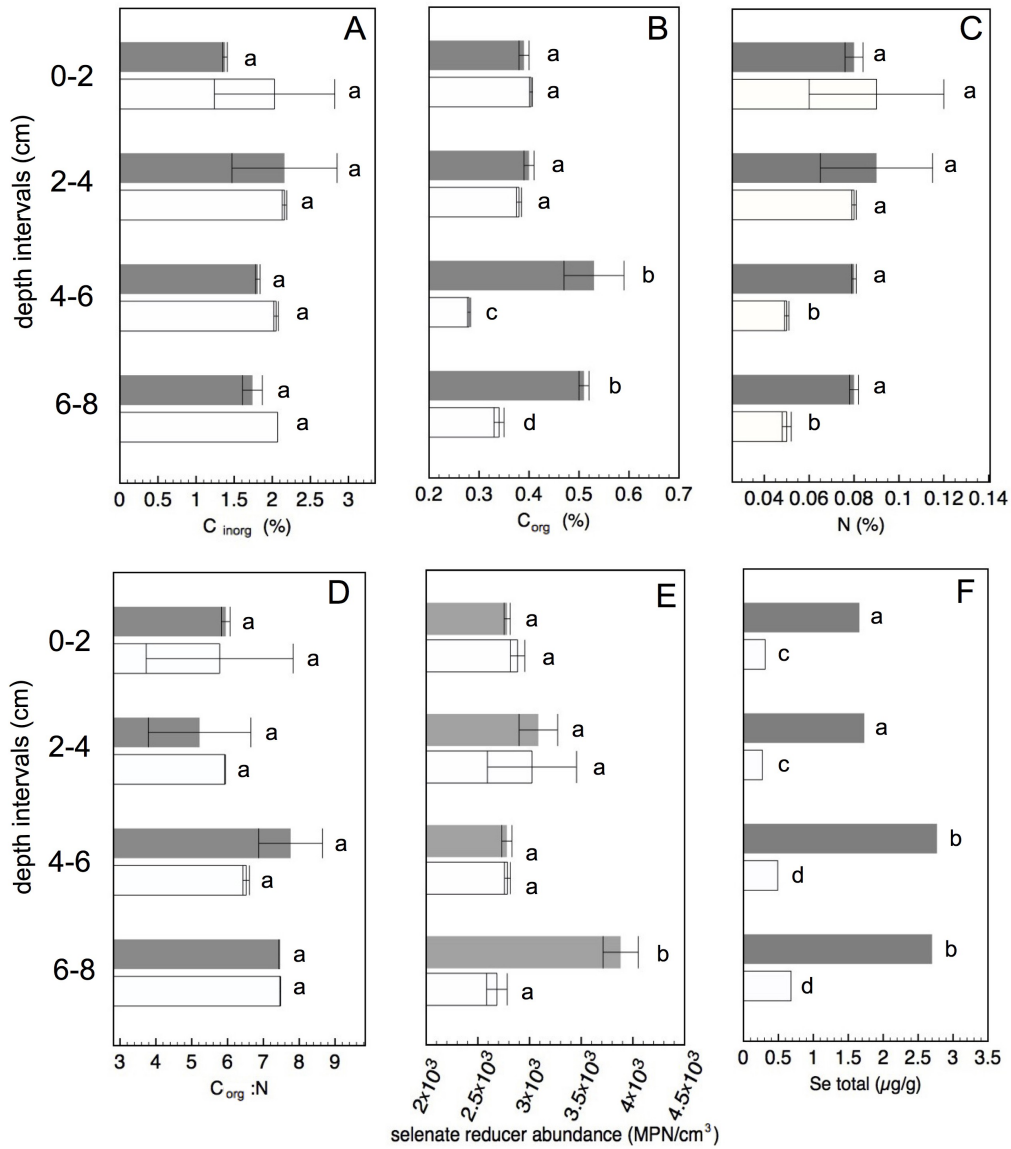
Figure 6: *Sediment inorganic carbon content (A), organic carbon content (B), nitrogen content (C), C_{org}:N (D), abundance of selenate reducers (E), and total selenium content (F) as a function of depth in the North (gray) and South (white) sites. Except for panel F, values represent the average of two replicates ± standard deviation and the absence of error bars represent standard deviations <0.02. Means with different letters are significantly different (Tukey's HSD, p<0.05).*
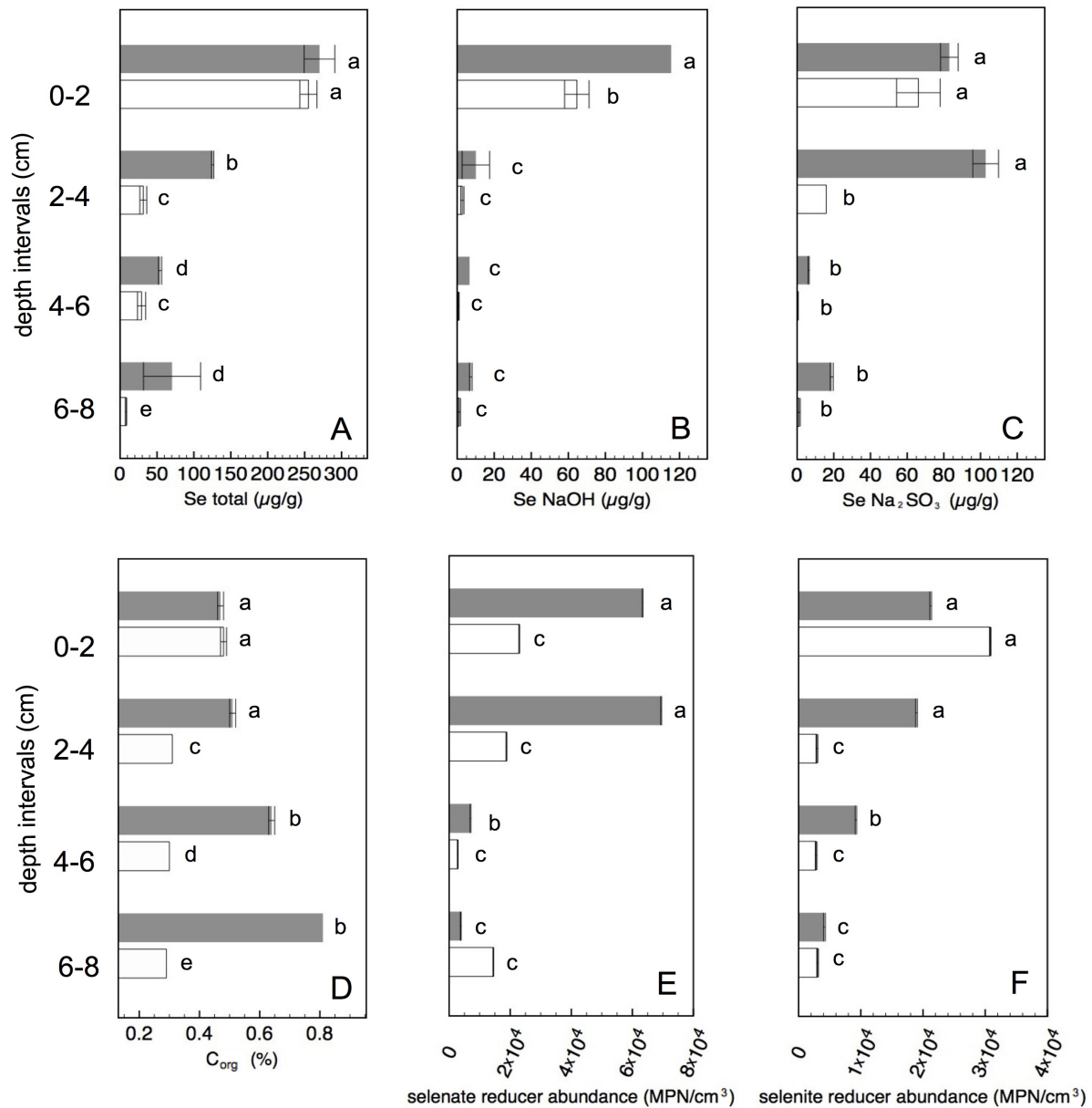
Figure 7: *Total selenium content (A), NaOH-associated selenium (B), elemental selenium content (C), organic carbon content (D), abundance of selenate-reducers (E) and abundance of selenite-reducers (F) as a function of depth in sediment from the North (gray) and South (white) sites recovered from FTRs. Values represent the average of two replicates ± standard deviation. The absence of error bars represent standard deviations <0.02. Means with different letters are significantly different (Tukey's HSD, p<0.05).*

4.2. Selenite and selenate sorption

We observed high selenite sorption in all sediments (Fig. 4 A) with adsorption potential increasing with depth and correlating positively with C_{org}:N suggesting an affinity of selenite for organic matter with proportionally lower N content. Our observation that selenite exhibits greater sorption than selenate is consistent with numerous previous work with soil, sediment and minerals (BarYosef & Meek, 1987; Su & Suarez, 2000; Hyun et al., 2006; Mandal et al., 2009). Selenite sorption to organic matter involves ternary complexation with metals and humic substances or associations with sediment polysacharides or fulvic acids (Fernández-Martínez & Charlet, 2009). Selenite sorption to organic matter remaind under investigation and could be greater than that associated with the mineral fraction (Coppin et al., 2006).

The unexpectedly high selenate sorption we observed in the sediment top 4 cm (Fig. 4 B) suggest that selenate sorption could be an important parameter controlling selenium retention in Salton Sea littoral sediment. Our observation of a high selenate sorption potential in the topmost 4 cm of North and South sediments was surprising since selenate has been shown to sorb only weakly to soil and sediment solid particles (Neal & Sposito, 1989; Zhang & Moore, 1997; Siddique et al., 2006; Amrhein & Doner, 2014). The lower sorption strength of selenate results from an electrostatic bonding mechanism, weaker if compared with the more stable ionic and covalent bonds that characterize selenite sorption (Sharmasarkar & Vance, 2002). Furthermore, selenate sorption decreases at alkaline pH due to the decrease of the aqueous $HSeO_4^-$ fraction (Singh et al., 1981; Rovira et al., 2008) and decreases with the increasing ionic strength of the solution (Singh et al., 1981; Jordan et al., 2011). On the other hand, organic matter (Singh et al., 1981; Balistrieri & Chao, 1987; Pezzarossa et al., 1999; Su & Suarez, 2000) and clays (Singh et al., 1981; Hyun et al., 2006) can be sorbants for selenate, however selenate sorption in usually negligible compared to selenite sorption. To our knowledge, three studies report high selenate sorption in soil. In a study by Singh et al. (1981), high organic carbon, calcareous, saline and alkali soils showed selenate sorption correlating positively with cation exchange capacity, organic carbon content, clay content and carbonate content, and negatively with salinity and alkalinity. Calcareous and saline soil sorbed, respectively, 46% and 31.8% of selenate in a 150 µM selenate solution, and all soils showed higher selenate sorption (between 26% and 40%) than selenite sorption (between 16% and 32%) at all selenium concentrations (Singh et al. 1981). In another study, selenate sorption to agricultural soil ranged between 3.6% and 24.6% and correlated positively with clay content, iron content and surface area, and negatively with sulfuric-acid extractable phosphorus (Vuori et al., 1989). A third study with coal mine soils found sorption percentages for selenate ranging between 44% and 95% (Sharmasarkar & Vance, 2002). High calcium content in sediment has been associated with an increase in the sorption of selenium oxyanions (Pezzarossa et al., 1999; Afzal et al., 2000; Wang et al., 2009). Salton Sea sediment has been shown to be saturated in regards to calcium carbonate, with average sediment $CaCO_3$ content of 24% and values as high as 50% in sediment from deeper parts of the lake (Anderson et al., 2008). We found inorganic carbon content to be between 3.4 and 6.6 times higher than organic carbon content in evaluated sediments, ranging between 1.4% and 2.2%. However, we did not find any significant correlations between inorganic carbon content and neither selenite nor selenate sorption. The role of high sulfate concentrations in Salton Sea water (9-13 g L^{-1}; Reese et al., 2008) in selenate sorption also has to be considered given that sulfate can suppress selenium sorption well above the enhancements related to calcium (Hyun et al., 2006). Therefore, organic carbon content, which correlated positively with selenate sorption, may explain the unexpectedly high selenate sorption values found in this study.

4.3. Sediment organic matter and selenium accumulation

Differences in selenium content between North and South littoral locations and across depth (Fig. 6 F) are influenced by sediment organic matter. Similar to Anderson et al. (2008), we found a strong and positive correlation between sediment C_{org} and total selenium content suggesting that higher accumulation of organic matter in North littoral locations leads to higher accumulation of selenium in sediments from the North site compared to those from the South site. Furthermore, we show a positive correlation between sediment C_{org} and selenate reducer abundance in North and South sediment. Organic matter thus seems to have a dual role during the retention of selenium in sediment. Organic matter can sorb selenium oxyanions (Coppin et al., 2009; Fernández-Martínez & Charlet, 2009), and also provides microbes with organic carbon, nitrogen and the reducing power required to grow and immobilize selenium (Oremland et al., 1989; Steinberg & Oremland, 1990; Ryu et al., 2011). The important role of sediment organic matter in selenium retention has been previously documented in soils and sediment from a variety of environments (Oades, 1988; Weres et al., 1990, Schroeder et al., 2002; Krantz, 2007; Martin et al., 2011; VillaRomero et al., 2013; Tolu et al., 2014).

The strong positive correlation found between sediment C_{org} and total selenium content in North and South sites corroborates previous studies that suggest selenium is bioassimilated and accumulates in trophic webs (Presser, 1994; Weres et al., 1990; Martin et al., 2011). The deposition of selenium-laden biomass can exacerbate selenium accumulation in Salton Sea littoral sediment. In shallow aquatic lacustrine environments from British Columbia and SE California, for example, the deposition of detritus containing selenium seems to govern selenium accumulation (Martin et al., 2011) in part because selenium enters the sediment environment in a fully bioassimilable form. In the Salton Sea littoral, dead fish, with tissue selenium concentration of 1.7-2.9 µg g^{-1} (Riedel et al., 2002; Moreau et al., 2007; Marti-Cardona et al., 2008), accumulate in areas where water birds intensively feed and can become an important source of selenium for both the littoral sediment and the piscivorous birds. This very same scenario has been thoroughly documented elsewhere in California and other Western states in the US (Presser et al., 1994).

4.4. Kinetic parameters for selenate reduction in FTRs: K_m and R_{max}

Our study is the first to report kinetic parameters for selenate reduction obtained from intact sediment and to demonstrate a wide cm-scale variation in R_{max} and K_m with depth (Fig. 3; Table 1). We showed a potential for selenate reduction in all sampled sediments, in which the Michaelis-Menten rate equation effectively described the consumption of selenate by Salton Sea sediment microbial communities (Fig. 3). Our data showed a positive correlation between K_m and R_{max}, linking low affinity for selenate with high potential for selenate reduction. We also show R_{max} values correlating positively the abundance of selenate reducers and total selenium content emphasizing the role of selenate reducers in selenium accumulation through microbial selenate reduction in the Salton Sea littoral.

R_{max} values obtained from FTRs at salinity 45 in this study, on the other hand, were within the range reported by Steinberg & Oremland, 1990, whom measured selenate reduction potential under salinities matching those of the original environment. R_{max} values obtained in this study were between one and three orders of magnitude lower than the largest values measured by Steinberg & Oremland, 1990. In a previous study with slurry experiments containing Salton Sea sediment collected from seven littoral locations, we found selenate reduction potential ranging between 29.1±13.3 and 294.9±40.8 nmol h^{-1} cm^{-3}. These R_{max} values are an order of magnitude higher than R_{max} reported in this study. VillaRomero et al., 2013,). In Salton Sea littoral sediment, highest selenate reduction potential occurred in the Alamo River delta which had a salinity of 3 (VillaRomero et al., 2013). Similar to

Steinberg & Oremland, 1990, VillaRomero et al., 2013 found no linear correlation between salinity and potential rates of selenate reduction. Microbial selenate reduction has been reported to occur at salinities between 100 and 240 in halophilic strains like *Selenihalanaerobacter shriftii* (Oren, 2011). Therefore, no significant impact of increasing salinity on selenate reduction would be expected in Salton Sea sediment.

K_m values in North and South Salton Sea sediment vary almost two orders of magnitude across depth (between 10 and 661 µM) (Fig. 3; Table 1) and are at least three orders of magnitude higher than selenate concentrations in Salton Sea water, which range between 0.5 and 2.0 µg L^{-1} (0.003 and 0.014 µM) (Holdren & Montaño, 2002; Schroeder et al., 2002). This indicates that, under *in situ* conditions, selenate reduction is limited by selenate availability and selenate-reducing microbial communities operate well below their selenate reduction potential. This diversity of affinities toward selenate compares to that obtained using sediment collected from 11 sampling sites across California and Nevada with pH, salinity and organic carbon content ranges of 7-9.8, 1-320 and 0.3%-10%, respectively (Steinberg & Oremland, 1990). That is, a range of K_m values similar to that found by Steinberg & Oremland, 1990, (7.9-720 µM) was found in a Salton Sea volume of sediment equal to 108 cm^3 (10-661 µM) (Fig. 3; Table 1) emphasizing the high degree of variability possible in a relatively small volume of sediment.

The lowest observed K_m values (Table 1) are close to the K_m value reported for the only known respiratory selenate reductase, SerA from *Thauera selenatis*, which has a K_m value of 16 µM (Schröder et al., 1997). This observation shows a high affinity towards selenate at 2-4 cm and 0-2 cm in North and South sediment, respectively, close to that of a purified selenate-specific selenate reductase and suggests that any incoming selenate would be rapidly reduced and immobilized in sediment from those depths.

Given that a selective pressure exists for sediment microbes to match K_m values to approximate environmental concentrations and optimize the responsiveness of microbial reaction rates (Sinsabaugh et al., 2014), the K_m values obtained in this study can be used to hypothesize the selenate concentrations that sediment microbes experience *in situ*. That is, K_m values not only reflect a broad diversity of affinities for selenate across sediment depth, but also suggest the range of selenate concentrations that microbial communities may experience in evaluated North and South littoral sediment. If correct, this interpretation suggests that in evaluated sediments selenate concentrations increase with depth. This interpretation would be consistent with an scenario in which incoming selenate is rapidly removed to reach low concentrations at 2-4 and 0-2 cm depth in North and South sediment, respectively, but accumulates to higher concentrations at lower depths. A simpler interpretation would be that microbial communities in sediment with K_m values for selenate above 15 µM are not exposed to significant selenate concentrations and given the availability of alternate electron acceptors, lack the selective pressure to lower their K_ms. A difficult point is the high K_m value detected in North sediment at 0-2 cm. We could speculate that selenate reduction in the North site takes place in the water column and reduced selenium species precipitate to the sediment surface, however, it is not possible to validate that hypothesis based on the available information.

The spatial segregation of maximal selenate reduction rates and R_{max} values corroborates previous observations regarding the prevalence of selenate reduction at the sediment surface (Oremland et al., 1989; Tokunaga et al., 1991, 1996; Velinsky & Cutter, 1991; Presser, 1994; Ryu et al., 2011) and highlights the importance of considering the method used to quantify selenate reduction rates during

data interpretation. In FTRs, microbes inhabiting the 2-4 cm depth in North sediment and the 0-2 cm depth in South sediment removed selenate at high rates (11.7±0.3 and 10.4±0.6 nmol cm^{-3} h^{-1} in North and South sediment, respectively) but showed R_{max} values lower than those measured in sediment from 6-8 cm (Fig. 3; Table 1). In contrast, sediment microbes at 6-8 cm showed both the highest K_m values for selenate and the highest R_{max} values but removed selenate from the FTR at lower rates (<6 nmol cm^{-3} h^{-1}). The fact that maximal selenate reduction rates were measured at the sediment surface while maximal R_{max} values were found at 6-8 cm also explains the significantly higher total selenium content found in Salton Sea littoral sediment at 4-8 cm depth (Fig. 6 F). That is, even though slurry experiments show that maximal selenate reduction rates occur at the sediment surface, FTR experiments show that maximal R_{max} values occur at 6-8 cm coinciding with maximal total selenium content in evaluated Salton Sea sediment.

Sediment slurries are convenient methods to rapidly quantify biogeochemical reaction rates under conditions that impose almost no limitations on microbial activity given that the tridimensional structure and distribution of microbes is destroyed, mass-transfer limitations are removed and therefore rates can achieve maximal values (Pallud & Van Cappellen, 2006; Pallud et al., 2007). These rates, however, may not be representative of field phenomena given that particular microbes may be selected and microbial-end products accumulate (Pallud & Van Cappellen, 2006; Pallud et al., 2007). Biogeochemical reaction rates and rate kinetic parameters derived from FTRs containing intact sediment samples, on the other hand, more closely reflect *in situ* processes because rate determinations are carried out under conditions of mass transfer limitation, microbial spatial distribution, and solid-bound substrate composition almost identical to those encountered in the field (Pallud & Van Cappellen, 2006). Consequently, K_m values obtained in slurry experiments can be highly variable, even for sediments from the same site, while K_m values obtained from FTR's fall within much narrower ranges (Pallud & Van Cappellen, 2006).

We show that elemental and organic-matter bound selenium forms represent the majority of reduced selenium in sediment recovered from FTRs, and account for 74% and 51% of total selenium in North and South sediment, respectively (Fig. 7 B and C). This suggests that microbial assimilatory reduction of selenate is more important than dissimilatory reduction during selenium accumulation and retention in sediment. The residual selenium fraction unaccounted by the sum of soluble, adsorbed, organic matter-bound, and elemental selenium fractions in North and South sediment most likely corresponds to reduced selenium forms recalcitrant to the extraction protocols employed. The recovery of adsorbed selenite with K_2HPO_4, for example, may be incomplete and miss between 36% and 19% of selenite in an inert silica matrix (Wright et al., 2003). Also, selenides incorporated into iron sulfide or pyrite may be more recalcitrant to extraction in either KCl, K_2HPO_4, NaOH or Na_2SO_3 but not in the $HClO_4$-HNO_3 digestion used to extract total selenium. On the other hand, our results agree with previous observations regarding the predominance of elemental and organic matter bound selenium as major products of selenate reduction in the environment (Keskinen et al., 2009; Martin et al., 2011; Ryu et al., 2011).

Our data show that the sorption of selenium oxyanions (Fig. 4) contributes more than microbial selenate reduction to the accumulation of selenium in Salton Sea littoral sediment. Selenate reduction is limited by the availability of selenate in sediment, as our K_m data show, while selenite and selenate sorption are high and potentially a more important during selenium accumulation. Given that the sediment K_m (10-15 µM) for selenate is at least 2 orders of magnitude higher than *in situ* selenate concentrations (0.0035-0.014 µM), selenate reduction in Salton Sea littoral sediment can not happen at

high rates. Selenium mobilized from the Colorado River delta enters the Salton Sea through seleniferous agricultural drainage water (Seiler, 2003). Incoming selenate is susceptible to unexpectedly high selenate sorption in the sediment surface of North and South sediment. Sediment from the 2-4 cm and 0-2 cm depths in North and South sediment, respectively, show the highest affinities toward selenate and can rapidly reduce it at high selenate reduction rates. However, selenate reduction potential is maximal at 6-8 cm which coincides with the significantly higher total selenium content, compared to the rest of evaluated depths, in sediment recovered from the Salton Sea. Selenite is produced from the dissimilatory reduction of selenate and is strongly retained in sediment, particularly that showing higher C_{org}:N values. We show that organic matter is an important parameter determining selenium retention in Salton Sea littoral sediment. In any case, elemental selenium and organic matter-bound selenium forms constitute the main products of microbial selenate reduction in sediment. Selenium sorption and bioaccumulation, in this way, represents a primary mechanism of selenium enrichment in evaluated sediment collected from the North and South Salton Sea littoral.

5. Conclusions

The diversity of sediment characteristics in North and South Salton Sea littoral sediment highlights the difficulties associated with predicting selenium accumulation patterns without sufficient information regarding the physical, chemical and microbial characteristics of sediment. In evaluated sediments, physical characteristics vary widely between locations and across depth due to the action of water currents. Differences in clay content lead to different patterns of C_{org} and N distribution across depth, which in turn influence selenium accumulation patterns by controlling the retention of selenate reducing microbes and the sorption of selenium oxyanions. Incoming selenate is reduced to biomass-associated and elemental selenium primarily. The interplay between sediment texture, organic carbon content, selenate and selenite sorption, selenate affinity, selenate reducer abundance, and maximum selenate reduction potential drive the accumulation of selenium in sediment with organic matter representing a key parameter due to its dual role as sorbant of selenium oxyanions and as a source of carbon, nitrogen and reducing power to support microbial selenate reduction. The prevalence of organic matter-bound selenium forms, compared to elemental selenium, suggests that microbial assimilatory selenate reduction is more important than microbial dissimilatory selenate reduction during selenium accumulation.

Our R_{max} and K_m data demonstrate that *in situ* selenate reduction across sediment depth is limited by the low availability of selenate and resident selenate-reducing microbial communities operate well below their maximum potential rate. In North and South sediment, the sediment surface has the greatest affinity for selenate and supports a microbial activity that can rapidly reduce increasing selenate concentrations. However, in the presence of selenate concentrations well below the K_m values measured here for sediment, microbial selenate reduction cannot achieve significantly high rates. Given the unexpectedly high selenate sorption found in evaluated sediment, sorption of selenium oxyanions seems to be more important that microbial selenate reduction during selenium accumulation in evaluated sediments.

Sediment at 6-8 cm shows the highest potential for selenate reduction which explains higher total selenium content at depths below 4 cm. Upon being immobilized in sediment, selenium is incorporated in sediment biomass and becomes accumulated in higher food-chain organisms through the consumption of a selenium rich diet. The rapid transference of selenium from dissolved pools in water to the sediment surface of sediment grains and biomass in selenium-ingesting sediment biota, coupled to the slow oxidation of reduced selenium species results in a net accumulation of selenium in

Salton Sea littoral sediment. Lastly, data obtained from hypersaline environments is scarce and FTRs represent powerful and convenient methods to quantify selenate reduction rates and reaction rate kinetics under the changing condition expected to affect the Salton Sea in the future.

6. References

Afzal, S., M. Younas, & K. Ali, 2000. Selenium Speciation Studies from Soan-Sakesar Valley, Salt Range, Pakistan. Water International 25: 425–436.

Amrhein, C., & H. Doner, 2014. Biogeochemistry of Trace Elements: Reactions in Soils. In Chang, A. C., & D. B. Silva (eds), Salinity and Drainage in San Joaquin Valley, California. Springer Netherlands: 123–146.

Anderson, M., L. Whiteaker, E. Wakefield, & C. Amrhein, 2008. Properties and distribution of sediment in the Salton Sea, California: an assessment of predictive models. In Hurlbert, S. H. (ed), The Salton Sea Centennial Symposium. Springer Netherlands: 97–110.

Balistrieri, L., & T. Chao, 1987. Selenium Adsorption by Goethite. Soil Science Society of America Journal 51: 1145.

BarYosef, B. & D. Meek, 1987. Selenium sorption by kaolinite and montmorillonite. Soil Science. 144:11-19.

Bianchi, T. S., 2012. Estuarine Chemistry. In Day, J. W., B. C. Crump, W. M. Kemp, & A. Yáñez-Arancibia (eds), Estuarine Ecology. John Wiley & Sons, Inc.: 39–83.

Butler, C., C. Debieux, E. Dridge, P. Splatt, & M. Wright, 2012. Biomineralization of selenium by the selenate-respiring bacterium *Thauera selenatis*. Biochemical Society Transactions 40: 1239–1243.

Byron, E., & H. Ohlendorf, 2007. Diffusive flux of selenium between lake sediment and overlying water: Assessing restoration alternatives for the Salton Sea. Lake and Reservoir Management 23: 630–636.

California Department of Water Resources, Department of Fish and Wildlife, 2013. Salton Sea, Species Conservation Habitat Project, Final Environmental Impact Statement/Environmental Impact Report.

Carter, M. & E. Gregorich, 2007. Soil Sampling and Methods of Analysis. CRC Press.

Chapman, P., W. Adams, M. Brooks, C. Delos, S. Luoma, W. Maher, H. Ohlendorf, T. Presser, & P. Shaw, 2010. Ecological assessment of selenium in the aquatic environment. CRC Press.

Coppin, F., C. Chabroullet, A. Martin-Garin, J. Balesdent, & J. Gaudet, 2006. Methodological approach to assess the effect of soil ageing on selenium behaviour: first results concerning mobility and solid fractionation of selenium. Biology and Fertility of Soils 42: 379–386.

Darcheville, O., L. Février, F. Haichar, O. Berge, A. Martin-Garin, & P. Renault, 2008. Aqueous, solid and gaseous partitioning of selenium in an oxic sandy soil under different microbiological states. Journal of Environmental Radioactivity 99: 981–992.

Duc, M., G. Lefevre, M. Fedoroff, J. Jeanjean, J. C. Rouchaud, F. Monteil-Rivera, J. Dumonceau, & S. Milonjic, 2003. Sorption of selenium anionic species on apatites and iron oxides from aqueous solutions. Journal of Environmental Radioactivity 70: 61–72.

Fernández-Martínez, A., & L. Charlet, 2009. Selenium environmental cycling and bioavailability: a structural chemist point of view. Reviews in Environmental Science and Biotechnology 8: 81–110.

Foster, A., G. Brown Jr., & G. Parks, 2003. X-ray absorption fine structure study of As(V) and Se(IV) sorption complexes on hydrous Mn oxides. Geochimica et Cosmochimica Acta 67: 1937–1953.

Frankenberger, 1994. Selenium in the Environment. CRC Press.

Frankenberger, W., & R. Engberg, 1998. Environmental Chemistry of Selenium. CRC Press.

Gobler, C., A. Lobanov, Y. Tang, A. Turanov, Y. Zhang, M. Doblin, G. Taylor, S. Sañudo-Wilhelmy, I. Grigoriev, & V. Gladyshev, 2013. The central role of selenium in the biochemistry and ecology of the harmful pelagophyte, Aureococcus anophagefferens. The ISME Journal 7: 1333–1343.

Godwin, C., & J. Cotner, 2015. Aquatic heterotrophic bacteria have highly flexible phosphorus content and biomass stoichiometry. The ISME Journal 9: 2324–2327.

Hamilton, S., 2004. Review of selenium toxicity in the aquatic food chain. Science of the total

environment 326: 1–31.

Holdren, G., & A. Montaño, 2002. Chemical and physical characteristics of the Salton Sea, California. Hydrobiologia 473: 1–21.

Hurlbert, A., T. Anderson, K. Sturm, & S. Hurlbert, 2007. Fish and fish-eating birds at the Salton Sea: a century of boom and bust. Lake and Reservoir Management 23: 469–499.

Hyun, S., P. Burns, I. Murarka, & L. Lee, 2006. Selenium(IV) and (VI) Sorption by Soils Surrounding Fly Ash Management Facilities. Vadose Zone Journal 5: 1110–1118.

Jellison, R., R. Anderson, J. Melack, & D. Heil, 1996. Organic matter accumulation in sediments of hypersaline Mono Lake during a period of changing salinity. Limnology and Oceanography 41: 1539–1544.

Jordan, N., H. Foerstendorf, S. Weib, K. Heim, D. Schild, & V. Brendler, 2011. Sorption of selenium(VI) onto anatase: Macroscopic and microscopic characterization. Geochimica et Cosmochimica Acta 75: 1519–1530.

Krantz, T., 2006. Salton Sea, California. In Encyclopedia of Earth. Eds. Brian Black. Environmental Information Coalition, National Council for Science and the Environment, Washington, D.C.

Lemly, D., 2002. Selenium Assessment in Aquatic Ecosystems: A Guide for Hazard Evaluation and Water Quality Criteria. Springer Science & Business Media.

Lemly, D., 2014. Teratogenic effects and monetary cost of selenium poisoning of fish in Lake Sutton, North Carolina. Ecotoxicology and Environmental Safety 104: 160–167.

Lenz, M., & P. Lens, 2009. The essential toxin: The changing perception of selenium in environmental sciences. Science of the total environment 407: 3620–3633.

Liao, C., X. Liang, M. Soupir, & L. Jarboe, 2015. Cellular, particle and environmental parameters influencing attachment in surface waters: a review. Journal of Applied Microbiology 119(2): 315–330.

Mandal, S., S. Mayadevi, & B. Kulkarni, 2009. Adsorption of Aqueous Selenite [Se(IV)] Species on Synthetic Layered Double Hydroxide Materials. Industrial & Engineering Chemistry Research 48: 7893–7898.

Marti-Cardona, B., T. Steissberg, S. Schladow, & S. Hook, 2008. Relating fish kills to upwellings and wind patterns in the Salton Sea In Hurlbert, S. (ed), The Salton Sea Centennial Symposium. Springer Netherlands: 85–95.

Martin, A., S. Simpson, S. Fawcett, C. Wiramanaden, I. Pickering, N. Belzile, Y. Chen, J. London, & D. Wallschläger, 2011. Biogeochemical Mechanisms of Selenium Exchange between Water and Sediments in Two Contrasting Lentic Environments. Environmental Science & Technology 45: 2605–2612.

McMahon, S., & J. Parnell, 2014. Weighing the deep continental biosphere. FEMS Microbiology Ecology 87: 113–120.

Miles, K., M. Ricca, A. Meckstroth, & S. Spring, 2009. Salton Sea Ecosystem Monitoring Project. U.S. Geological Survey Open-File Report 2009–1276.

Monteil-Rivera, F., M. Fedoroff, J. Jeanjean, L. Minel, M. Barthes, & J. Dumonceau, 2000. Sorption of selenite (SeO_3^{2-}) on hydroxyapatite: An exchange process. Journal of Colloid and Interface Science 221: 291–300.

Moreau, M., J. Surico-Bennett, M. Vicario-Fisher, R. Gerads, R. Gersberg, & S. Hurlbert, 2007. Selenium, arsenic, DDT and other contaminants in four fish species in the Salton Sea, California, their temporal trends, and their potential impact on human consumers and wildlife. Lake and Reservoir Management 23: 536–569.

Neal, R., & G. Sposito, 1989. Selenate Adsorption on Alluvial Soils. Soil Science Society of America Journal 53: 70.

Oades, J., 1988. The retention of organic matter in soils. Biogeochemistry 5: 35–70.

Oremland, R., J. Hollibaugh, A. Maest, T. Presser, L. Miller, & C. Culbertson, 1989. Selenate Reduction to Elemental Selenium by Anaerobic Bacteria in Sediments and Culture: Biogeochemical Significance of a Novel, Sulfate-Independent Respiration. Applied and Environmental Microbiology 55: 2333–2343.

Oremland, R., N. Steinberg, A. Maest, L. Miller, & J. Hollibaugh, 1990. Measurement of in situ rates of selenate removal by dissimilatory bacterial reduction in sediments. Environmental Science & Technology 24: 1157–1164.

Pallud, C., C. Meile, A. Laverman, J. Abell, & P. Van Cappellen, 2007. The use of flow-through sediment reactors in biogeochemical kinetics: Methodology and examples of applications. Marine Chemistry 106: 256–271.

Pallud, C., & P. Van Cappellen, 2006. Kinetics of microbial sulfate reduction in estuarine sediments. Geochimica et Cosmochimica Acta 70: 1148–1162.

Pezzarossa, B., D. Piccotino, & G. Petruzzelli, 1999. Sorption and desorption of selenium in different soils of the mediterranean area. Communications in Soil Science and Plant Analysis 30: 2669–2679.

Presser, T., 1994. The Kesterson effect. Environmental Management 18: 437–454.

Presser, T., M. Sylvester, & W. Low, 1994. Bioaccumulation of selenium from natural geologic sources in western states and its potential consequences. Environmental Management 18: 423–436.

Reese, B., & M. Anderson, 2009. Dimethyl sulfide production in a saline eutrophic lake, Salton Sea, California. Limnology and Oceanography 54: 250–261.

Reese, B., M. Anderson, & C. Amrhein, 2008. Hydrogen sulfide production and volatilization in a polymictic eutrophic saline lake, Salton Sea, California. Science of the total environment 406: 205–218.

Riedel, R., D. Schlenk, D. Frank, & B. Costa-Pierce, 2002. Analyses of organic and inorganic contaminants in Salton Sea fish. Marine Pollution Bulletin 44: 403–411.

Rovira, M., J. Giménez, M. Martínez, X. Martínez-Lladó, J. de Pablo, V. Martí, & L. Duro, 2008. Sorption of selenium (IV) and selenium (VI) onto natural iron oxides: Goethite and hematite. Journal of Hazardous Materials 150: 279–284.

Roychoudhury, A., E. Viollier, & P. Van Cappellen, 1998. A plug flow-through reactor for studying biogeochemical reactions in undisturbed aquatic sediments. Applied Geochemistry 13: 269–280.

Ryu, J., S. Gao, & K. Tanji, 2011. Accumulation and speciation of selenium in evaporation basins in California, USA. Journal of Geochemical Exploration 110: 216–224.

Saha, U., & P. Huang, 2010. Surface coverage effects on the desorption kinetics of selenite from a hydroxyaluminum–montmorillonite complex. Journal of colloid and interface science 350: 320–329.

Santos, I., B. Eyre, & M. Huettel, 2012. The driving forces of porewater and groundwater flow in permeable coastal sediments: A review. Estuarine, Coastal and Shelf Science 98: 1–15.

Schladow, S., W. Fleenor, F. Bombardelli, & E. Chung, 2007. Quantifying sediment resuspension linkages to nutrient enrichment in the existing and future Salton Sea. University of California Water Resources Center Technical Completion Report No. W-998.

Schroeder, R., W. Orem, & Y. Kharaka, 2002. Chemical evolution of the Salton Sea, California: nutrient and selenium dynamics. In Barnum, D., J. Elder, D. Stephens, & M. Friend (eds), The Salton Sea. Springer Netherlands.

Schroeder, R. & W. Orem, 2000. Nutrient Dynamics in the Salton Basin--implications from Calcium, Uranium, Molybdenum, and Selenium. U.S. Geological Survey.

Schroeder, R. & M. Rivera, 1993. Physical, chemical, and biological data for detailed study of

irrigation drainage in the Salton Sea area, California. U.S. Geological Survey Open-File Report 93-83.

Schulthess, C., & Z. Hu, 2001. Impact of Chloride Anions on Proton and Selenium Adsorption by an Aluminum Oxide. Soil Science Society of America Journal 65: 710.

Seiler, R., 2003. Irrigation-induced contamination of water, sediment, and biota in the western United States: Synthesis of data from the National Irrigation Water Quality Program. U.S. Department of the Interior, U.S. Geological Survey.

Sharmasarkar, S., & G. Vance, 2002. Selenite–selenate sorption in surface coal mine environment. Advances in Environmental Research 7: 87–95.

Siddique, T., Y. Zhang, B. Okeke, & W. Frankenberger Jr., 2006. Characterization of sediment bacteria involved in selenium reduction. Bioresource Technology 97: 1041–1049.

Singh, M., N. Singh, & P. Relan, 1981. Adsorption and desorption of selenite and selenate selenium. Soil Science 132: 2.

Steinberg, N., & R. Oremland, 1990. Dissimilatory Selenate Reduction Potentials in a Diversity of Sediment Types. Applied and Environmental Microbiology 56: 3550–3557.

Stolz, J., P. Basu, J. Santini, & R. Oremland, 2006. Arsenic and Selenium in Microbial Metabolism. Annual Review of Microbiology 60: 107–130.

Stolz, J., & R. Oremland, 1999. Bacterial respiration of arsenic and selenium. FEMS Microbiology Reviews 23: 615–627.

Su, C., & D. Suarez, 2000. Selenate and Selenite Sorption on Iron Oxides. Soil Science Society of America Journal 64: 101.

Tokunaga, T., D. Lipton, S. Benson, A. Yee, J. Oldfather, E. Duckart, P. Johannis, & K. Halvorsen, 1991. Soil selenium fractionation, depth profiles and time trends in a vegetated site at Kesterson Reservoir. Water, Air, and Soil Pollution 57-58: 31–41.

Tokunaga, T., I. Pickering, & G. Brown, 1996. Selenium Transformations in Ponded Sediments. Soil Science Society of America Journal 60: 781.

Tolu, J., Y. Thiry, M. Bueno, C. Jolivet, M. Potin-Gautier, & I. Le Hécho, 2014. Distribution and speciation of ambient selenium in contrasted soils, from mineral to organic rich. Science of the total environment 479–480: 93–101.

Turner, A., 2013. Selenium in sediments and biota from estuaries of southwest England. Marine Pollution Bulletin 73: 192–198.

US Environmental Protection Agency, 2010. California's 2008-2010 Section 303(d) list of impaired waters. California State Water Resources Control Board, Sacramento.

US Environmental Protection Agency, 2015. Draft aquatic life chronic criterion for selenium in freshwater, Vol. EPA-822-P-15-001. US Environmental Protection Agency, Washington, DC.

vanDuren, L. & Middelburg, 2011. The Benthic Boundary Layer: Transport Processes and Biogeochemistry. Eos Transactions. AGU 82(52) 658-659.

Velinsky, D., & G. Cutter, 1991. Geochemistry of selenium in a coastal salt marsh. Geochimica et Cosmochimica Acta 55: 179–191.

Vuori, E., J. Vääriskoski, H. Hartikainen, P. Vakkilainen, J. Kumpulainen, & K. Niinivaara, 1989. Sorption of selenate by finnish agricultural soils. Agriculture, Ecosystems & Environment 25: 111–118.

VillaRomero, J., M. Kausch, & C. Pallud, 2013. Selenate reduction and adsorption in littoral sediments from a hypersaline California lake, the Salton Sea. Hydrobiologia 709: 129–142.

Vogl, R., & R. Henry, 2002. Characteristics and contaminants of the Salton Sea sediments. Hydrobiologia 473: 47–54.

Wang, T., J. Wang, Y. Tang, H. Shi, & K. Ladwig, 2009. Leaching Characteristics of Arsenic and

Selenium from Coal Fly Ash: Role of Calcium. Energy & Fuels 23: 2959–2966.

Weres, O., H. Bowman, A. Goldstein, E. Smith, L. Tsao, & W. Harnden, 1990. The effect of nitrate and organic matter upon mobility of selenium in groundwater and in a water treatment process. Water, Air, and Soil Pollution 49: 251–272.

Weres, O., A. Jaouni, & L. Tsao, 1989. The distribution, speciation and geochemical cycling of selenium in a sedimentary environment, Kesterson Reservoir, California, U.S.A. Applied Geochemistry 4: 543–563.

Woomer, P. L., 1994. Most Probable Number Counts. In Methods of Soil Analysis: Part 2 - Microbiological and Biochemical Properties 59–79.

Xu, X., W. Li, M. Fujibayashi, M. Nomura, O. Nishimura, & X. Li, 2015. Predominance of terrestrial organic matter in sediments from a cyanobacteria- blooming hypereutrophic lake. Ecological Indicators 50: 35–43.

Zhang, Y., & J. Moore, 1997. Controls on selenium distribution in wetland sediment, Benton Lake, Montana. Water, Air, and Soil Pollution 97: 323–340.

Chapter 3 — Potential microbial pathways and thermodynamic constraints of selenate reduction in an halophilic microbial consortium isolated from Salton Sea littoral sediment capable of selenium removal

Juan Fernando Villa-Romero

Department of Plant and Microbial Biology, University of California, Berkeley

Abstract

Selenium accumulation in Salton Sea littoral sediment and the transfer of selenium from inorganic pools to trophic webs represent a threat to important waterfowl populations that rely on vital resources the Salton Sea habitat provides. The accumulation of selenium in sediment results from the adsorption of water-soluble selenium oxyanions and from the microbial reduction of incoming selenate through assimilatory pathways that lead to selenium incorporation in aminoacids or dissimilatory pathways that led to the formation of less mobile reduced selenium species, selenite and elemental selenium. I isolated a microbial consortia from North Salton Sea littoral sediment collected from the 6-8 cm depth interval. This consortia, referred here as SS-1, is capable of growing at 30°C and salinity 45 in 10 mM selenate and consistently produced red elemental selenium in minimal media supplemented with 10 mM lactate. SS-1 was capable of growing in nitrate, but not in selenite, nitrite, sulfate or sulfite. When incubated in the presence of nitrate and selenate, the removal of selenate by SS-1 followed the removal of nitrate and was completed only after all nitrate was consumed from the media. Multiple attempts to obtain axenic cultures from SS-1 were unsuccessful.

I also performed slurry experiments with sediment collected from two Salton Sea littoral sites to show that higher nitrate reduction rates corresponded to higher selenate reduction rates.

These observations corroborate previous reports regarding the role of nitrate reducers in selenium cycling and suggest nitrate reducers play an important role during the immobilization of selenium in Salton Sea littoral sediment. Once immobilized in sediment, selenium enters the trophic webs that ultimately lead to selenium bioaccumulation in waterfowl. In barnacle shells recovered from the Salton Sea littoral, I found selenium concentrations reaching 7.22 µg g^{-1}, a value almost twice that of total selenium content in sediment. This chapter evaluates these preliminary data and provides an in-depth review of the biogeochemical cycle of selenium in sediment. I review the assimilatory and dissimilatory microbial pathways that lead to selenium retention in sediment, bioenergetic data relevant to selenate respiration and microbial biomass synthesis in natural environments, and the microbial diversity of the Salton Sea ecosystem. This chapter concludes with an outline of the potential mechanisms linking selenium sorption, microbial selenate reduction and selenium bioaccumulation in the Salton Sea ecosystem.

1. Introduction

Selenium (Se) is a chalcogen, an essential micronutrient (Gladyshev et al., 2012; Winkel et al., 2012), and one of the most common toxic trace elements in contaminated soils (Navarro et al., 2015). Selenium naturally occurs in four oxidation states: -II, 0, IV, and VI. In oxic environments, water-soluble selenium oxyanions predominate either as selenate (Se(VI), as SeO_4^{2-}), a highly mobile ion, and/or selenite (Se(IV), as SeO_3^{2-}) which is highly susceptible to sorption and therefore considered immobile (Saha & Huang, 2010; Amrhein & Doner, 2014). Selenate, selenite and organic selenides are toxic and known to bioaccumulate (Lemly, 2014) whereas elemental selenium is solid, insoluble, virtually immobile and biologically inert (Stolz et al., 2006; Gladyshev et al., 2012). In sediment, microbes can couple the oxidation of organic carbon to the reduction of selenium oxyanions through a variety of pathways, including assimilatory reduction that incorporates selenium into aminoacids

45

(Gladyshev et al., 2012) and dissimilatory reduction that couples growth to the reduction of selenate to selenite and of selenite to elemental selenium (Stolz et al., 2002). Microbial dissimilatory selenate reduction is a key process transferring selenium from water to sediment in aquatic ecosystems (Oremland et al., 1989; Steinberg & Oremland, 1990). Selenium immobilized in sediment represents more than 90% of the total selenium present in wetland environments (Afzal et al., 2000) and may become available to microorganisms, animals and plants that can bioaccumulate selenium to concentrations 1-3 orders of magnitude higher than those present in water (Turner, 2013; US Environmental Protection Agency, 2014).

The Salton Sea is the largest lake in California, and is part of the state's 303(d) list of impaired water bodies (US Environmental Protection Agency, 2012). Selenate concentrations in waters that feed the Salton Sea frequently exceed federal regulatory concentration limits for selenium for protection of aquatic life (3.1 µg L^{-1}, 0.022 µM) (US Environmental Protection Agency, 2015), however, dissolved selenium concentrations in Salton Sea water are low and range between 0.5 and 2.0 µg L^{-1} (0.003-0.014 µM) (Holdren & Montaño, 2002; Schroeder et al., 2002). Salton Sea sediments showed high potential selenate reduction rates (VillaRomero et al., 2013; Chapter 2) and a high selenium content that ranged between 0.27 and 15 µg g^{-1}, about 30 times larger than that in surrounding soil (Schroeder et al., 2000; Byron & Ohlendorf, 2007; VillaRomero et al., 2013; Chapter 2). Salton Sea sediments are considered major selenium sinks for selenium mobilized from the Colorado River Basin (Schroeder & Rivera, 1993; Schroeder et al., 2002). Only minor loss of selenium through volatilization occurs in the Salton Sea (Schroeder et al., 2002) and virtually all of the selenium entering the lake is currently sequestered within its sediments.

In anoxic sediment, microbes can couple the oxidation of organic matter to the reduction of inorganic ions (Lovley, 1993; Bianchi, 2012). Sulfate is the dominant terminal electron acceptor in the Salton Sea given its elevated concentrations in water (9-13 g L^{-1}) (Reese & Anderson, 2009; Swan et al., 2010). Nitrate concentrations in Salton Sea water, on the other hand, are below 0.2 mg L^{-1} (Reese et al., 2008). Selenate respiration can support microbial growth in Salton Sea littoral sediment but is limited by the availability of selenate (Chapter 2). The reduction of selenate to selenite is energetically favored at a pE below 7.5 (neutral pH) placing it between nitrate and manganese oxides on the redox ladder (Sposito et al., 1991). Therefore, sulfate levels and sulfate reduction are not expected to inhibit selenate reduction in the Salton Sea. The role of nitrate-reducers in selenate reduction in aquatic environments has been extensively documented. Most organisms capable of selenate reduction are classified as nitrate-reducers (Stolz & Oremland, 1999) and both, nitrate inhibition of selenate reduction (Oremland et al., 1989; Fellowes et al., 2013) and the simultaneous reduction of nitrate and selenate (Bailey et al., 2013) have been reported.

After oxidized selenium forms are microbially reduced, selenium becomes bioavailable and can enter the trophic webs that threaten waterfowl, primarily through ingestion (Presser & Luoma, 2010, 2013; US Environmental Protection Agency, 2015). Invertebrates inhabiting sediment accumulate selenium largely through ingestion of selenium-containing particulate matter and sediment biota (Turner, 2013; US Environmental Protection Agency, 2014). Barnacles dominate sediment in the Salton Sea North littoral region (Detwiler et al., 2002; Schroeder et al., 2002) (Fig. 1) and can be of special concern, however, no studies have been done regarding the selenium content of these invertebrates in the Salton Sea littoral. Barnacles are abundant in many littoral areas of the Salton Sea (California Department of Water Resources, Department of Fish and Wildlife, 2013), show the highest known accumulated trace metal concentrations among marine invertebrates (Rainbow & Wang, 2005),

and have been shown to accumulate selenium up to 72.59 µg g^{-1} in selenium contaminated marine environments (Muhamed Ashraf et al., 2007). Most reports of selenium concentration in barnacles recovered from selenium contaminated and non-contaminated environments range between 0.7 and 81 µg g^{-1} (Gay & Maher, 2003; Muhamed Ashraf et al., 2007) with no clear effect reported regarding differences between selenium contaminated and non contaminated sites.

Figure 1. A core sample collected from Salton City shown to illustrate the abundance of barnacles in littoral sediment collected across a vertical depth gradient. Each ring has a depth equal to 2 cm (Photo: Juan Fernando Villa-Romero)

In previous chapters we show that organic carbon has a dual role as sorbant of selenium oxyanions and as a source of reducing power for microbes that drive selenate reduction in Salton Sea sediment. However, the link that connects microbial selenate reduction to selenium bioaccumulation in

the Salton Sea environment has not been investigated. An explanation to the higher selenium contents found in North littoral sediment, compared to South littoral sediment, for example, remains elusive. Given the abundance of barnacles in sediment from the North littoral region, it is possible that this organism serves as a link between the microbial pathways that transfer selenium from water to sediment, and the bioavailable selenium forms that enter and accumulate in trophic webs that lead to selenium poisoning in waterfowl.

Microbial selenate reduction, like most biogeochemical reactions, is an autocatalytic process, meaning that an increase in the population of microbes catalyzing a particular reaction leads to an increase in reaction rate (Jin & Bethke, 2007). Therefore, the ability to predict the rate of microbial biomass synthesis, for selenate reducers in this case, would be useful inform models that incorporate microbially driven selenate reduction rates to better understand selenium accumulation in Salton Sea littoral sediment. The recovery of axenic cultures is crucial to understand not only the molecular mechanisms of selenate reduction, but also the possible range of physiologies that microbes performing similar operations in the same environment have. In the case of selenium, data regarding the microbes and microbial mechanisms that cycle selenium in the environment remains limited. In this chapter I provide a broad evaluation of the microbial mechanisms that lead to selenium accumulation in Salton Sea sediment to provide a reference during future research.

To better define the microbial pathways that lead to selenium accumulation in the Salton Sea littoral, I performed experiments with a microbial consortia isolated from North littoral sediment and with slurries prepared with sediment recovered from littoral locations impacted by urban and agricultural development. In order to evaluate the risk associated with selenium accumulation in barnacles inhabiting the Salton Sea North littoral region, I also quantified the selenium content in barnacles collected from this site. I present data suggesting that nitrate-reduction pathways are important and participate in microbial processes that lead to selenium accumulation in sediment from the Salton Sea littoral. I also present data regarding the selenium content of barnacle shells collected across a depth gradient 0-8 cm at 2 cm depth intervals in a site located in the North Salton Sea littoral to show that selenium content in barnacles is almost twice that of total selenium content in sediment.

Given that recovering axenic cultures from the isolated consortia was unsuccessful, I review here the microbial pathways that lead to selenium immobilization in sediment, the thermodynamic constraints associated with microbial growth and microbial selenate respiration, and the microbial diversity reported in Salton Sea water and sediment. I hope this information is useful to future research efforts aimed at characterizing selenium accumulation in the Salton Sea, and to efforts aimed at applying the vastly unexplored selenate reduction potential of microbes to solve the global problem of selenium pollution.

2. Materials and Methods
2.1. Nitrate and selenate reduction in sediment slurries
Salton Sea sediment was collected from the water-sediment interface down to a depth of 5 cm using a hand pushed corer 1-2 m from the shore line at a water depth no greater than 0.5 m. Two sites located in the Salton Sea littoral were sampled in February 2010 (Fig. 2) due to their location close to urban and agricultural development areas.
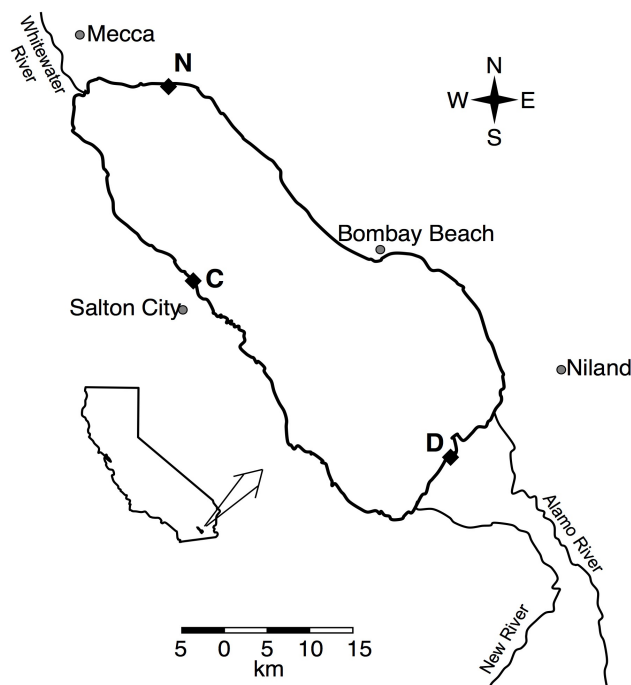
Figure 2. *Map showing the location of the Salton Sea in California and of three sites (diamonds) sampled along the littoral of the Salton Sea*

Site C was located on the shoreline of Salton City (N33.32875° W115.941778°), one of the largest urban developments on the Salton Sea coast, while site D was located at the South end of the lake (N33.153917° W115.649111°), in between the Alamo and New Rivers heads and across a large agricultural field (Fig. 2). Site C was located close to the Marina at West Shores on a mudflat surrounded by rocks and extending 1-2 m to the border of the lake (Fig. 3). Barnacles, fish carcasses and fish bones were visible but not abundant. Water in site C was calm and the water-sediment interface was easy to identify. Collected sediments were uniformly black-to-grey and gave a slight sulfidic smell (Fig. 4).

Site D was located on a narrow sandy playa free from barnacle shells, fish bones and fish carcasses (Fig. 5). Water overlying the sampling site was calm and clear, and the water-sediment interface was easy to identify. Collected sediments gave a slight smell of hydrogen sulfide and consisted of a thin brown layer (~5 mm depth) underlain by a gray layer (Fig. 6). Sediment samples were preserved at 4°C under anoxic conditions during transportation and immediately used to assemble sediment slurries at the laboratory.

Ten replicate anoxic slurries (50% w/v) for site C, and four replicate anoxic slurries (50% w/v) for site D were prepared in 125-ml sterile borosilicate glass serum bottles by mixing sediment sample with an equal volume of a sterile anoxic NaCl solution simulating the salinity of the Salton Sea (45 g L^{-1}) and either 4 mM $NaNO_3$ or 0.5 mM Na_2SeO_4 as terminal electron acceptors. Anoxic solutions were prepared by boiling prepared solutions briefly under a N_2 atmosphere. Slurries were degassed with nitrogen, sealed with butyl rubber stoppers, crimped with aluminum seals, and incubated during 141 and 308 hours for nitrate and selenate slurries, respectively, in the dark at 21°C under gentle orbital

shaking to maintain the sediment in suspension. Slurries were regularly sampled under anaerobic conditions. Aliquots of 0.5 mL were collected from all slurries at four different timepointsand immediately analyzed for selenate and nitrate using a Dionex ion chromatograph (electrochemical detector, ED40; analytical column, AS23/AG23; anion self-regenerating suppressor, ASRS-I, 4 mm) supplied with a carbonate eluent (4.8 mM Na_2CO_3 and 1 mM $NaHCO_3$) at a flow rate of 1.0 mL min^{-1}. Reduction rates for nitrate and selenate were calculated from the initial linear decrease in ion concentration as a function of time.

Figure 3. *Picture of sampling site at location C, Salton City (Photo: Juan Fernando Villa-Romero)*

2.2. Isolation of microbial consortia from Salton Sea littoral sediment

A microbial consortium was isolated from Salton Sea sediment collected from the 6-8 cm depth interval in the North littoral region (site N, N33.52338˚; W115.98176˚; Fig. 2) on November 2012. This site was selected due to the abundance of barnacles and fish carcasses and its proximity to the drainage area of agricultural areas irrigated by the nearby Whitewater River (Fig. 2). Five grams of wet sediment were suspended in 45 mL of sterile saline solution (NaCl, 2%; $MgCl_2$, 0.3%) and shaken thoroughly. Tenfold dilution series (eight replicates) were made directly in sterile culture medium dispensed in 96-well microtiter plates (see Chapter 2, section *Enumeration of selenate reducers in sediment*). From each well showing the presence of selenate-reducers, as indicated by the presence of red precipitate, a subsample was aseptically collected and transferred to Hungate tubes flushed with N_2

and containing 9 mL of anoxic medium of the following composition (in L^{-1}): NaCl, 45 g; $MgCl_2$ì$6H_2O$, 3 g; KH_2PO_4, 0.2 g; NH_4Cl, 0.3 g; KCl, 0.3 g; Na_2SO_4, 0.3 g; yeast extract, 0.1 g; Na_2SeO_4, 1.89 g (10 mM); ATCC MD-TMS (trace mineral solution), 10 mL; ATCC MD-VS (vitamin solution), 10 mL; Na-lactate, 10 mM; pH was adjusted to 7.5. Tubes were sealed and incubated at 30°C in the dark for 3 weeks. Cultures were transferred to fresh anoxic medium every three weeks at a 1:10 dilution and those leading to inconsistent results after incubation were discarded. Inconsistent results were those could not be replicated after three or more transfers. The domesticated microbial consortium was capable of consistently forming an intensely red precipitate (Fig. 7) and will be referred heretofore as SS-1. Experiments to determine the range of terminal electron acceptors that SS-1 was capable to reduce were done in media of identical composition to that used for isolation, but supplemented with 10 mM of sodium selenite, nitrate, nitrite, sulfate or sulfite, instead of selenate.

2.3. Recovery of axenic cultures

Stable cultures of SS-1 were plated on 1% agar plates containing media of identical composition to that used during isolation and incubated anaerobically at 30°C in the dark using hermetically sealed pouches containing BD anaerobic GasPaks. The appearance of colonies was monitored periodically and detectable colonies were transferred to 9 mL of liquid medium of identical composition to that used during isolation and incubated anaerobically at 30°C in the dark for 3 weeks. Additionally, stable SS-1 cultures maintained during three successive transfers in a medium of identical composition to that used during isolation were serially diluted twelve-fold at 1:10 ratios across the horizontal axis of 96-well microtiter plates. Dilutions 10^{-8}-10^{-12} were transferred to 9 mL of liquid media of identical composition to that used during isolation and incubated anaerobically at 30°C in the dark for 3 weeks.

2.4. Evaluation of selenate reduction in the presence of nitrate by the isolated microbial consortium

SS-1 was maintained during three successive transfers in a medium of identical composition to that used during isolation. For the experiment, this culture was transferred to fresh anoxic media in three sets of triplicate Hungate tubes at a 1:10 dilution. One set contained 5 mM selenate and 20 mM nitrate as terminal electron acceptors. Nitrate was supplied in excess to selenate to evaluate the effect of nitrate saturation on selenate reduction. The two remaining sets contained only 5 mM selenate and were used as controls. One control set was autoclaved at 121°C for 15 minutes to sterilize the incubation and monitor any changes in nitrate or selenate concentration not attributable to biological activity. Microbial growth was followed using absorbance at 600 nm (OD_{600}). All tubes were incubated in the dark at 30°C and 2 mL of liquid sample were collected at 19.5, 65.5, 89.5 and 114 hours to quantify nitrate and selenate concentrations using a Dionex ion chromatograph (electrochemical detector, ED40; analytical column, AS23/AG23; anion self-regenerating suppressor, ASRS-I, 4 mm) supplied with a carbonate eluent (4.8 mM Na_2CO_3 and 1 mM $NaHCO_3$) at a flow rate of 1.0 mL min^{-1}.

2.5. Selenium quantification in barnacle shells

Barnacle shells were carefully separated manually from a core sample collected at four depth intervals from site N (Fig. 2). From each depth interval, 1 gram of recovered shell sample was processed using a method developed at the laboratory: the sample was digested with 6 mL of 6M HCl in a 30 mL graduated digestion glass tube. This mix was placed on a hotplate at 70°C overnight and evaporated to near dryness. The remaining sample was diluted in 3 mL of 3 M HCl and filtered through a 0.45 μm PTFE filter membrane. Total selenium in these samples was measured using a Perkin Elmer 5300 DV Inductively Coupled Plasma-Optical Emission Spectrometer (ICP-OES) operating in regular mode. Selenium standards were prepared from certified reference stock solutions (VHG Labs) in a 3 M

HCl matrix to match the composition of the samples.

Figure 4. A view of the sediment core collected form site C. Each ring
has a depth equal to 2 cm (Photo: Juan Fernando Villa-Romero)

3. Results
3.1. Selenate reduction in slurries
A lag phase of about 45 hours in nitrate reduction and about 150 hours in selenate reduction was
observed in slurries containing sediment from site D, while no lag phase was apparent in slurries containing
sediment from site C (Fig. 8). Nitrate and selenate were completely removed from slurries containing

sediment from site C at about 45 hours and 300 hours, respectively (Fig. 8). In contrast, nitrate and selenate were present at 0.93±0.35 mM and 0.36±0.16 mM, respectively, by the end of the incubation period in slurries containing sediment from site D. Selenate and nitrate reduction rates were 13.44±1.13 and 0.66±0.03 μM h^{-1} g^{-1} dry sediment, respectively, for site C, and 1.13±0.15 and 0.31±0.19 μM h^{-1} g^{-1} dry sediment, respectively, for site D.

Figure 5. *Picture of sampling site at location D (Photo: Juan Fernando Villa-Romero)*

3.2. Microbial consortium SS-1

A microbial consortium was successfully isolated from sediment collected from site N (Fig. 2) at 6-8 cm depth and will be referred to as SS-1 (Fig. 7). Experiments with SS-1 showed that it could grow in 10 mM nitrate but not in 10 mM selenite, nitrite, sulfate or sulfite. However, after several transfers in nitrate, the capacity to grow in selenate was greatly diminished and could not match the selenate reducing capabilities of the original culture. This was evident by the lack of consistent growth of nitrate-grown cultures when returned to media containing selenate only. SS-1 cultures incubated in nitrate and returned to selenate failed to grow, grew inconsistently or did not produce the intensely red precipitate observed in selenate-grown cultures. Several unsuccessful attempts were made to obtain axenic cultures from SS-1. Colonies recovered on 1% agar plates of composition identical to that of the liquid medium failed to grow or did not led to consistent growth patterns when transferred to liquid

medium. The dilution-to-extinction approach resulted in one tube showing a pattern of growth that was different to that observed in SS-1 but poorly reproducible. This second consortium isolated from SS-1 produced a black precipitate (SS-2 in Fig. 7), however, this result was inconsistent and could not be replicated after several transfers.

Figure 6. *A view of the sediment core collected form site D. Each ring has a depth equal to 2 cm (Photo: Juan Fernando Villa-Romero)*
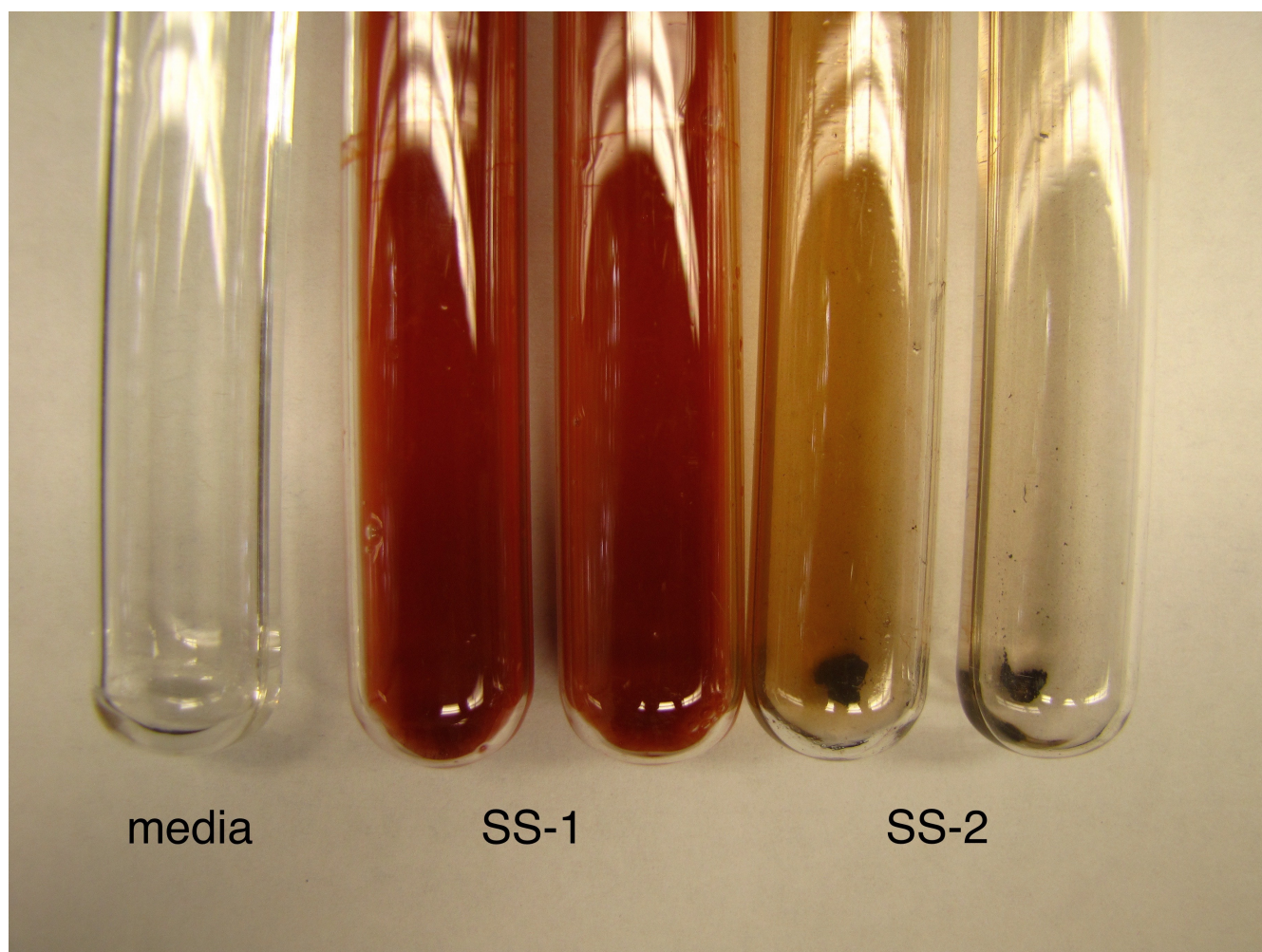
Figure 7. A comparison of isolation media containing selenate (left tube), media containing consortium SS-1 (duplicate tubes), media containing consortium SS-2 (duplicate tubes)

3.3. Selenate reduction in the presence of nitrate by the microbial consortium SS-1

When SS-1 was cultured in the presence of 20 mM nitrate, selenate removal followed nitrate removal and was not complete until all nitrate was removed from the medium (Fig. 9 B). A 60 hour lag-phase in selenate removal was observed when SS-1 was grown in selenate alone and in selenate and nitrate (Fig. 9 A and B). The calculated rates for selenate and nitrate reduction were 37.9 and 549.6 µM h^{-1}, respectively. Absorbance at 600 nm (OD$_{600}$) reached 7.40 in selenate-grown cultures and 1.11 in selenate-nitrate grown cultures (data not shown). A relatively short lag phase in nitrate removal could be inferred from the experiment with selenate and nitrate. At 65 hours nitrate was almost completely consumed in the nitrate-selenate experiment (Fig. 9 B) while selenate was still at initial concentrations in the selenate control (Fig. 9 A). Selenate was almost completely removed from the liquid phase at about 120 hours in both, the nitrate-selenate and selenate only incubation. A 65 hour lag-phase in OD$_{600}$ absorbance was also detected in both experiments, however, the formation of colloidal elemental selenium in the selenate-grown experiment may interfere with OD$_{600}$ measurements leading to growth overestimations. Colloidal elemental selenium was also evident in the SS-1 experiment with selenate and nitrate but it did not reach the intensity observed in the selenate grown culture.

3.4. Selenium content of barnacle shells

Selenium was detected in all tested barnacle shells with a content ranging between 0.1 µg g^{-1} at 6-8 cm and 7.22 µg g^{-1} at 0-2 cm (Fig. 10).
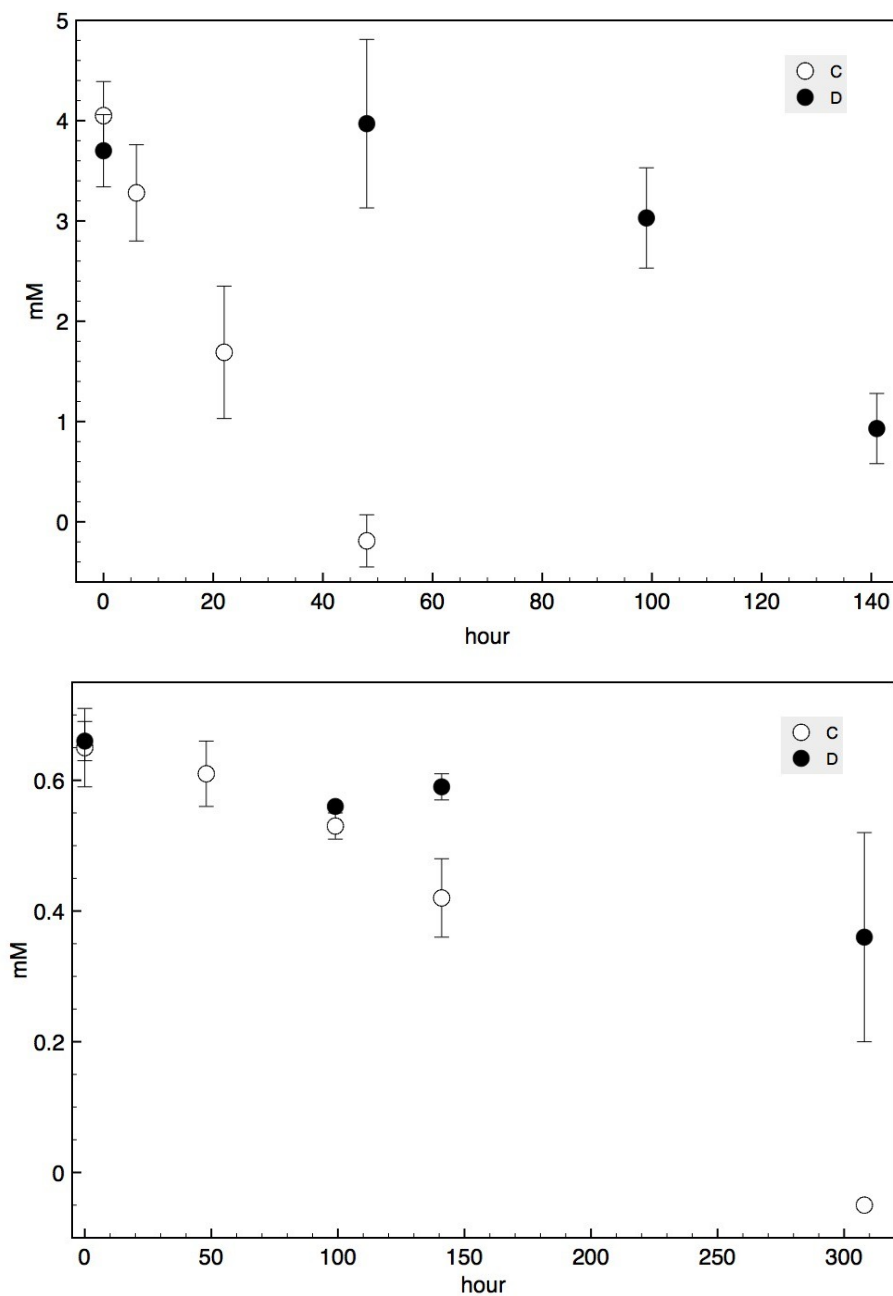

Figure 8. *Nitrate (top) and selenate (bottom) concentrations in sediment slurries prepared with sediment from site C (open circles) and site D (closed circles) as a function of time. Values represent the average of ten replicates for site C, and four replicates for site D ± standard deviation.*

4. Discussion

4.1. Selenate and nitrate reduction in SS-1

The consortium SS-1 was capable of tolerating 10 mM selenate concentrations and a salinity of 45, and seems to grow coupling the dissimilatory reduction of selenate to the oxidation of lactate. The presence of a red precipitate strongly suggests the formation of elemental selenium, which is the product of the microbial dissimilatory reduction of selenate. The lack of selenate removal in the autoclaved controls shows that the removal of selenate is a biological process. Obtaining axenic cultures from SS-1 was unsuccessful due to the poor growth of colonies on agar plates. However, the consortium SS-1 was successfully domesticated and consistently resulted in growth of identical characteristics. This was determined visually as growth of identical characteristics after similar incubation times. SS-1 maintained in selenate containing media removed 20 mM nitrate from the liquid phase without a significant lag phase suggesting that the active selenate reduction pathway in SS-1 is capable of reducing nitrate because a lag phase in microbial activity is usually interpreted as the time required to induce an inactive enzymatic pathway (Pierru et al., 2006). Many microbial isolates capable of nitrate respiration are capable of reducing selenate, and vice versa (Stolz & Oremland, 1999; Watts et al., 2005). In SS-1, the role of colloidal selenium during the estimation of microbial growth using absorbance at 600 nm cannot be properly evaluated and thus growth data remains inconclusive.
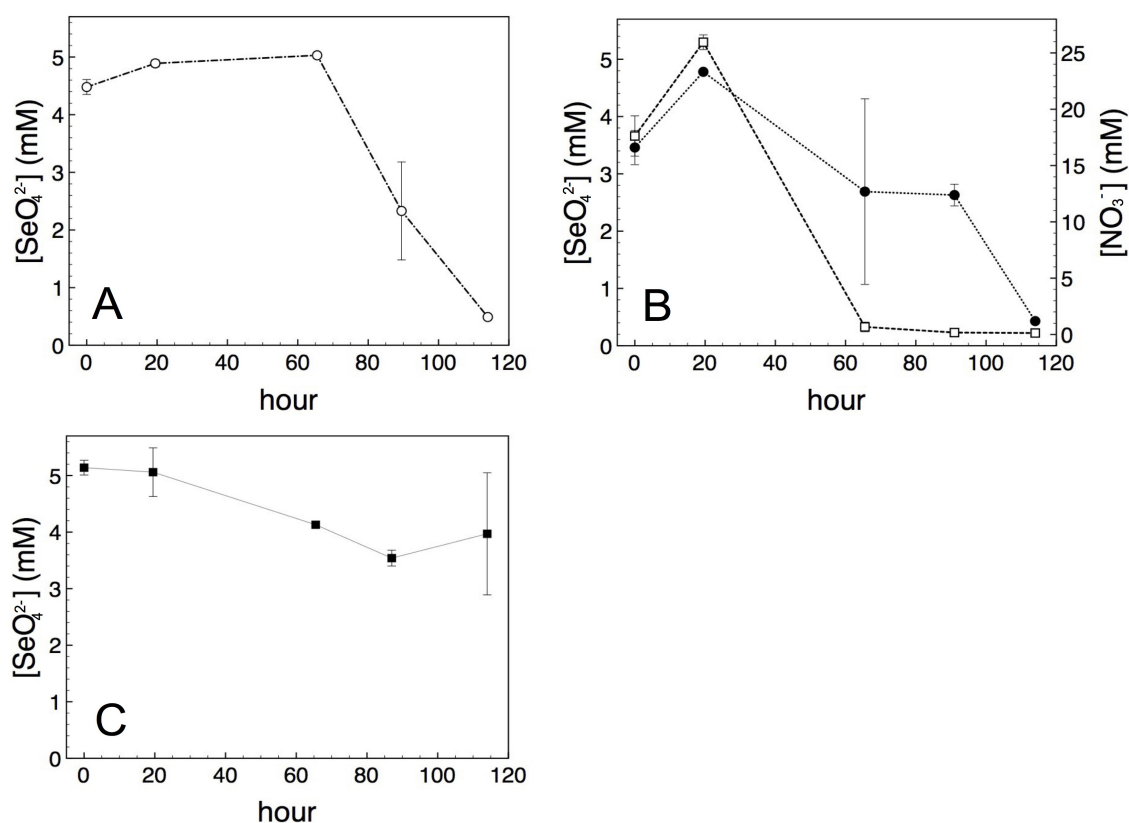
Figure 9. *Selenate and nitrate reduction by consortia SS-1. (A) 5 mM selenate only control, (B) 5 mM selenate (closed circles), 20 mM nitrate (open squares) incubation, (C) 5 mM selenate in autoclaved control*

4.2. Selenate and nitrate reduction in sediment slurries

In slurry incubations using sediment from sites C and D, high nitrate reduction rates occurred in sediment slurries showing high selenate reduction rates, an observation consistent with a previous report of selenate reduction and denitrification rates correlating in a study of slurries prepared with sediment collected from eleven locations across California and Nevada (Steinberg & Oremland, 1990).

4.3. Selenium in barnacles recovered from the Salton Sea

Barnacle shells recovered from the Salton Sea littoral showed selenium concentrations almost twice that of those found for total selenium content in sediment. Most reports of selenium concentration in barnacles recovered from selenium contaminated and non-contaminated environments range between 0.7 and 81 µg g^{-1} (Gay & Maher, 2003; Muhamed Ashraf et al., 2007) with no clear effect reported regarding differences between selenium contaminated and non contaminated sites. *Balanus amphitrite* Darwin, or "stripped" barnacle, were probably introduced to the Salton Sea by military seaplanes during the 1940s and have since adapted to the hypersaline conditions of the lake showing particularly high growth rates between January and May due to the warm water temperature and the abundance of phytoplankton (Geraci et al., 2008). *Balanus amphitrite* shows high and prey-dependent assimilation efficiencies for selenium, 63%-76% when feeding on zooplankton and 79% when feeding on diatoms, for example (Wang et al., 1999).
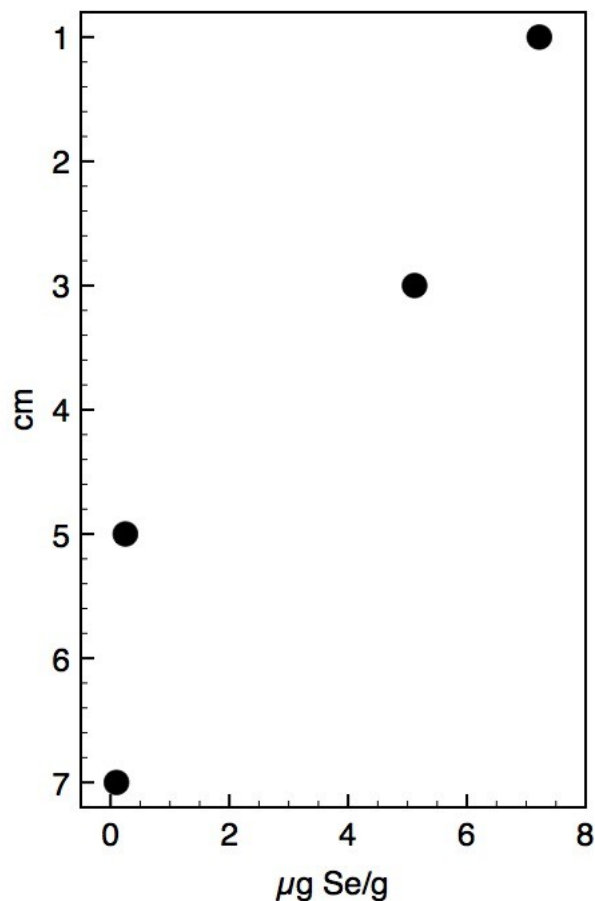
Figure 10. *Selenium concentrations in barnacles recovered from the North Salton Sea littoral*

58

4.4. Microbial selenate, nitrate and sulfate reduction in the environment

Teasing out the biogeochemical pathways that process selenium in sediment is complicated by our lack of knowledge regarding selenium-exclusive microbial metabolic pathways, and by the overlap between the nitrogen, sulfur and selenium cycles in the environment. Only one microbial reductase exclusive for selenate, SerA from *Thauera selenatis*, has been characterized (Schröder et al., 1997) and microbial pathways involved in nitrate, nitrite, sulfate and sulfite reduction are suspected to reduce selenate to selenite and elemental selenium in nature (Zannoni et al., 2007). Microbial pathways involved in nitrate reduction, more importantly, drive selenate reduction (Oremland et al., 1999; Watts et al., 2005) in part due to the virtually equivalent redox potentials of the SeO_4^{2-}-SeO_3^{2-} and NO_3^{-}-NO_2^{-} couples (+0.44 and +0.42 V, respectively) (Steinberg et al., 1992). The nitrate reductase of *Escherichia coli*, *Rhodobacter sphaeroides*, *Ralstonia eutropha*, *Paracoccus denitrificans* and *Paracoccus pantotrophus*, for example, can use selenate as electron acceptor, however, V_{max} for nitrate reduction was 140-fold higher than that for selenate reduction (Sabaty et al., 2001). Microbial nitrate reductases (NarG) and *T. selenatis*' SerA belong to the DMSO reductase family (Stolz et al., 2006). Archaeal nitrate reductases, on the other hand, show a high level of sequence similarity with annotated selenate reductases (Martinez-Espinosa et al., 2007). Sulfate reducing bacteria can reduce selenate enzymatically in at least three ways (Hockin & Gadd, 2003, 2006): via dissimilatory sulfate-reduction to hydrogen selenide; via assimilatory reduction to biomass selenide and/or volatile alkylated selenides; and via a third pathway that reduces selenium oxyanions to elemental selenium but it is uncoupled from microbial growth. Sulfate-reducing bacteria can also reduce selenite to elemental selenium with bacterially generated sulfide outside the cell producing red colloidal elemental selenium at the end of an incubation with selenate and sulfate (Hockin & Gadd, 2003, 2006). The range of environmental circumstances under which these selenium processing pathways occur in nature, however, remains poorly understood (Hockin & Gadd, 2003).

4.5. Assimilatory reduction pathways for selenium

Formate dehydrogenases exist only in prokaryotes, are the most widespread and abundant selenoproteins, and are present in most obligate anaerobes or facultative aerobes (Gladyshev et al., 2012), including the Gram negative bacterium *Escherichia coli* (Stolz et al., 2006). This suggests that selenium-containing formate dehydrogenases provide an advantage during anaerobic respiration, however, the required selenium assimilation pathways must confer a selective advantage to be preserved (Gladyshev et al., 2012). Microbes can assimilate selenate to selenomethionine via ATP sulfurylases of the sulfur assimilation pathway, but selenate-specific assimilation pathways may exist (Stolz et al., 2006). At concentrations above 1 μM, *E. coli* uptakes selenate via the sulfate ABC transporter and reduces it to selenide through assimilatory reduction pathways (Gladyshev et al., 2012; Shaw et al., 2012). In the presence of selenite, *E. coli* incorporates selenium via chemical interactions with thiol compounds, e.g. glutathione that lead to the synthesis of seleno aminoacids (Stolz et al., 2006; Gladyshev et al., 2012). A selenocysteyl-tRNA with unique sequence and structural properties, can incorporate selenocysteine into proteins with varying degrees of specificity in response to UGA, a universally conserved codon for selenocysteine (Stolz et al., 2006; Gladyshev et al., 2012; Nancharaiah & Lens, 2015). Selenomethionine, on the other hand, is almost indiscriminately incorporated into proteins in place of methionine (Gladyshev et al., 2012). The synthesis of selenium-containing aminoacids depends on the presence of selenium, but no selenium storage proteins have been described and little is known regarding selenium transport in bacteria (Shaw et al., 2012). *Ralstonia metallidurans*, a gram negative *β-Proteobacterium* that tolerates high heavy-metal concentrations removes selenium from water through two slow reactions with similar kinetics, which lead to the production of two reduced selenium species in equivalent proportions: a period of assimilatory uptake

that leads to alkyl selenide production, and a detoxification pathway that leads to elemental selenium (Sarret et al., 2005).

Colloidal nanoparticles of elemental selenium can directly enter living cells, which is a common occurrence in the case of nanomaterials (Winkel et al., 2012).
A study of selenium accumulation in aquatic biota from seven agricultural drains in the southern border of the Salton Sea showed the highest selenium concentrations in midge larvae (6.5 µg g^{-1}), Western mosquitofish (6.81 µg g^{-1}), and Sailfin molly (6.89 µg g^{-1}), compared to filtered water (5.62 µg g^{-1}), particulate organic detritus (5.48 µg g^{-1}), plankton (2.42 µg g^{-1}), and filamentous algae (2.22 µg g^{-1}) (Saiki et al., 2011). Neither algae nor plankton seem to contribute substantially to selenium accumulation in midge larvae or fish given the strong correlations found between selenium concentration in organic detritus, midges and fish, the lack of significant correlations between selenium concentrations in algae, plankton and fish, and the analysis of 235 fish gut contents showing algae and planktonic invertebrates accounting for only 1-2% of consumed biomass. (Saiki et al., 2011).

4.6. Dissimilatory reduction pathways for selenium

Dissimilatory reduction of selenium oxyanions is widespread among prokaryotes (Lovley, 1993; Stolz et al., 2002) and has been reported in both Bacteria and Archaea (Nancharaiah & Lens, 2015). In experimental enrichments prepared to isolate selenate-reducers from environmental samples, the rapid appearance of selenate- and selenite-reducers suggests these microorganisms are metabolically active in nature (Stolz & Oremland, 1999). Selenate-reducing bacteria are not only phylogenetically diverse but also functionally diverse and can couple growth to the oxidation of a wide range of electron donors, including H$_2$, glucose, pyruvate, lactate, acetate, citrate, glycerol, formate and hydroxybenzoate (Nancharaiah & Lens, 2015).

Eighteen strains of *Clostridium*, *Citrobacter*, *Flavobacterium*, *Pseudomonas*, *Sedimenticola*, and *Desulfurispirillum* species, and members of *γ-Proteobacteria*, *δ-Proteobacteria*, *Deferribacteres*, and *Chrysiogenetes* taxa have been reported to reduce selenate to elemental selenium (Lovley, 1993; Stolz et al., 2002; Nancharaiah & Lens, 2015) (Table 1). A number of these, including *Duganella* sp., *Agrobacterium* sp., *Geobacter sulfurreducens*, *Shewanella oneidensis*, *Veillonella atypica*, *Rhodospirillum rubrum*, *Sulfurospirillum barnesii*, *Bacillus selenitireducens*, *Selenihalanerobacter shriftii* and *Thauera selenatis* can form selenium nanoparticles from the reduction of selenium oxyanions (Bajaj et al., 2012; Butler et al., 2012). Only four, namely *Bacillus selenitireducens* and three strains of an *Aquificales* species (HGMK-1, 2, and 3) (Stolz et al., 2006) are reported to use selenite as terminal electron acceptor and reduce it to elemental selenium. The molecular basis of selenate reduction was described first in *T. selenatis* (Schröder et al., 1997) and later in *Enterobacter cloaceae* SLD1a-1 (Yee & Kobayashi, 2008) and *Citrobacter freundii* (Theisen & Yee, 2014). Expression of the selenate reductase gene of *C. freudii*, *E. cloacae*, *E. coli*, *Bacillus selenatarsenatis* SF-1 and *T. selenatis* is regulated by oxygen-sensing transcription factors and a fumarate-nitrate reduction (FNR) operon (Theisen & Yee, 2014). All known selenate reductases seem to be assembled and folded prior to export by the Tat export pathway (Theisen & Yee, 2014).

T. selenatis is a *β-Proteobacterium* isolated from seleniferous waters of the San Joaquin Valley in California (Macy & Lawson, 1993). The periplasmic selenate reductase of *T. selenatis*, SerA, is selenate-specific, contains molybdenum, iron, and acid-labile sulfur as prosthetic groups, and consists of α, β and γ subunits of 96 kDa, 40 kDa, and 23 kDa, respectively, located in the cell periplasm (Schröder et al., 1997). Kinetic parameters V_{max}, the maximum reaction rate when the enzyme is

saturated with substrate, and K_m, the affinity of the enzyme towards the substrate, describe the relationship between substrate concentration and the rate of an enzyme-catalyzed reaction. The K_m for selenate in *T. selenatis*' selenate reductase catalytic subunit, SerA, was determined to be 16 µM, and the V_{max} was 40 µmol min^{-1} mg^{-1} of protein (Schröder et al., 1997). Selenite formed in the periplasm of *T. selenatis* is transported to the cytoplasm via a sulfate transporter, and reduced via thiol-mediated reduction to elemental selenium nanospheres putatively stabilized by a 95-kDa protein, SefA (selenium factor A) (Debieux et al., 2011; Butler et al., 2012). Alternatively, *T. selenatis* reduces selenite to elemental selenium through a nitrite reductase (Bébien et al., 2002). Accumulation of red elemental selenium nanospheres in *T. selenatis* cultures has been observed in the cytoplasm and in spent extracellular medium (Nancharaiah & Lens, 2015).

Table 1. Microbial strains capable of selenate respiration (adapted from Saiki, 2011)

	Group
Pyrobaculum aerophilum	Crenarchaeota
Pyrobaculum arsenicum	Crenarchaeota
Salana multivorans	Gram +, high G+C
Bacillus selenitireducens	Gram +, low G+C
Bacillus arsenicoselenatis	Gram +, low G+C
Desulfitobacterium sp. OhF2	Gram +, low G+C
Selenihalanaerobacter schriftii	*Halanaerobacter*
Bordetella petrii	*β-Proteobacteria*
Thauera selenatis	*β-Proteobacteria*
Aeromonas hydrophila	*γ-Proteobacteria*
Citrobacter sp. TCA-1	*γ-Proteobacteria*
JSA	*γ-Proteobacteria*
TSA	*γ-Proteobacteria*
AK4OH1	*γ-Proteobacteria*
Ke4OH1	*γ-Proteobacteria*
Enterobacter cloacae SLD1a-1	*γ-Proteobacteria*
Wolinella succinogenes	*ε-Proteobacteria*
Wolinella succinogenes R-1	*ε-Proteobacteria*
Sulfurospirillum barnesii	*ε-Proteobacteria*

E. cloaceae is a fermentative, facultative anaerobic bacterium isolated from seleniferous water of the San Luis Drain in California (Losi & Frankenberger, 1997) that reduces selenate after oxygen depletion through a tungstate-sensitive, membrane-bound, trimeric complex with a catalytic molybdoenzyme of 100 kDa facing the periplasmic side of the cytoplasmic membrane (Yee & Kobayashi, 2008; Nancharaiah & Lens, 2015). The enzyme complex is ~600 kDa and has a $\alpha_3\beta_3\gamma_3$ subunit composition with masses of ~100, ~55 and ~36 for the α, β and γ subunits, respectively (Yee & Kobayashi, 2008). The catalytic subunit contains molybdenum, heme and non-heme iron as prosthetic groups, a b-type cytochrome in the active complex, and can reduce chlorate and bromate but not nitrate, nitrite, sulfate, arsenate, nor dimethylsulfoxide triethylamine N-oxide (Yee & Kobayashi, 2008).

B. selenatarsenatis SF-1 was isolated from sediments exposed to effluents from a glass manufacturing plant and reduces selenate through a membrane-bound trimeric molybdoenzyme that

faces the outside of the cell and transfers electrons from a quinol pool to the catalytic unit (SrdA) via SrdC and SrdB (Kuroda et al., 2011). *B. selenatarsenatis* SF-1 can respire selenate, arsenate and nitrate, however, a mutation targeting the *srdBCA* operon leads to the disruption of selenate reduction activity only suggesting that respiratory selenate reduction is independent from arsenate and nitrate reduction in this Gram-positive bacterium (Kuroda et al., 2011). SrdBCA is a membrane-bound, molybdopterin-containing oxidereductase that reduces selenate to selenite releasing an oxide ion and forming water as a result (Kuroda et al., 2011). SrdC binds quinol and transfers two electrons to the iron-sulfur cluster of SrdB which then passes electrons to selenate through the molybdenum cofactor (Kuroda et al., 2011).

In *C. freundii*, a facultative anaerobic *γ-Proteobacterium*, selenate reduction is predicted to occur through a molybdenum-containing Tat-secreted protein with a highly conserved molybdopterin-binding site (Theisen & Yee, 2014). *C. freundii*'s selenate reductase is encoded by the *ynfEGH* gene cluster which was 79%, 86% and 73% identical to *E. coli*'s YnfE, YnfG and YnfH proteins, respectively (Theisen & Yee, 2014). The *ynfE* gene contains the FNR operon and Tat signal sequence (Theisen & Yee, 2014). The *ynfG* gene codes for a sulfur-iron subunit analogous to the DmsB subunit of the DMSO reductase complex that connects the selenate reductase of *E. coli* to the electron transport chain (Theisen & Yee, 2014). The *ynfH* gene, a membrane-anchoring subunit 65% identical to *E. coli*'s DmsC protein, may attach the selenate reductase complex to the inner membrane, and bind to menaquinol to mediate transfer of electrons from the metaquinone electron pool (Theisen & Yee, 2014). The YnfE active site of *C. freundii*'s selenate reductase faces the periplasmic side of the cytoplasmic membrane, receives electrons from the menaquinone pool via YnfG and transfers them to selenate reducing it to selenite (Theisen & Yee, 2014).

In *E. coli* and *Salmonella*, two facultative anaerobic *γ-Proteobacteria*, selenate reduction is catalyzed by a molybdenum-containing selenate reductase distinct from *T. selenatis*' SerA or *B. selenatarsenatis*' SrdA (Theisen & Yee, 2014). *E. coli* mutants impaired in selenate reduction showed gene alterations in molybdopterin biosynthesis and putative oxidoreductase proteins suggesting that a molybdopterin-containing complex including YgfK, YfgM and YfgN proteins, carries out selenate reduction in the bacterium (Bébien et al., 2002).

Given the diversity of microbial pathways capable of selenate reduction, it is plausible to hypothesize that assimilatory reduction of selenium oxyanions through sulfur assimilation pathways, and dissimilatory reduction of selenate through nitrate reduction pathways can contribute to selenium immobilization in Salton Sea littoral sediment. But, to what extent SS-1 relies on assimilatory or dissimilatory reduction to drive selenate removal from liquid media can not be properly evaluated from the present data. Despite these limitations, understanding the molecular mechanisms microbes use to process selenium is required to develop reliable models of selenate reduction in the environment (Yee & Kobayashi, 2008).

4.7. Thermodynamic and stoichiometric constraints of microbial selenate reduction

Given that the MPN method used to estimate selenate-reducer abundance in sediment (see Chapter 1 and Chapter 2) and the OD_{600} approach used to monitor growth in SS-1 cultures could not be validated using colony counts in solid media, it is important to review the potential that selenate reduction has to support anaerobic microbial growth. The ability to predict the rate of biomass synthesis in microbes performing a particular geochemical reaction is important because these reactions are autocatalytic, that is, the reaction rate increases with increasing biomass (Jin & Bethke, 2007).

The synthesis of microbial biomass in natural settings requires the production of extracellular degradative enzymes that scavenge the required elements from the environment outside the cell, therefore linking microbial growth and organic matter decomposition (Sinsabaugh et al., 2009, 2014; Sinsabaugh & Shah, 2012). Thus, microbial growth regulates the geochemical cycling of biologically active elements under limits imposed by thermodynamic and stoichiometric constraints. Thermodynamic constraints refer to the energetic yields and requirements associated with microbial respiration and biomass synthesis, respectively, while stoichiometric constraints refer to the limits imposed by narrow ranges of possible microbial and organic matter C:N (Sinsabaugh & Shah, 2012; Helton et al., 2015). Microbial respiration, microbial biomass synthesis and organic matter decomposition in sediment are thus constrained by the energy required to synthesize and maintain microbial biomass, the energy yield of a particular form of microbial respiration, the availability and concentrations of electron donors and acceptors, and the C:N stoichiometry of microbial cells and electron donors (Moorhead et al., 2012; Sinsabaugh et al., 2014; Helton et al., 2015). Conceptual biogeochemical models that integrate these thermodynamic and stoichiometric data would therefore be powerful tools to understand biogeochemical patterns on local scales (Helton et al., 2015).
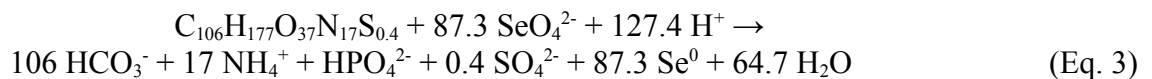
In anaerobic sediments of the Salton Sea, the mechanisms of selenium accumulation are closely linked to the quantity and characteristics of photosynthetic biomass (Weres et al., 1990; Zhang & Moore, 1997; Afzal et al., 2000; Vogl & Henry, 2002; Moreau et al., 2007a; Miles et al., 2009). The Salton Sea photosynthetic biomass, which we consider to have an average composition of $C_{106}H_{177}O_{37}N_{17}S_{0.4}$, based on mixed plankton tows from five ocean sites (Hedges et al., 2002) contributes importantly to organic matter accumulating in littoral sites (Anderson et al., 2008). Microbial dissimilatory metabolism couples the oxidation of an electron donor with the reduction of several inorganic terminal electron acceptors (Lovley, 1993). The energy liberated by coupling the oxidation of organic matter to the reduction of a particular inorganic ion is proportional to the number of electrons gained by the electron acceptor (Panikov & Flickinger, 2009; White et al., 2011). The number of electron moles available from the oxidation of one mole of organic matter with the general formula $C_aH_bO_c$ can be calculated as (Clark & Blanch, 1995; Jin & Bethke, 2007):

$$4a + 1b - 2c \qquad \text{(Eq. 1)}$$

The complete oxidation of organic matter with formula $C_{106}H_{177}O_{37}N_{17}S_{0.4}$, based on Eq. 1, releases 527 moles of electrons. Selenate reduction, on the other hand, requires 6 electrons to reduce selenate to elemental selenium:

$$SeO_4^{2-} + 6\ e^- + 8\ H^+ \rightarrow Se^0 + 4\ H_2O \qquad \text{(Eq. 2)}$$

By dividing the 527 electron moles available from $C_{106}H_{177}O_{37}N_{17}S_{0.4}$ oxidation by the 6 electron moles required to reduce one mole of selenate to elemental selenium, we find that 87.3 moles of selenate can be reduced with one mole of organic matter. Therefore, the balanced redox reaction coupling the oxidation of average marine organic matter to the reduction of selenate would be:

$$C_{106}H_{177}O_{37}N_{17}S_{0.4} + 87.3\ SeO_4^{2-} + 127.4\ H^+ \rightarrow$$
$$106\ HCO_3^- + 17\ NH_4^+ + HPO_4^{2-} + 0.4\ SO_4^{2-} + 87.3\ Se^0 + 64.7\ H_2O \qquad \text{(Eq. 3)}$$

In denitrifying prokaryotes, the translocation of 1 proton follows the transport of 1 electron to nitrate during nitrate reduction (White et al., 2011). As presented earlier, denitrification is a

geomicrobial process closely related to selenate reduction. So, assuming that i) all the energy released from electron transport is allocated to proton translocation, ii) the microbial enzymes involved in nitrate and selenate respiration are comparable, and iii) the phosphorylation of ADP to ATP requires the translocation of 3 protons (White et al., 2011), 527 electrons available from the oxidation of one mole of organic matter would lead to the formation of about 175.6 moles of ATP. This value is obtained by dividing the 527 electrons available for selenate reduction by 3, which is number of electrons that need to translocated to phosphorylate ADP to ATP.

A yield coefficient that links the energy available from respiration and the energy required for the synthesis of a unit of microbial biomass is required to calculate the theoretical yield of microbial biomass associated with a particular form of respiration. The ATP yield coefficient for anaerobic microbial growth ranges between 8.3 and 12.6 g of cell dry weight (CDW) mol^{-1} ATP, with an average of 10.7 g CDW mol^{-1} ATP (Clark & Blanch, 1995; Xiao & VanBriesen, 2007). Multiplying the 10.7 g CDW mol^{-1} ATP average by 175.6 moles of ATP derived from the oxidation of one mole of organic matter with formula $C_{106}H_{177}O_{37}N_{17}S_{0.4}$, we find that 1879.6 g CDW could be synthesized. Assuming an average 70% water content for microbial cells (Feijó Delgado et al., 2013), 1879.6 g CDW would correspond to 6265.4 g of microbial cells.

In summary, the oxidation of one mole of organic matter (OM) with formula $C_{106}H_{177}O_{37}N_{17}S_{0.4}$ (FW= 2325.4 g mol^{-1}) coupled to the reduction of 87.3 moles of selenate (FW= 142.96 g mol^{-1}) would lead to the formation of 87.3 moles of elemental selenium (FW= 78.96 g mol^{-1}) and 6265.4 g of microbial biomass (MB):

$$0.34 \text{ g of organic matter} + 1.81 \text{ g of } SeO_4^{2-} \rightarrow 1 \text{ g of } Se^0 + 0.9 \text{ g of microbial biomass}$$
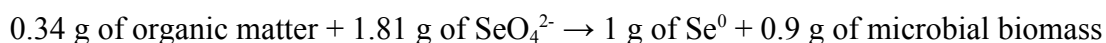
These values correspond to 0.5 g of microbial biomass synthesized for every gram of selenate reduced to elemental selenium.

The molar cell protein yield of *T. selenatis* using acetate to reduce selenate to selenite was found to be 7.8 g of cell protein mol^{-1} of selenite formed (Macy & Lawson, 1993). Assuming a protein content of 52.5% CDW (Feijó Delgado et al., 2013), this CDW yield corresponds to 14.9 g of microbial biomass, or 0.1 g of microbial biomass synthesized for every gram of selenate reduced to selenite, which is five times less than the theoretical microbial biomass yield resulting from oxidation of more complex organic matter, as calculated above. This illustrates the strong effect that organic matter characteristics have on the extent of microbial biomass synthesis.

As seen above, microbial biomass yield values link the energy generated from a particular form of respiration with the energy required to synthesize microbial biomass. A microbial biomass yield coefficient for anaerobic microbial growth coupled to selenate reduction based on energy available as ATP should be similar to that associated with anaerobic microbial growth in general (8.3-12.6 g of cell dry weight (CDW) mol^{-1} ATP) (Clark & Blanch, 1995; Xiao & VanBriesen, 2007). However, the only available microbial biomass yield value specific for the dissimilatory reduction of selenate is that reported for *T. selenatis* using acetate (7.8 g of cell protein mol^{-1} of selenite formed from selenate reduction) (Macy & Lawson, 1993). The molar cell protein yield of *T. selenatis* is the only datapoint available to link the energy yield and energy requirement associated with selenate reduction and microbial biomass synthesis, respectively, and was obtained from a pure culture grown under laboratory conditions. This dearth of data impedes the application of mathematical approaches that

couple the energy available from coupled redox reactions between terminal electron donors and acceptors to microbial growth in sediment. For example, another approach to estimate microbial biomass yields in sediment necessitates knowledge of the concentrations of microbial electron donors and acceptors and the rates of reactions describing potential catabolic processes (LaRowe & Amend, 2015a). This information can be used to compute the energy available to synthesize microbial biomass in sediment but requires having more precise knowledge regarding the microbial biomass yield values as outlined above. In Salton Sea FTR experiments (Chapter 2), biomass yields for selenate reducers were found to be 2 to 3 orders of magnitude lower than the expected yields based on the calculations presented in this section (data not shown). Elaborating further on the implications of this observation is not a straightforward exercise. First, bacterial growth efficiencies, the amount of new bacterial biomass produced per unit of organic carbon substrate assimilated, can range widely, between 0.01 and 0.6 in oligotrophic and eutrophic systems, for example, and is not a constant value regardless of the parameter to which one may attempt to normalize it (Giorgio & Cole, 1998). Second, data regarding the physiology of selenium utilization in microbes is much scarcer compared to that available to describe microbial cycling of nitrogen and sulfur, for example. It is worth noticing that predicted biomass yield values using the approach outlined above is close to the value expected based on the bacterial growth efficiency values proposed by Giorgio & Cole, 1998. Clearly, validating the theoretical biomass yields of microbes in their natural environments with experimental data obtained under conditions that closely represent their natural habitats is an avenue of promising future research.

4.8. Phylogenetic diversity in Salton Sea littoral sediment

Here I review data regarding the phylogenetic diversity of microbes in the Salton Sea to accompany information provided above regarding the diversity of microbial selenate reduction pathways. I will then use this information better define the microbial groups that may be driving selenate reduction in consortia SS-1 and in Salton Sea sediment and water.

Salton Sea water is populated by 46 distinct phyla dominated by *α-* and *γ-Proteobacteria* (>50.0% RA), *Bacteroidetes* (8.5-11.19% RA), *Spirochaetes* (5.9% RA), *Planctomycetes* (4-2-5.1% RA), unclassified bacterial groups (4.3-7.5% RA) and *Cyanobacteria* (4.2% RA) (Hawley et al., 2014) that showed significant seasonal variability in species diversity, richness, and community composition (Dillon et al., 2009).Salton Sea sediment communities, on the other hand, are dominated by anaerobes (e.g., *Clostridia*), *δ-Proteobacteria* (32% of relative abundance, RA), a group associated with dissimilatory sulfate reduction (Castro et al., 2000) , *γ-Proteobacteria* (10% RA) and *Crenarchaeota* groups (Dillon et al., 2009; Swan et al., 2010) with *δ-Proteobacteria* detected only between 16 and 21 cm of depth (Swan et al., 2010). *Crenarchaeota* abundance, specifically, ranged between 0.4 and 22% across a 0-35 cm sediment depth interval, and increased with decreasing carbon content and increasing salinity (Swan et al., 2010). Bacterial groups from *γ-Proteobacteria* are capable of growing coupling selenate reduction to the oxidation of aromatic compounds which currently contaminates some littoral regions of the Salton Sea (Schroeder et al., 2002). Salinity structured sediment bacterial communities with increasing salinity leading to an increase in *ß-Proteobacteria*, the phylogenetic group to which *T. selenatis* belongs to, and a decrease in *α-* and *γ-Proteobacteria,* but exerted no significant control on archaeal communities, which were weakly correlated with sediment total carbon content (Swan et al., 2010). *Pyrobaculum aerophilum* and *Pyrobaculum arsenicum*, members of the *Crenarchaeota*, have been shown to use selenate as terminal electron acceptor (Stolz et al., 2006). Given that sulfate levels and sulfate reduction are not expected to inhibit selenate reduction in the Salton Sea, the role of *δ-Proteobacteria* on selenate reduction has to be considered. On one hand, *δ-Proteobacteria* are the most abundant microbial group in sediment, and, as presented above, selenate is primarily uptaken through

sulfate assimilation pathways. On the other, *δ-Proteobacteria* in Salton Sea sediment has been reported at depths below those targeted in this study, and SS-1 was incapable of growing on sulfate or sulfite. Taken all together, these results suggest that nitrate reducers and nitrate reducing pathways process the low concentrations of selenate potentially present in Salton Sea littoral sediment. However, nitrate reducers are phylogenetically and metabolically diverse and microbial community data poorly constrains the possible list of microbial actors driving selenate reduction in the Salton Sea.

Salinity is a known global determinant of microbial diversity (Lozupone & Knight, 2007) and is probably the main constraint on microbial diversity in the Salton Sea. High salinities constrain metabolic diversity by selecting against bioenergetic pathways incompatible with increasing osmotic stress (Oren, 1999, 2011) given the potentially high energetic costs of osmoregulation (Oren, 2011; LaRowe & Amend, 2015a, 2015b). Selenate, however, has been found to drive anaerobic respiration at high salinity with halophilic strains like *Selenihalanaerobacter shriftii* capable of growing at salt concentrations between 100 and 240 g L^{-1} (Oren, 2011).

5. Conclusion

The consortium SS-1 was consistently capable of producing red elemental selenium in a minimal medium supplemented with 10 mM lactate and reduced selenate probably through nitrate reduction pathways. The potential role of nitrate-reducers in selenate reduction in evaluated Salton Sea sediments could be inferred from the rapid removal of nitrate by SS-1 maintained in selenate, high nitrate reduction rates occurring in sediment slurries showing also high selenate reduction rates in slurries containing sediment from sites C and D, and previous observations regarding the role of nitrate-reducers in selenium cycling (Steinberg & Oremland, 1990; Oremland et al., 1999; Watts et al., 2005).

Microbes in sediment not only catalyze the reduction of selenate but also constitute the trophic base of detrital food webs (Sinsabaugh et al., 2009). Selenium is more bioavailable in organic forms (Zhang & Moore, 1997; Ryu et al., 2011) and selenium accumulated in bacteria is more bioavailable to predators than selenium accumulated in sediment (Turner, 2013). Invertebrates inhabiting sediment accumulate selenium from a variety of sources (Peters et al., 1997) but largely through ingestion of selenium-containing particulate matter and sediment biota (Turner, 2013; US Environmental Protection Agency, 2014). The ingestion of selenium seems to drive the accumulation of selenium in animals (Presser & Luoma, 2010, 2013). Selenium utilization is widespread across life kingdoms. Yeast and higher plants do not utilize selenoproteins, while vertebrates depend on selenoproteins for their survival (Gladyshev et al., 2012). Selenium is a sulfur analog and can be assimilated through sulfur assimilation pathways (Stolz et al., 2006).

Areas of future research include the recovery, isolation and characterization of microbial cultures capable of selenate reduction, particularly targeting data on biomass yields for selenate reducers, and the periodic monitoring of selenium in Salton Sea invertebrates and fish that constitute the base of trophic webs supporting important bird populations.

The role of microbes in selenium immobilization is significant but the phylogenetic and functional diversity associated with selenium cycling in the environment has been inconclusively explored. Even though selenium-exclusive metabolic pathways exist and most likely remain to be discovered, the overlap between the nitrogen, sulfur and selenium cycles in nature complicates our understanding of selenium biogeochemistry in Salton Sea sediment. Better defining microbial biomass synthesis associated with the energy yield of dissimilatory selenate reduction could be coupled to

existing information regarding the concentration of electron donors and acceptors and may be used to better predict the rates of particular biogeochemical reactions (Helton et al., 2015). In this sense, multidisciplinary experiments that integrate geophysical, geochemical, microbial and kinetic data are powerful means to complete a scenario that better describes selenium behavior in sediment.

The roles of invertebrates and fish in selenium bioaccumulation in the Salton Sea should be further investigated. The polychaete *Neanthes* (*Nereis*) *succinea N. succinea* is the Salton Sea's most abundant macroinvertebrate (between $1.5 \cdot 10^{10}$ kg and $6.7 \cdot 10^{7}$ kg) (Swan et al., 2007), may accumulate selenium and is the primary food source for Salton Sea fish and some waterfowl species (Swan et al., 2007). Massive fish die-offs that each year reach up to 20 million individuals (Hurlbert et al., 2007; Moreau et al., 2007a, 2007b), each with selenium concentrations in tissue ranging between 1.7 and 2.9 µg g^{-1} (Riedel et al., 2002; Moreau et al., 2007a, 2007b; Marti-Cardona et al., 2008), on the other hand, would recycle selenium between contaminated biota and sediment. Monitoring of selenium in these populations would be more attuned with the latest approaches to evaluate risk associated with selenium, not on the basis of environmental exposure but on the basis of diet (US Environmental Protection Agency, 2014).

6. References

Afzal, S., M. Younas, & K. Ali, 2000. Selenium Speciation Studies from Soan-Sakesar Valley, Salt Range, Pakistan. Water International 25: 425–436.

Amrhein, C., & H. Doner, 2014. Biogeochemistry of Trace Elements: Reactions in Soils. In Chang, A. C., & D. B. Silva (eds), Salinity and Drainage in San Joaquin Valley, California. Springer Netherlands.

Anderson, M., L. Whiteaker, E. Wakefield, & C. Amrhein, 2008. Properties and distribution of sediment in the Salton Sea, California: an assessment of predictive models In Hurlbert, S. H. (ed), The Salton Sea Centennial Symposium. Springer Netherlands.

Bailey, R., T. Gates, & A. Halvorson, 2013. Simulating variably-saturated reactive transport of selenium and nitrogen in agricultural groundwater systems. Journal of Contaminant Hydrology 149: 27–45.

Bajaj, M., S. Schmidt, & J. Winter, 2012. Formation of Se (0) Nanoparticles by *Duganella* sp. and *Agrobacterium* sp. isolated from Se-laden soil of North-East Punjab, India. Microbial Cell Factories 11: 1–14.

Balistrieri, L., & T. Chao, 1987. Selenium Adsorption by Goethite. Soil Science Society of America Journal 51: 1145.

Bar-Yosef, B., & D. Meek, 1987. Selenium sorption by kaolinite and montmorillonite. Soil Science. 144: 11-19.

Bébien, M., J. Kirsch, V. Méjean, & A. Verméglio, 2002. Involvement of a putative molybdenum enzyme in the reduction of selenate by *Escherichia coli*. Microbiology 148: 3865–3872.

Bianchi, T., 2012. Estuarine Chemistry, In Day, J., B. Crump, W. Kemp, & A. Yáñez-Arancibia (eds), Estuarine Ecology. John Wiley & Sons, Inc.: 39–83.

Butler, C., C. Debieux, E. Dridge, P. Splatt, & M. Wright, 2012. Biomineralization of selenium by the selenate-respiring bacterium *Thauera selenatis*. Biochemical Society Transactions 40: 1239–1243.

Byron, E., & H. Ohlendorf, 2007. Diffusive flux of selenium between lake sediment and overlying water: Assessing restoration alternatives for the Salton Sea. Lake and Reservoir Management 23: 630–636.

Castro, H. F., N. H. Williams, & A. Ogram, 2000. Phylogeny of sulfate-reducing bacteria. FEMS Microbiology Ecology 31: 1–9.

Charlet, L., A. Scheinost, C. Tournassat, J. Greneche, A. Géhin, A. Fernández-Martínez, S. Coudert, D. Tisserand, & J. Brendle, 2007. Electron transfer at the mineral/water interface: Selenium reduction by ferrous iron sorbed on clay. Geochimica et Cosmochimica Acta 71: 5731–5749.

Clark, D., & H. Blanch, 1995. Biochemical Engineering, Second Edition. CRC Press.

Debieux, C., E. Dridge, C. Mueller, P. Splatt, K. Paszkiewicz, I. Knight, H. Florance, J. Love, R. Titball, R. Lewis, D. Richardson, & C. Butler, 2011. A bacterial process for selenium nanosphere assembly. Proceedings of the National Academy of Sciences 108: 13480–13485.

Dillon, J., L. McMath, & A. Trout, 2009. Seasonal changes in bacterial diversity in the Salton Sea. Hydrobiologia 632: 49–64.

Duc, M., G. Lefevre, M. Fedoroff, J. Jeanjean, J. Rouchaud, F. Monteil-Rivera, J. Dumonceau, & S. Milonjic, 2003. Sorption of selenium anionic species on apatites and iron oxides from aqueous solutions. Journal of Environmental Radioactivity 70: 61–72.

Feijó Delgado, F., N. Cermak, V. Hecht, S. Son, Y. Li, S. Knudsen, S. Olcum, J. Higgins, J. Chen, W. H. Grover, & S. Manalis, 2013. Intracellular Water Exchange for Measuring the Dry Mass, Water Mass and Changes in Chemical Composition of Living Cells. PLoS ONE 8: e67590.

Frankenberger, W., & R. Engberg, 1998. Environmental Chemistry of Selenium. CRC Press.

Gay, D., & W. Maher, 2003. Natural variation of copper, zinc, cadmium and selenium concentrations

in *Bembicium nanum* and their potential use as a biomonitor of trace metals. Water Research 37: 2173–2185.

Geraci, J., C. Amrhein, & C. Goodson, 2008. Barnacle growth rate on artificial substrate in the Salton Sea, California, In Hurlbert, S. H. (ed), The Salton Sea Centennial Symposium. Springer Netherlands: 77–84.

Giorgio, P. , & J. Cole, 1998. Bacterial Growth Efficiency in Natural Aquatic Systems. Annual Review of Ecology and Systematics 29: 503–541.

Gladyshev et al. (ed), 2012. Selenium - Its Molecular Biology and Role in Human Health. Springer Biochemistry and Biophysics.

Hamilton, S., 2004. Review of selenium toxicity in the aquatic food chain. Science of the total environment 326: 1–31.

Hawley, E., W. Schackwitz, & M. Hess, 2014. Metagenomic Sequencing of Two Salton Sea Microbiomes. Genome Announcements 2:1.

Hedges, J., J. Baldock, Y. Gélinas, C. Lee, M. Peterson, & S. Wakeham, 2002. The biochemical and elemental compositions of marine plankton: A NMR perspective. Marine Chemistry 78: 47–63.

Helton, A., M. Ardón, & E. Bernhardt, 2015. Thermodynamic constraints on the utility of ecological stoichiometry for explaining global biogeochemical patterns. Ecology Letters 18: 1049–1056.

Hockin, S., & G. Gadd, 2006. Removal of selenate from sulfate-containing media by sulfate-reducing bacterial biofilms. Environmental Microbiology 8: 816–826.

Hockin, S., & G. Gadd, 2003. Linked Redox Precipitation of Sulfur and Selenium under Anaerobic Conditions by Sulfate-Reducing Bacterial Biofilms. Applied and Environmental Microbiology 69: 7063–7072.

Holdren, G., & A. Montaño, 2002. Chemical and physical characteristics of the Salton Sea, California. Hydrobiologia 473: 1–21.

Hurlbert, A., T. Anderson, K. Sturm, & S. Hurlbert, 2007. Fish and fish-eating birds at the Salton Sea: a century of boom and bust. Lake and Reservoir Management 23: 469–499.

Jin, Q., & C. Bethke, 2007. The thermodynamics and kinetics of microbial metabolism. American Journal of Science 307: 643–677.

Kang, M., B. Ma, F. Bardelli, F. Chen, C. Liu, Z. Zheng, S. Wu, & L. Charlet, 2013. Interaction of aqueous Se(IV)/Se(VI) with $FeSe/FeSe_2$: Implication to Se redox process. Journal of Hazardous Materials 248–249: 20–28.

Kuroda, M., M. Yamashita, E. Miwa, K. Imao, N. Fujimoto, H. Ono, K. Nagano, K. Sei, & M. Ike, 2011. Molecular Cloning and Characterization of the srdBCA Operon, Encoding the Respiratory Selenate Reductase Complex, from the Selenate-Reducing Bacterium *Bacillus selenatarsenatis* SF-1. Journal of Bacteriology 193: 2141–2148.

LaRowe, D., & J. Amend, 2015a. Power limits for microbial life. Extreme Microbiology 718.

LaRowe, D., & J. Amend, 2015b. Catabolic rates, population sizes and doubling/replacement times of microorganisms in natural settings. American Journal of Science 315: 167–203.

Lemly, A. 2014. Teratogenic effects and monetary cost of selenium poisoning of fish in Lake Sutton, North Carolina. Ecotoxicology and Environmental Safety 104: 160–167.

Losi, M., & W. Frankenberger, 1997. Reduction of Selenium Oxyanions by *Enterobacter cloacae* SLD1a-1: Isolation and growth of the bacterium and its expulsion of selenium particles. Applied and Environmental Microbiology 63: 3079–3084.

Lovley, D., 1993. Dissimilatory Metal Reduction. Annual Review of Microbiology 47: 263–290.

Lozupone, C., & R. Knight, 2007. Global patterns in bacterial diversity. Proceedings of the National Academy of Sciences 104: 11436–11440.

Macy, J., & S. Lawson, 1993. Cell yield (Y_M) of *Thauera selenatis* grown anaerobically with acetate

plus selenate or nitrate. Archives of Microbiology 160: 295–298.

Mandal, S., S. Mayadevi, & B. Kulkarni, 2009. Adsorption of Aqueous Selenite [Se(IV)] Species on Synthetic Layered Double Hydroxide Materials. Industrial & Engineering Chemistry Research 48: 7893–7898.

Marti-Cardona, B., T. Steissberg, S. Schladow, & S. Hook, 2008. Relating fish kills to upwellings and wind patterns in the Salton Sea. In Hurlbert, S. (ed), The Salton Sea Centennial Symposium. Springer Netherlands: 85–95.

Martinez-Espinosa, R., E. Dridge, M. Bonete, J. Butt, C. Butler, F. Sargent, & D. Richardson, 2007. Look on the positive side! The orientation, identification and bioenergetics of "Archaeal" membrane-bound nitrate reductases. FEMS Microbiology Letters 276: 129–139.

Miles, K., M. Ricca, A. Meckstroth, & S. Spring, 2009. Salton Sea Ecosystem Monitoring Project. U.S. Geological Survey.

Moorhead, D., G. Lashermes, & R. Sinsabaugh, 2012. A theoretical model of C- and N-acquiring exoenzyme activities, which balances microbial demands during decomposition. Soil Biology and Biochemistry 53: 133–141.

Moreau, M., J. Surico-Bennett, M. Vicario-Fisher, D. Crane, R. Gerads, R. Gersberg, & S. Hurlbert, 2007a. Contaminants in tilapia (*Oreochromis mossambicus*) from the Salton Sea, California, in relation to human health, piscivorous birds and fish meal production. Hydrobiologia 576: 127–165.

Moreau, M., J. Surico-Bennett, M. Vicario-Fisher, R. Gerads, R. Gersberg, & S. Hurlbert, 2007b. Selenium, arsenic, DDT and other contaminants in four fish species in the Salton Sea, California, their temporal trends, and their potential impact on human consumers and wildlife. Lake and Reservoir Management 23: 536–569.

Muhamed Ashraf, P., B. Meenakumari, & T. Saly, 2007. Seasonal Variation of Metal Concentration in Barnacles (*Balanus* sp.) of Cochin Estuary, South West Coast of India. Fishery Technology 44.

Nancharaiah, Y., & P. Lens, 2015. Ecology and Biotechnology of Selenium-Respiring Bacteria. Microbiology and Molecular Biology Reviews 79: 61–80.

Navarro, R., T. Aoyagi, M. Kimura, H. Itoh, Y. Sato, Y. Kikuchi, A. Ogata, & T. Hori, 2015. High-Resolution Dynamics of Microbial Communities during Dissimilatory Selenate Reduction in Anoxic Soil. Environmental Science & Technology 49: 7684–7691.

Neal, R., & G. Sposito, 1989. Selenate Adsorption on Alluvial Soils. Soil Science Society of America Journal 53: 70.

Oades, J., 1988. The retention of organic matter in soils. Biogeochemistry 5: 35–70.

Oremland, R., J. Hollibaugh, A. Maest, T. Presser, L. Miller, & C. Culbertson, 1989. Selenate Reduction to Elemental Selenium by Anaerobic Bacteria in Sediments and Culture: Biogeochemical Significance of a Novel, Sulfate-Independent Respiration. Applied and Environmental Microbiology 55: 2333–2343.

Oremland, R., J. Blum, A. Bindi, P. Dowdle, M. Herbel, & J. Stolz, 1999. Simultaneous Reduction of Nitrate and Selenate by Cell Suspensions of Selenium-Respiring Bacteria. Applied and Environmental Microbiology 65: 4385–4392.

Oren, A., 1999. Bioenergetic Aspects of Halophilism. Microbiology and Molecular Biology Reviews 63: 334–348.

Oren, A., 2011. Thermodynamic limits to microbial life at high salt concentrations. Environmental Microbiology 13: 1908–1923.

Panikov, N., & M. Flickinger, 2009. Kinetics, Microbial Growth Encyclopedia of Industrial Biotechnology. John Wiley & Sons, Inc.

Peters, G., W. Maher, J. Barford, & V. Gomes, 1997. Selenium Associations in Estuarine Sediments: Redox Effects. In Evans, R., J. Wisniewski, & J. Wisniewski (eds), The Interactions Between

Sediments and Water. Springer Netherlands: 275–282.

Pierru, B., S. Grosse, D. Pignol, & M. Sabaty, 2006. Genetic and Biochemical Evidence for the Involvement of a Molybdenum-Dependent Enzyme in One of the Selenite Reduction Pathways of *Rhodobacter sphaeroides* f. sp. *denitrificans* IL106. Applied and Environmental Microbiology 72: 3147–3153.

Presser, T., & S. Luoma, 2010. Ecosystem-Scale Selenium Modeling in Support of Fish and Wildlife Criteria Development for the San Francisco Bay-Delta Estuary, California. U.S. Geological Survey.

Presser, T., & S. Luoma, 2013. Ecosystem-scale Selenium Model for the San Francisco Bay-Delta Regional Ecosystem Restoration Implementation Plan. San Francisco Estuary and Watershed Science 11.

Presser, T., M. Sylvester, & W. Low, 1994. Bioaccumulation of selenium from natural geologic sources in western states and its potential consequences. Environmental Management 18: 423–436.

Rainbow, P., & W. Wang, 2005. Trace metals in barnacles: the significance of trophic transfer. Science in China Series C: Life Sciences 48: 110–117.

Reese, B., & M. Anderson, 2009. Dimethyl sulfide production in a saline eutrophic lake, Salton Sea, California. Limnology and Oceanography 54: 250–261.

Reese, B., M. Anderson, & C. Amrhein, 2008. Hydrogen sulfide production and volatilization in a polymictic eutrophic saline lake, Salton Sea, California. Science of the total environment 406: 205–218.

Riedel, R., D. Schlenk, D. Frank, & B. Costa-Pierce, 2002. Analyses of organic and inorganic contaminants in Salton Sea fish. Marine Pollution Bulletin 44: 403–411.

Ryu, J., S. Gao, & K. Tanji, 2011. Accumulation and speciation of selenium in evaporation basins in California, USA. Journal of Geochemical Exploration 110: 216–224.

Sabaty, M., C. Avazeri, D. Pignol, & A. Vermeglio, 2001. Characterization of the Reduction of Selenate and Tellurite by Nitrate Reductases. Applied and Environmental Microbiology 67: 5122–5126.

Saha, U., & P. Huang, 2010. Surface coverage effects on the desorption kinetics of selenite from a hydroxyaluminum–montmorillonite complex. Journal of Colloid and Interface Science 350: 320–329.

Saiki, M., B. Martin, & T. May, 2011. Selenium in aquatic biota inhabiting agricultural drains in the Salton Sea Basin, California. Environmental Monitoring and Assessment 184: 5623–5640.

Sarret, G., L. Avoscan, M. Carrière, R. Collins, N. Geoffroy, F. Carrot, J. Covès, & B. Gouget, 2005. Chemical Forms of Selenium in the Metal-Resistant Bacterium Ralstonia metallidurans CH34 Exposed to Selenite and Selenate. Applied and Environmental Microbiology 71: 2331–2337.

Scheinost, A., & L. Charlet, 2008. Selenite Reduction by Mackinawite, Magnetite and Siderite: XAS Characterization of Nanosized Redox Products - Environmental Science & Technology (ACS Publications).

Schröder, I., S. Rech, T. Krafft, & J. Macy, 1997. Purification and Characterization of the Selenate Reductase from *Thauera selenatis*. Journal of Biological Chemistry 272: 23765–23768.

Schroeder, R., W. Orem, & Y. Kharaka, 2002. Chemical evolution of the Salton Sea, California: nutrient and selenium dynamics. In Barnum, D., J. Elder, D. Stephens, & M. Friend (eds), The Salton Sea. Springer Netherlands: 23–45.

Schroeder, R. & W. Orem, 2000. Nutrient Dynamics in the Salton Basin--implications from Calcium, Uranium, Molybdenum, and Selenium. U.S. Geological Survey.

Schroeder, R. & M. Rivera, 1993. Physical, chemical, and biological data for detailed study of irrigation drainage in the Salton Sea area, California. U.S. Geological Survey Open-File Report 93-83.

Shaw, F., F. Mulholland, G. Le Gall, I. Porcelli, D. Hart, B. Pearson, & A. van Vliet, 2012. Selenium-dependent biogenesis of formate dehydrogenase in *Campylobacter jejuni* is controlled by the *fdhTU* accessory genes. Journal of Bacteriology 194: 3814–3823.

Sinsabaugh, R., J. Belnap, S. Findlay, J. Shah, B. Hill, K. Kuehn, C. Kuske, M. Litvak, N. Martinez, D. Moorhead, & D. Warnock, 2014. Extracellular enzyme kinetics scale with resource availability. Biogeochemistry 121: 287–304.

Sinsabaugh, R., B. Hill, & J. Follstad Shah, 2009. Ecoenzymatic stoichiometry of microbial organic nutrient acquisition in soil and sediment. Nature 462: 795–798.

Sinsabaugh, R., & J. Shah, 2012. Ecoenzymatic Stoichiometry and Ecological Theory. Annual Review of Ecology, Evolution, and Systematics 43: 313–343.

Sposito, G., A. Yang, A. Mackzum, & R. H. Neal, 1991. Selenate Reduction in an Alluvial Soil. Soil Science Society of America Journal 55: 1597.

Steinberg, N., J. Blum, L. Hochstein, & R. Oremland, 1992. Nitrate Is a Preferred Electron Acceptor for Growth of Freshwater Selenate-Respiring Bacteria. Applied and Environmental Microbiology 58: 426–428.

Steinberg, N., & R. Oremland, 1990. Dissimilatory Selenate Reduction Potentials in a Diversity of Sediment Types. Applied and Environmental Microbiology 56: 3550–3557.

Stolz, J., P. Basu, & R. Oremland, 2002. Microbial transformation of elements: the case of arsenic and selenium. International Microbiology 5: 201–207.

Stolz, J., P. Basu, J. Santini, & R. Oremland, 2006. Arsenic and Selenium in Microbial Metabolism. Annual Review of Microbiology 60: 107–130.

Stolz, J., & R. Oremland, 1999. Bacterial respiration of arsenic and selenium. FEMS Microbiology Reviews 23: 615–627.

Su, C., & D. Suarez, 2000. Selenate and Selenite Sorption on Iron Oxides. Soil Science Society of America Journal 64: 101.

Swan, B., C. Ehrhardt, K. Reifel, L. Moreno, & D. Valentine, 2010. Archaeal and Bacterial Communities Respond Differently to Environmental Gradients in Anoxic Sediments of a California Hypersaline Lake, the Salton Sea. Applied and Environmental Microbiology 76: 757–768.

Swan, B., J. Watts, K. Reifel, & S. Hurlbert, 2007. Role of the polychaete *Neanthes succinea* in phosphorus regeneration from sediments in the Salton Sea, California. Hydrobiologia 576: 111–125.

Theisen, J., & N. Yee, 2014. The Molecular Basis for Selenate Reduction in *Citrobacter freundii*. Geomicrobiology Journal 31: 875–883.

Tokunaga, T., D. Lipton, S. Benson, A. Yee, J. Oldfather, E. Duckart, P. Johannis, & K. Halvorsen, 1991. Soil selenium fractionation, depth profiles and time trends in a vegetated site at Kesterson Reservoir. Water, Air, and Soil Pollution 57-58: 31–41.

Turner, A., 2013. Selenium in sediments and biota from estuaries of southwest England. Marine Pollution Bulletin 73: 192–198.

US Environmental Protection Agency, 2012. California's 2008-2010 Section 303(d) list of impaired waters. California State Water Resources Control Board, Sacramento.

US Environmental Protection Agency, 2015. Draft aquatic life chronic criterion for selenium in freshwater, Vol. EPA-822-P-15-001. US Environmental Protection Agency, Washington, DC.

VillaRomero, J., M. Kausch, & C. Pallud, 2013. Selenate reduction and adsorption in littoral sediments from a hypersaline California lake, the Salton Sea. Hydrobiologia 709: 129–142.

Vogl, R., & R. Henry, 2002. Characteristics and contaminants of the Salton Sea sediments. Hydrobiologia 473: 47–54.

Wang, W., J. Qiu, & P. Qian, 1999. The trophic transfer of Cd, Cr, and Se in the barnacle *Balanus*

amphitrite from planktonic food. Marine Ecology Progress Series 187: 191–201.

Watts, C., Ridley H, Dridge E, Leaver J, Reilly A, Richardson D, & Butler C, 2005. Microbial reduction of selenate and nitrate: common themes and variations. Biochemical Society Transactions 33: 173–175.

Weres, O., H. Bowman, A. Goldstein, E. Smith, L. Tsao, & W. Harnden, 1990. The effect of nitrate and organic matter upon mobility of selenium in groundwater and in a water treatment process. Water, Air, and Soil Pollution 49: 251–272.

Weres, O., A. Jaouni, & L. Tsao, 1989. The distribution, speciation and geochemical cycling of selenium in a sedimentary environment, Kesterson Reservoir, California, U.S.A. Applied Geochemistry 4: 543–563.

White, D., J. Drummond, & C. Fuqua, 2011. The Physiology and Biochemistry of Prokaryotes. Oxford University Press, New York.

Winkel, L., C. Johnson, M. Lenz, T. Grundl, O. Leupin, M. Amini, & L. Charlet, 2012. Environmental Selenium Research: From Microscopic Processes to Global Understanding. Environmental Science & Technology 46: 571–579.

Xiao, J., & J. VanBriesen, 2007. Expanded thermodynamic true yield prediction model: adjustments and limitations. Biodegradation 19: 99–127.

Yee, N., & D. Kobayashi, 2008. Chapter 3 Molecular Genetics of Selenate Reduction by *Enterobacter cloacae* SLD1a- 1 Advances in Applied Microbiology. Academic Press: 107–123.

Zannoni, D., F. Borsetti, J. Harrison, & R. Turner, 2007. The Bacterial Response to the Chalcogen Metalloids Se and Te. In Poole, R. K. (ed), Advances in Microbial Physiology. Academic Press: 1–312.

Zhang, Y., & J. Moore, 1997. Controls of selenium distribution in wetland sediment, Benton Lake, Montana. Water, Air, and Soil Pollution 97: 323–340.

Zhang, Y., Z. Zahir, & W. Frankenberger, 2004. Fate of colloidal-particulate elemental selenium in aquatic systems. Journal of Environmental Quality 33: 559–564.

Conclusions

Salton Sea littoral sediments show a high spatial variability in selenate reduction rates. In Salton Sea littoral sediment, K_m values for selenate are orders of magnitude higher than selenium concentrations in Salton Sea water. That is, selenate-reducing microbial communities in Salton Sea littoral sediment operate well below their maximum potential and, therefore, *in situ* microbial selenate reduction is limited by the low availability of selenate. Selenate adsorption, on the other hand, was unexpectedly high. Both selenate reduction and the sorption of selenium oxyanions are affected by sediment organic carbon content, which acts as a sorbant for selenium oxyanions and provides sediment microbial communities with the reducing power required to grow and reduce selenate to biomass-associated and elemental selenium, primarily. While microbial selenate reduction in sediment is capable of fully removing the low concentrations of selenate in Salton Sea water, the sorption of selenium oxyanions, more importantly, seems to drive selenium accumulation in littoral sediments of the lake. The diversity of sediment characteristics in The Salton Sea littoral highlights the difficulties associated with predicting selenium accumulation patterns without sufficient information regarding the sediment physical, chemical and microbial characteristics.

The interpretation of data pertaining biogeochemical rates and rate kinetics must consider the methods used to obtain them. Data obtained using sediment slurries, for example, can only poorly reflect environmental processes given that rate limitations are removed by destroying the tridimensional structure of the sediment. As a result, reaction rates obtained using slurries are generally orders of magnitude higher than those at which reactions occur in natural settings. I showed, for example, that surficial sediment at the water-sediment interface has the highest affinity for selenate and supports microbial cells capable of rapidly removing high selenate concentrations in FTRs. Deeper sediment, on the other hand, showed lower overall selenate reduction rates in FTRs but the highest R_{max} values for selenate reduction, potentially explaining higher selenium content in Salton Sea sediment collected from North and South locations at depths below 4 cm.

The observation that surficial sediment shows high selenate reduction rates corroborates previous observations regarding the spatial segregation and predominance of selenate reduction in surface sediment. However, the overlap between the nitrogen, sulfur and selenium cycles in sediment, whereby selenate can be processed through microbial nitrate and sulfate reduction pathways, and the spatial segregation of nitrate and sulfate reduction in sediment, whereby nitrate reduction is generally considered a surface process while sulfate reduction is considered a process that occurs at greater depths, complicates the explanation regarding why total selenium contents were significantly higher below 4 cm depth in evaluated sediment from North and South littoral locations. This is the first study quantifying selenate reduction rates using an approach the preserves the tridimensional structure of the sediment, and suggests that past observations regarding the prevalence of selenate reduction in surface sediment may be an artifact related to the generalized use of sediment slurries to quantify biogeochemical rates.

A microbial consortium isolated from littoral sediments collected from the depth intervbal 6-8 cm in the North littoral region tolerated 10 mM selenate concentrations and salinity of 45 and was consistently capable of producing red elemental selenium in minimal media supplemented with 10 mM lactate. The data presented suggest that this consortium removed selenate through nitrate reduction pathways. Sulfate is not expected to suppress microbial selenate reduction in sediment from the Salton Sea littoral and reports of selenate reduction at salinities close to saturation suggest selenium

immobilization driven by microbial activity is likely to continue in the Salton Sea littoral despite the increase of water salinity expected to affect the lake in the near future.

Selenium immobilization in Salton Sea sediments has prevented aqueous selenium concentrations from reaching levels that pose an environmental hazard. However, selenium immobilized in sediment becomes available to invertebrates inhabiting Salton Sea sediment and enters the trophic webs that lead to toxic effects in waterfowl largely through ingestion of selenium-containing particulate matter and sediment biota. Barnacle shells are abundant in the north Salton Sea littoral and I showed they accumulate selenium up to concentrations almost twice of those found in littoral sediment.

Areas of future research include the recovery, isolation and characterization of halophilic microbial cultures capable of selenate reduction to obtain data on biomass yields for selenate reducers, and the periodic monitoring of selenium in Salton Sea invertebrates and fish that constitute the base of trophic webs. The role of microbes in selenium immobilization is significant but the phylogenetic and functional diversity associated with selenium cycling in the environment has been inconclusively explored.